University of Zagreb

Faculty of Geotechnical engineering

Nada Glumac

POTENTIOMETRIC SURFACTANT SENSORS BASED ON NEW IONOPHORES

DOCTORAL DISSERTATION

Varaždin, 2026.

University of Zagreb

Faculty of Geotechnical engineering

Nada Glumac

POTENTIOMETRIC SURFACTANT SENSORS BASED ON NEW IONOPHORES

DOCTORAL DISSERTATION

Mentors:

Full Professor Nikola Sakač

Associate Professor Marija Jozanović

Varaždin, 2026.

Sveučilište u Zagrebu

Geotehnički fakultet

Nada Glumac

POTENCIOMETRIJSKI SENZORI ZA TENZIDE NA BAZI NOVIH IONOFORA

DOKTORSKI RAD

Mentori:

prof.dr.sc. Nikola Sakač

izv. prof. dr. sc. Marija Jozanović

Varaždin, 2026.

SUPERVISORS

Full professor Nikola Sakač, PhD
Department of Environmental Engineering
Faculty of Geotechnical Engineering
University of Zagreb

Prof. Nikola Sakač is a full professor within the scientific field of chemistry and chemical engineering at the Faculty of Geotechnical Engineering, University of Zagreb, where he currently serves as Vice-Dean for science (2024–2027) and Head of the Unit for Chemical Sensors in the Laboratory for Environmental Engineering. His research focuses on chemical sensors, electrochemical sensing systems, environmental analytical chemistry, and development of advanced materials for detection of environmental pollutants and biomarkers.

In particular, his work addresses the development of potentiometric sensors, ion-selective electrodes, nanomaterial-based sensing layers, and hybrid electrochemical-opticalsensing platforms for detection of micropollutants, surfactants, heavy metals, and biological markers.

Prof. Sakač obtained his PhD in analytical chemistry from the Faculty of Chemical Engineering and Technology, University of Zagreb in 2011. Since 2023 he has held the position of full professor at the University of Zagreb, after previously serving as associate professor and assistant professor at the same institution and earlier at the Department of Chemistry,University of Osijek.

His scientific work has produced high-impact publications in international journals, particularly in the field of chemical sensors and analytical chemistry with 1009 citation and h-index 19. Prof. Sakač has extensive experience in national and international research projects, including Croatian Science Foundation projects, EU-funded research initiatives, and multiple COST Actions focused on analytical platforms, environmental monitoring, and supramolecular chemosensors. His work often involves interdisciplinary collaboration combining analytical chemistry, materials science, nanotechnology, and environmental engineering. He maintains a broad international collaboration network with leading researchers and institutions, including the Institute of Macromolecular Chemistry (Czech Academy of Sciences), the University of Naples Federico II, the University of Pécs, and other European institutions working on sensor technologies and environmental monitoring.

In addition to research, Prof. Sakač is actively engaged in academic teaching and supervision at undergraduate, graduate, and doctoral levels. He has delivered 17 invited lectures internationally, particularly on chemical sensor technologies, and has served on editorial boards of scientific journals. Prof. Sakač has received several recognitions for his scientific work, including a gold and silver medals for innovations at the ARCA Innovation Fair (2024 and 2025) and institutional awards for scientific excellence.

Assoc. Prof. Marija Jozanović, PhD
Josip Juraj Strossmayer University of Osijek
Department of Chemistry
Subdepartment of Analytical, Organic and Applied Chemistry

Associate Professor Marija Jozanović began her academic career in the Department of Chemistry at Josip Juraj Strossmayer University of Osijek, where she has been employed since 2011. She teaches undergraduate and graduate courses, including Organic Chemistry, Food Chemistry, and Basic Principles of Forensic Chemistry. She currently serves as Vice Head for Research at the Department of Chemistry.

She obtained her PhD in Engineering Chemistry in 2015 from the Faculty of Chemical Engineering and Technology, University of Zagreb, with the dissertation Electroanalytical Characterization and Electrophoretic Determination of Histidine Dipeptides, Carnosine and Anserine Using a C4D Detector. She previously graduated as Mag. Educ. of Chemistry and Biology from Josip Juraj Strossmayer University of Osijek in 2009, with a thesis focused on spectroscopic and potentiometric studies of starch–triiodide complexes for the development of an amylase sensor.

She was appointed Assistant Professor in 2018 and Associate Professor in 2023. Between 2021 and 2023, she served as Head of the Subdepartment of Analytical, Organic, and Applied Chemistry.

Her research focuses on electrochemical sensors, potentiometric methods, microchip electrophoresis, and analytical methods for environmental, pharmaceutical, and food analysis. In recent years, her work has particularly emphasized the synthesis and application of quaternary ammonium salts and nanomaterials as sensor materials, antimicrobial agents, and microfluidic analysis of dietary supplements.

She has co-authored more than 35 scientific papers indexed in the Web of Science database and has presented her research at numerous international scientific conferences. In 2024, she received the Gold Medal at the ARCA/AGRO-ARCA International Innovation Exhibition for an innovation developed in collaboration with the industry.

ACKNOWLEDGMENTS

This doctoral thesis is the result of the work of numerous institutions and individuals who have found themselves along the way and have left their smaller or larger mark on it. The most meritorious person in shaping the research and connecting all the institutions and people was my mentor, Prof. Dr. Nikola Sakač.

I would like to express my deepest gratitude to my mentor, Prof. Dr. Nikola Sakač, on whose encouragement I enrolled in the doctoral programme. I thank him for his trust, patience and all the time, knowledge and useful advice that went into this work, as well as for the extensive help and co-operation at all stages of the thesis.

I would also like to thank my co-author, Assoc. Prof. Marija Jozanović, under whose guidance the new chemical compounds on which my research was based were synthesised. I would like to thank her for her composure and encouragement in moments of crisis.

I would also like to thank my colleague and friend Nikolna Novotni Horčička, because we have travelled the same path together with different research topics. We supported each other and I thank her for her enthusiasm when sometimes it seemed that everything was lost.

I would like to thank the Međimurje Waters Administration for supporting my scientific education and especially my colleagues and friends Natalija, Katarina and Zoran for their support and technical help in developing the experimental part of the research.

I would like to thank my family for the help and support they gave me when I needed it most. And finally, a big thank you to everyone who in any way in the creation of this work.

ABSTRACT

Surfactants are widely used in industrial, household, and personal care products and frequently occur as environmental contaminants, necessitating reliable analytical methods for their determination. This doctoral research focuses on the development of new potentiometric sensors for the determination of ionic surfactants based on novel ionophores based on quaternary ammonium compounds and doped carbon-based nanocomposites.

In the first part of the study, a new triazolium-based quaternary ammonium compound, 1,3-dioctadecyl-1*H*-1,2,3-triazol-3-ium bromide (DODTA-Br), was synthesized and used for DODTA–TPB ionophore synthesis. DODTA–TPB was incorporated into PVC-based liquid membrane surfactant sensor. The developed DODTA–TPB sensor exhibited a near-Nernstian response to cationic surfactants (CTAB 56.2 and CPC 58.5 mV/decade) and anionic surfactants (SDS −59.2 and DBS −57.5 mV/decade) with a linear working range between approximately 10^{-7} and 10^{-3} mol L^{-1} and fast response time (<10 s). The sensor was successfully applied as an end-point indicator in potentiometric titrations of ionic surfactants in commercial products and environmental samples.

In the second part of the research, a nanocomposite surfactant sensor based on Pt-doped multiwalled carbon nanotubes (Pt@MWCNT) and the cationic surfactant 1,3-dihexadecyl-1*H*-benzo[d]imidazol-3-ium ionophore was developed. The Pt@MWCNT–DHBI sensor demonstrated near-Nernstian response for anionic surfactants (SDS -59.1 and DBS -57.5 mV/decade*),* improved membrane stability, reduced signal noise, and long-term operational stability exceeding six months. The sensor was successfully applied in potentiometric titrations of commercial detergent samples, yielding results in good agreement with the classical two-phase titration method.

The developed sensors were validated through analysis of technical surfactants, commercial detergents, mouthwash products, and environmental water samples. Recovery values ranged from 94.2 to 99.2%, confirming the high accuracy and reliability of the proposed analytical methods.

Computational modeling using quantum-chemical calculations and molecular dynamics simulations was applied to investigate the formation and stability of the DODTA–TPB ion pair. Theoretical analysis demonstrated that the ionic associate is primarily stabilized by electrostatic

interactions, with additional contributions from van der Waals and hydrophobic interactions, supporting its suitability as an ionophore for potentiometric sensors.

The results demonstrated that newly designed ionophores significantly improve the analytical performance and stability of potentiometric surfactant sensors. The developed sensors represent simple, sensitive, and cost-effective analytical tools for the determination of surfactants in environmental and industrial samples.

Keywords: surfactants, potentiometric surfactants sensor, quaternary ammonium compounds, metal-doped MWCNT, carbon nanocomposite, ion-pair, water analysis

Prošireni sažetak

Surfaktanti predstavljaju važnu skupinu kemijskih spojeva koji se široko primjenjuju u deterdžentima, proizvodima za osobnu higijenu, farmaceutskim pripravcima te brojnim industrijskim formulacijama. Zbog njihove široke uporabe značajne količine surfaktanata dospijevaju u okoliš, osobito u vodene sustave, gdje mogu uzrokovati negativne ekološke učinke. Stoga je pouzdano određivanje surfaktanata od velikog značaja za kontrolu kvalitete proizvoda, praćenje onečišćenja okoliša te ispunjavanje regulatornih zahtjeva. Klasične analitičke metode, poput dvostruko-fazne titracije, i dalje se često koriste, ali su povezane s uporabom organskih otapala i relativno dugotrajnim postupcima. U tom kontekstu, potenciometrijski senzori temeljeni na ionsko-selektivnim membranama predstavljaju jednostavnu, brzu i ekološki prihvatljiviju alternativu za određivanje surfaktanata.

Ovo doktorsko istraživanje usmjereno je na razvoj novih potenciometrijskih senzora za određivanje ionskih surfaktanata temeljenih na novim ionoforima baziranim na kvaternim amonijevim spojevima i dopiranim ugljikovim nanokompozitima.

U prvom dijelu istraživanja sintetiziran je novi heterociklički kvaterni amonijev spoj, 1,3-dioktadecil-1*H*-1,2,3-triazol-3-ijev bromid (DODTA-Br), koji je korišten za pripravu ionskog para DODTA–TPB. Dobiveni ionski par ugrađen je u PVC membranu tekućeg tipa i primijenjen kao aktivni ionofor u potenciometrijskom senzoru za surfaktante. Razvijeni DODTA–TPB senzor pokazao je gotovo Nernstovski odziv prema kationskim surfaktantima (CTAB 56,2 i CPC 58,5 mV/dekada) te prema anionskim surfaktantima (dodecil sulfata (SDS) −59,2 i dodecilbenzen sulfonata (DBS) −57,5 mV/dekada), s linearnim radnim područjem koncentracija približno od 10^{-7} do 10^{-3} mol L^{-1} i brzim vremenom odziva (<10 s).

Analitička primjenjivost senzora potvrđena je potenciometrijskim titracijama tehničkih surfaktanata poput SDS, DBS i lauril eter sulfata (LES), pri čemu su dobivene titracijske krivulje imale izražen sigmoidalni oblik s velikim promjenama potencijala (ΔE do približno 301 mV).

Senzor je uspješno primijenjen i za određivanje surfaktanata u komercijalnim proizvodima, uključujući vodice za ispiranje usta i deterdžente različitih formulacija. Dobiveni rezultati pokazali su dobro slaganje s rezultatima dobivenim klasičnom titracijom u dvije faze. Dodatno je ispitana primjenjivost senzora u okolišnim uzorcima vode (rijeke Drava i Mura, jezero

Motičnjak i akumulacija Drava). Metodom standardnog dodatka, dobivene su vrijednosti iskorištenja u rasponu od 94,2 do 96,5 %, što potvrđuje izostanak značajnog utjecaja matriksa i pouzdanost predložene metode.

U drugom dijelu istraživanja razvijen je potenciometrijski senzor temeljen na platinski dopiranim višestijenčanim ugljikovim nanocjevčicama (Pt@MWCNT) i kationskom surfaktantu 1,3-diheksadecil-1*H*-benzo[d]imidazol-3-ijev kao nanokompozitnom ionoforu. Pt@MWCNT–DHBI senzor pokazao je gotovo Nernstovski odziv prema anionskim surfaktantima (SDS−59,1 i DBS−57,5 mV/dekadi), poboljšanu stabilnost membrane, smanjeni šum signala te dugoročnu operativnu stabilnost dulju od šest mjeseci, bez značajnog drifta potencijala ili ispiranja ionofora iz membrane.

Nanokompozitni senzor uspješno je primijenjen u potenciometrijskim titracijama komercijalnih deterdženata. Određeni sadržaji anionskih surfaktanata iznosili su 6,1–6,3 % za praškaste deterdžente, 2,1 % za tekuće/gel deterdžente te 13,2–15,1 % za deterdžente za ručno pranje posuđa. Dobiveni rezultati bili su u dobroj podudarnosti s rezultatima dobivenim referentnim metodama i drugim senzorima.

Kako bi se bolje razumio mehanizam stvaranja i stabilnosti ionskog para DODTA–TPB, provedeno je računalno modeliranje primjenom kvantno-kemijskih izračuna i molekulske dinamike. Rezultati su pokazali da je stabilnost ionskog para prvenstveno posljedica elektrostatskih interakcija između triazolijeve kationske jezgre i tetrafenilboratnog aniona, uz dodatni doprinos van der Waalsovih i hidrofobnih interakcija. Dobiveni rezultati potvrđuju da teorijsko modeliranje može značajno doprinijeti racionalnom dizajnu novih ionofora i razumijevanju njihovog ponašanja u membranskim senzorima.

Rezultati istraživanja pokazuju da novo sintetizirani ionofori mogu značajno unaprijediti analitička svojstva potenciometrijskih senzora za surfaktante. Razvijeni senzori predstavljaju jednostavne, osjetljive i ekonomične analitičke alate za određivanje surfaktanata u okolišnim uzorcima, industrijskim formulacijama i komercijalnim proizvodima.

Ključne riječi: surfaktanti, potenciometrijski senzor, kvaterni amonijevi spojevi, višestjenčane ugljikove nanocjevčice dopirane metalom, ugljikov nanokompozit, ionski par, analiza vode

TABLE OF CONTENTS

LIST OF ABBREVIATIONS

CMC	Critical micelle concentration
CAGR	Compound annual growth rate
MBAS	Methylene Blue Active Substance
HPLC	High-Performance Liquid Chromatography
GC	Gas Chromatography
ISE	Ion-Selective electrode
TPB	tetraphenyl borate
PVC	Polyvinyl chloride
QACs	Quaternary alkyl ammonium compounds
EAC	Electroactive material
SWCNTs	Single-wall carbon nanotubes
MWCNTs	Multi-wall carbon nanotubes
CTAB	Hexadecyltrimethylammonium
SDS	Sodium dodecyl sulfate
CPC	Cetylpyridinium chloride
DMI-TPB	1,3-didecyl-2-methylimidazole-tetraphenylborate
AS^-	Anionic surfactant
CS^+	Cationic surfactants
$K^{pot}AB$	Selectivity coefficient
aRXm	Occupied binding sites in the membrane
LOD	Limit of detection
IUPAC	International Union of Pure and Applied Chemistry
LOQ	Limit of quantification
DBS	Dodecylbenzenesulfonate
TDA-DBS	Tetradodecylammonium - dodecylbenzenesulfonate
THA-SDS	Tetrahexadecylammonium-dodecyl sulfate
NPOE	2-Nitrophenyl octyl ether
DMI-TPB	1,3-didecyl-2-methylimidazolium-tetraphenylborate
HDTA-TPB	Hexadecyltrioctadecylammonium-tetraphenylborate
DTA-DBS	Dodecyltrimethylammonium-dodecylbenzenesulphonate
CTA	Cetyltrimethylammonium
TPB	Tetraphenylborate
CTA-SDS	Cetyltrimethylammonium - dodecyl sulfate
CTA-TPB	Ccetyltrimethylammonium-tetraphenylborate
DDA	Dimethyldioctadecylammonium
TODA	Tetraoctadecylammonium
DODTA-Br	1,3-dioctadecyl-1*H*-1,2,3-triazol-3-ium bromide
DODTA–TPB	1,3-dioctadecyl-1*H*-1,2,3-triazol-3-ium-tetraphenylborate
Hyamine 1622	Benzethonium chloride
FIM	Fixed interference method
Pt@MWCNT	Pt-doped multiwalled carbon nanotubes
DHBI	1,3-dihexadecyl-1*H*-benzo[d]imidazol-3-ium
Pt@MWCNT- DHBI	Pt-doped multiwalled carbon nanotubes - 1,3-dihexadecyl-1*H*-benzo[d]imidazol-3-ium
Pt@MWCNT- DBS	Pt-doped multiwalled carbon nanotubes – dodecylbenzenesulfonate
ESP	Electrostatic potential
FTIR	Fourier Transform Infrared Spectroscopy

CDA	Charge decomposition analysis
vdW	Van der Waals
DMIC	1,3-didecyl-2- methyl-imidazolium
TEM	Transmission electron microscopy
HOMO	Highest occupied molecular orbital
LUMO	Lowest unoccupied molecular orbital
DMIC–TPB	1,3-didecyl-2- methyl-imidazolium – tetraphenylborate
LES	Lauryl ether sulfate
ESI-MS/MS	Electrospray ionisation mass spectrometry

LIST OF SCIENTIFIC PAPERS

This PhD thesis comprises three original scientific papers on the topic of new surfactant sensors.

List of published scientific papers:

Published paper	**Database**	**Paper category and quartile**	**Impact factor (IF)**
I. N. Glumac, M. Fizer, N. Sakač, D. Marković, L. Vrban, R. Vianello, B. Šarkanj, M.K. Sakač, M. Jozanović, Study of a 1,3-dioctadecyl-1*H*-1,2,3-triazol-3-ium cation for potentiometric surfactants sensing applications, J. Mol. Liq. 432 (2025) 127831. https://doi.org/10.1016/j.molliq.2025.127831	WoSCC-SCIE	CHEMISTRY, PHYSICAL (Q2/2024) PHYSICS, ATOMIC, MOLECULAR & CHEMICAL (Q1/2024)	IF=5.2/2024
II. Glumac, L. Vrban, R. Vianello, M. Jozanović, M. Fizer, M.K. Sakač, R. Velotta, V. Iannotti, B. Della Ventura, M. Cvetnić, D. Marković, N. Sakač, A DODTA–TPB-Based Potentiometric Sensor for Anionic Surfactants: A Computational Design and Environmental Application, Chemosensors. 13 (2025) 321. https://doi.org/10.3390/chemosensors13090321	WoSCC-SCIE	EnvCHEMISTRY, ANALYTICAL (Q2/2024) ELECTROCHEMISTRY (Q2/2024) INSTRUMENTS & INSTRUMENTATION (Q2/2024)	IF=3,7/2024
III. N. Glumac, M. Momčilović, I. Kramberger, D. Štraus, N. Sakač, E. Kovač-Andrić, B. Đurin, M. Kraševac Sakač, K. Đambić, M. Jozanović, Potentiometric Surfactant Sensor with a Pt-Doped Acid-Activated Multi-Walled Carbon Nanotube-Based Ionophore Nanocomposite, Sensors. 24 (2024). https://doi.org/10.3390/s24082388	WoSCC-SCIE	CHEMISTRY, ANALYTICAL (Q2/2024) ENGINEERING, ELECTRICAL & ELECTRONIC (Q2/2024) INSTRUMENTS & INSTRUMENTATION (Q2/2024)	IF=3,5/2024

1. INTRODUCTION

1.1. Surfactants

Surfactants, or surface-active agents, are amphiphilic compounds widely utilized across industries for their ability to lower surface and interfacial tension between different phases, such as liquid-liquid, liquid-gas, or liquid-solid. These molecules consist of hydrophilic (water-attracting) heads and hydrophobic (water-repelling) tails, making them particularly effective in applications ranging from detergents for cleaning and disinfection to pharmaceuticals, cosmetics, food production, petroleum refining, and nanotechnology.

Because of their structural properties, surfactants spontaneously form aggregates such as micelles, bilayers, and liquid crystals, depending on concentration and environmental conditions. The most well-known example is micelle formation, which occurs when the surfactant concentration reaches the critical micelle concentration (CMC). CMC is a crucial parameter that defines the behavior of surfactants in solution and is frequently used in their characterization.

Surfactants are classified according to the charge on their hydrophilic head group. Anionic surfactants (e.g., dodecyl sulfates and alkylbenzenesulfonates) carry a negative charge and are most commonly used in detergents and cleaning agents. [1] Cationic surfactants (e.g., quaternary ammonium compounds) are positively charged and often used as biocides, disinfectants, and in textile processing.

Nonionic surfactants carry no net charge and are used in cosmetics and the food industry, while amphoteric surfactants display both positive and negative charges depending on the pH of the medium. [2]

Population growth and extensive urbanization have led to the increased production of surfactants. Anionic surfactants dominate global production, accounting for approximately 70% of the market, driven primarily by expanding consumer demand in home and personal care products. [3] With the surfactant industry valued at $45.57 billion in 2024 and projected to reach $76.81 billion by 2034 at a compound annual growth rate (CAGR) of 5.36% from 2025 to 2034. [3] Their widespread use has necessitated improvements in both formulation and monitoring to address associated health and environmental challenges.

Surfactants are known to disrupt cellular structures, impede oxygen exchange in aquatic environments, and irritate human skin, emphasizing the need for constant water quality monitoring and stringent production controls.

Standard methods for detecting surfactants such as two-phase titration [4] and the Methylene Blue Active Substance (MBAS) method [5] are labor-intensive, lack reproducibility, require skilled personnel, and involve hazardous organic solvents, conflicting with principles of green chemistry. Instrumental approaches, including High-Performance Liquid Chromatography (HPLC) [6], Gas Chromatography (GC) [7], Ion-Exchange Chromatography [8] and Size-Exclusion Chromatography [9], provide greater accuracy but are costly and unsuitable for routine or on-site applications. Waste containing anionic surfactants is one of the most widespread water pollutants, leading to the need for new, cost-effective, accurate, and practical methods for detecting anionic surfactants. [9–12] From this perspective, the use of potentiometric sensors appears to be a highly promising method.

1.2. Potentiometry

Potentiometry is an electroanalytical method based on the dependence of the potential of an indicator electrode on the concentration of a particular ionic species with which it is in contact in solution. During the measurement, a very small electric current flows through the cell, which does not affect the equilibrium state of the electrodes. The principle of potentiometric measurements is based on the correlation between the composition of the sample and the magnitude of the potential formed between the reference and indicator electrodes. The reference electrode provides a stable potential over a long period of time, while the indicator electrode shows a variable potential depending on the activity of the primary ion or analyte in direct potentiometry, a high-impedance potential measuring device (millivoltmeter) is located between the two electrodes. Electrochemical sensors convert the effect of electrochemical interaction into a useful signal. Chemical sensors consist of a receptor that serves for recognition and a transducer that is responsible for receiving the signal. [13] Potentiometry appeared at the beginning of the 20th century, and the first potentiometric sensors for surfactants in the 1960s and 1970s of the last century.

Direct potentiometry

Direct potentiometry can be used to determine the activity of many cations and anions in a fast, simple and convenient way. This method uses a device with an immersed ion-selective sensor that translates the activity of ions into an electrical potential. The cell voltage depends only on the activity of the ionic species in the solution in which it is found. The direct potentiometry measurement procedure consists of several steps. Solutions of different concentrations, or activities, are prepared. Then, the electrode potential value is measured with the prepared solutions, on the basis of which a calibration diagram $E = f$ (log a) is constructed. The diagram shows the dependence of the electrode potential on the logarithm of the activity of ions in solutions. The linear part of the curve is used to determine the unknown activity. By measuring the activity potential based on the calibration diagram, its concentration is read. The electrical potential of the electrodes of an electrochemical cell is expressed by the Nernst equation:

$$E = E^0 + \frac{2{,}303 \cdot RT}{nF} \cdot \log a \qquad (1)$$

where is it:

E - measured potential,

E^0 - standard electrode potential,

R - gas constant, 8.314 J K^{-1} mol^{-1} ,

T- temperature in Kelvin,

n - ion charge,

F - Faraday's constant, 96500 C,

a - activity of the analyte.

Activity is a measure of the interaction of different molecules in a non-ideal system, and represents the effective concentration of ions, which is usually less than the actual concentration of ions in solution. The activity of an ion is equal to the product of the mean activity coefficient (f) and the molar concentration of the ion (c):

$$a = c \cdot f \qquad (2)$$

The value of the activity coefficient under ideal conditions is 1 (in very dilute solutions where the ionic strength is minimal), which means that the activity of an ion is equal to its concentration. The activity coefficient can be calculated using the Debye-Hückel equation:

$$-\log f = \frac{A \cdot n^2 \cdot \sqrt{\mu}}{1+B \cdot r_x \cdot \sqrt{\mu}} \qquad (3)$$

where:

μ - ionic strength of the solution

rx - effective diameter of the hydrated ion X in angstroms (1Å = 10^{-8} cm).

A, B - constants depending on temperature and nature of solvent (for aqueous solutions at 25°C, A is 0.51 and B is 0.33).

Potentiometric titration

Potentiometric titration is a volumetric method in which the potential difference between two electrodes is measured as a function of the added volume of reagent. The method is based on the determination of the unknown concentration of the test solution by titration with a standard solution, where a significant change in the potential of the indicator electrode occurs (titration endpoint). The measuring potential is proportional to the logarithm of the analyte activity, and the measurement is based on the volume of titrant that causes a rapid change in potential near the equivalence point. The advantage of this method is the determination of analytes in turbid samples without the use of chloroform.

1.3. Ion-Selective electrodes for surfactants

Potentiometric sensors are an important class of electrochemical sensors that detect changes in electrode potential during analyte-receptor interactions. Ion-Selective electrodes (ISEs) with polymer membranes containing selective transducers (ionophores) are the most commonly used potentiometric sensors. [14–16]The composition of ISEs is based on three important components: a sensing material- ionophore (an ion-pair consisting a cationic and anionic surfactant or some other high molecular weight anion; like tetraphenyl borate (TPB) - an organoboron anion consisting of a central boron atom with four phenyl groups [17], PVC and a plasticizer. [18] Therefore, the sensitivity, selectivity, and lifetime of ISEs largely depend on the properties of the ionophores. [19–23] The development of new highly lipophilic ionophores is thus a promising approach to ensure the best properties of potentiometric sensors. [23,24]

Various ionic pairs are used for constructing ISEs for anionic surfactants: tetrahexadecylammonium-dodecyl sulfate [25], 1,3-didecyl-2-methylimidazolium-tetraphenylborate [26], hexadecyltrioctadecylammonium-tetraphenylborate [27], cetyltrimethylammonium-dodecyl sulfate [28], dodecyltrimethylammonium-dodecylbenzene sulfonate [29], cetyltrimethylammonium-tetraphenylborate [30], hyamine-tetraphenylborate [31], etc. Quaternary alkyl ammonium compounds (QACs) are used as the active component of the ionic pair to detect anionic surfactants. QACs are cationic surfactants with a nitrogen atom carrying a positive charge, enabling interaction with anionic surfactants. The quaternary nitrogen atom of QACs can be part of an aromatic or aliphatic ring. [32] The hydrophobic part of QACs is usually an alkyl chain of varying lengths, while the hydrophilic group differs. QACs also exhibit antimicrobial activity and are used as biocides and antimicrobial therapeutic agents. [33] Due to these properties, QACs are widely used as disinfectants and water treatment agents to control microbiological contamination in water systems. An ideal ion-pair should exhibit high lipophilicity, low aqueous solubility, strong selectivity toward the target analyte, and sufficient membrane compatibility. [15,34,35] In this way, the fabricated surfactant sensors could have high response, extended lifetime and broad useful concentration range. [22,23] A major challenge in constructing ISEs is the reliable immobilization of electroactive material (EAC) in the PVC matrix. Leaching of the EAC causes significant changes in sensor response and shortens its lifespan. [16,36] This issue can be improved by modifying the membrane composition, using EACs with lower water solubility. [37] Reduced solubility of newly synthesized compounds through alkylation with extremely long alkyl chains will minimize EAC leaching from the membrane, positively affecting sensor response stability and lifespan. The ability of ionophores to act as sensors is determined by complex chemical interactions at their binding sites. [34] Ionophore properties are influenced by a sensitive balance between the rigidity required for selectivity and the flexibility needed for rapid ion transfer. Aromatic QACs possess both these properties: rigidity due to the planar aromatic ring and flexibility due to rotation around the nitrogen atom. The development of new ISEs is limited by the use of commercially available ionophores. Thus, the synthesis of new ionophores would enable the development of new ISEs with significantly improved properties.

The other part of the sensor is the membrane medium in which the ion pair is dissolved. This is usually a mixture of high molecular weight PVC with a lipophilic plasticizer. The choice of the plasticizer affects the final response of the sensor [18,38] The plasticizer should also prevent

water penetration into the membrane and by improving the flexibility of PVC, also increase the solubility of the ionophore in the final sensing membrane matrix.

1.4. Nanomaterials in potentiometric surfactant sensors

Nanomaterials play an important role in the field of potentiometric testing because they possess excellent electrical properties and good hydrophobicity. Advances in nanotechnology have introduced carbon-based materials like single-wall and multi-wall carbon nanotubes (SWCNTs and MWCNTs) as innovative sensor components, offering advantages such as enhanced electron transfer, superior mechanical strength, adjustable surface reactivity, which makes them suitable for solid membrane ion selective electrodes. [1,39–42]

Nanomaterials in ion-selective electrodes for the determination of anionic surfactants were first used by Najafi in 2011. [41] Using a modified single-walled carbon nanotube (SWCNT) was constructed by Najafi et al. where hexadecyltrimethylammonium (CTAB) and dodecylsulfate (SDS), adsorbed to the SWCNTs, act as ionophores. The electrodes showed a fast response time of 30 s and could be used for 3 months. The membrane electrodes showed a Nernst slope (59.5 mV/decade) for SDS and (57.2 mV/decade) for CTAB. Furthermore, nanomaterials are used to prevent leaching of sensor material from the membrane. [1,42–44]

Sakač et al. described a solid-contact electrode with multilayer carbon tubes. [45] The sensing material used was the ion pair 1,3-didecyl-2-methylimidazole-tetraphenylborate (DMI-TPB). The multi-walled carbon nanotubes (MWCNTs) were homogeneously distributed in a PVC matrix, resulting in a more stable response with low noise (2.6 mV/h). They used MWCNTs to immobilize the sensing material with the ion pair 1,3-didecyl-2-methylimidazole-tetraphenylborate (DMI-TPB) implemented in a PVC membrane. The use of MWCNTs reduced the membrane resistance, increased the active surface area, and improved the repeatability. The sensor had a lifetime of 6 months.

Nanomaterials can be chemically bound to the ion pair. On the other hand, an inclusion complex with an ion pair or charged surfactant can also act as an ionophore. [45–48]

Carbon-based nanomaterials doped with metals (e.g. Pt or Ag) will further increase the electrical conductivity of the sensor membrane itself, which will further increase the sensitivity and lifespan of the sensor. Metal-doping further improves sensitivity, selectivity, stability, and detection range, enabling faster response times and extended operational functionality. [49]

Doped carbon nanotubes with platinum nanoparticles exhibit synergetic effects that enhance sensor stability and catalysis, reducing fouling and facilitating miniaturization. [50,51]

So far, the use of metal-doped carbon nanomaterials in the construction of surfactant sensors has not been described.

1.5. Response of ion-selective electrode to anionic surfactants

An important property of surfactant monomers is their ability to form ion-associates with ions of the opposite charge:

$$CS^+ + AS^- \rightleftarrows CSAS \qquad (4)$$

where they are CS^+- cations of cationic surfactants (quaternary ammonium compounds, pyridinium, arsonium phosphonium cations), cationic dyes, large complex cations formed by metal ion and ligand, large organic cations, etc.; AS^- - anions of anionic surfactants, large organic and inorganic anions.

Increasing the concentration of surfactant above the critical micellar concentration often leads to solubilization of the associated ion in the micelle. Ionic associates (ion pairs) are most often insoluble in water and can be extracted in nonpolar solvents (a property used in the isolation of sensor material). In surfactant analysis, only monovalent cations and anions are used, so the ions within ionic associates are always in a 1:1 ratio.

The mechanisms of interaction between the analyte and the membrane containing the sensor material are as follows:

a) analyte ion: AS^-, which originates from the fully dissociated anionic surfactant MAS

$$MAS \leftrightarrows M^+ + AS^- \qquad (5)$$

where:

M^+ - monovalent cation (usually K^+, Na^+, NH_4^+)

AS^- - anion of anionic surfactant (highly lipophilic)

b) sensor material: electrically charged CSAS

Dissociation CSAS:

$$CSAS_{(m)} \rightleftarrows CS^{+}{}_{(m)} + AS^{-}{}_{(m)} \qquad (6)$$

(m = membrane)

Ion exchange reaction in the membrane:

$$CSAS_{(m)} + AS^{-} \rightleftarrows CSAS_{(m)} + AS^{-} \qquad (7)$$

A liquid membrane with an ion-exchange pair is in contact with aqueous solutions of anions (analyte anions and interfering anions). The dominant species that exist within such a membrane are free CS^+ sites and free interfering ions, and the following competitive reactions are possible in the membrane phase:

$$CS^{+} + AS^{-}_{det} \rightleftarrows CSAS_{(det)} \qquad (8)$$

$$CS^{+} + AS^{-}_{int} \rightleftarrows CSAS_{(int)} \qquad (9)$$

And with the corresponding stability constants:

$$\beta_{CSAS_{det}} = \frac{\left[CSAS_{det}\right]}{\left[CS^{+}\right]\left[AS^{-}_{det}\right]} \qquad (10)$$

$$\beta_{CSAS_{int}} = \frac{\left[CSAS_{int}\right]}{\left[CS^{+}\right]\left[AS^{-}_{int}\right]} \qquad (11)$$

Discussion of the selectivity of surfactant electrodes with a liquid membrane requires the consideration of two limiting cases: complete dissociation in the membrane phase and the case of complete association, which is related to the polarity of the membrane medium and the affinity of the active sites of the membrane to interferents.

1.6. Analytical characteristics of the sensor

Ion-selective surfactant electrodes have specific properties, which are: selectivity and dynamic range, linearity range or working range, detection limit, quantification limit, response time and reproducibility, accuracy, precision, and trueness.

Selectivity and dynamic range

Selectivity is the ability of a potentiometric sensor to determine a specific type of analyte in the presence of other interfering chemical species that affect the response signal. [52] The response of a membrane in the presence of several different ions is determined by the equilibrium constants of the primary and interfering ion exchange reactions between the organic and aqueous phases. The resulting potential can be described by the potentiometric selectivity coefficient. If the solution contains only primary ions, the response is generated according to the Nernst equation. In case the solution contains other ions that affect the creation of electromotive force, the response is generated according to the Nicolskii-Eisenman equation. [15] In practice, the selectivity coefficient can be determined by the following methods:

1. Mixed solution methods (constant primary ion method, constant interference method, two-solution method, parallel potential method).

2. Separate solution methods (separate solution method of equal activities, equal potential solution method). [52,53]

For highly selective electrodes, the selectivity coefficient $K^{pot}AB$ is very small and the electromotive force depends only on the activity of the primary ion. The potentiometric selectivity coefficient $K^{pot}AB$ depends on the membrane composition, the complex constant of the ligand and the test ion, and the lipophilicity of the test ions.

Dynamic range

The dynamic range of an ion-selective electrode is determined by the difference between the maximum and minimum activity of the occupied binding sites in the membrane. This is the range in which the sensor responds, and is calculated according to the expression:

$$\text{Dynamic range} = (aRXm)_{max} - (aRXm)_{min} \qquad (12)$$

Linearity range and measurement (working) range

The linear operating range is determined by the calibration graphs and is defined as the area in which the data points on the calibration curve do not deviate by more than 2mV from linearity. [54] This is the range within which the change in the sensor signal is linearly dependent on the observed analyte property (concentration). Linearity can be defined as the ability of the sensor to provide a response proportional to the analyte concentration in the sample within a certain concentration range. The slope of the linear part of the calibration curve at 298 K is 59.16 mV for monovalent ions and 29.58 mV for divalent ions. At low and high activities, there is a deviation from linearity, so this is the range in which the electrode begins to lose sensitivity to the primary ion. [55] The test is carried out at five concentrations in the desired working range of the method and is determined mathematically and graphically according to equation:

$$y = a\,x + b \qquad (13)$$

where: y - measurement parameter; a - ordinate intercept; x – concentration; b - slope of the line.

The measurement or working range is the range between the minimum and maximum values of the analyte concentration the sensor has acceptable accuracy and precision, linearity and Nernst slope. Within the measurement range, the change in the sensor signal is linear and depends on the measured quantity (analyte concentration).

Limit of detection and limit of quantification

Limit of detection (LOD) is the smallest amount of analyte that can be measured. At low analyte concentrations, the lower limit of detection and deviation from the Nernst slope of the direction occur. A lower slope occurs due to interfering ions or when the response of ion-selective electrodes is mostly non-linear at high and low analyte activities. According to the International Union of Pure and Applied Chemistry (IUPAC) definition, the limit of detection for potentiometric measurements differs from that for other methods due to differences in the nature of the ISE response (logarithmic response). [56]

The limit of quantification (LOQ) is the smallest amount of analyte that can be quantitatively determined.

Response time and reproducibility

The response time is defined according to IUPAC recommendations as the time elapsed from the first contact when the ion-selective electrode is immersed in the solution or from a change

in the concentration of the primary ion to the moment when the potential does not change by more than 1 mV or when it reaches 90% of the final value. [57] The response time depends on the type of electrode, interference, the magnitude and direction of the concentration changes and the temperature.

Reproducibility is the standard deviation of data collected in a series of measurements in solutions of different concentrations of chemical species (after removing, rinsing, or wiping the electrode). [56]

Sensitivity

Sensitivity is the ability of a method or instrument to distinguish between analyte samples of different concentrations with a defined level of confidence, i.e., a measure of the change in the value of the measured sensor signal per unit change in analyte concentration. It can be increased by introducing additional signal stages, which increases the precision of the sensor and lowers the detection limit.

Accuracy, precision and trueness

Accuracy is the degree of agreement between test results and an accepted reference value. For a measurement to be accurate, it must be within ± 5%. The deviation is calculated according to the equation:

$$\text{percentage error}(\%) = \frac{\text{obtained result} - \text{expected result}}{\text{expected result}} \cdot 100 \qquad (14)$$

Sensor precision is the degree of agreement between a series of measurements made from the same homogeneous sample according to a prescribed analytical procedure. Precision is expressed by the mean square deviation and relative standard deviation. If systematic error is not present, the dispersion of results is a consequence of random error.

Trueness is the degree of agreement between the mean value and an accepted reference value. Trueness is calculated as the systematic error of the measuring device, and is calculated as the difference between the arithmetic mean and the reference value. [58]

$$b = \bar{x} - x_{ref} \qquad (15)$$

where: b - systematic error of the measuring device, $\bar{x}$ - mean value, x_{ref} - reference value.

1.7. Objectives, hypothesis and Expected Scientific contribution

The main objective of this research is to develop and construct new potentiometric sensors based on newly synthesized QAC surfactants, which will serve as sensing materials for ionic surfactants quantification. Additionally, composite sensor membranes based on carbon nanomaterials doped with noble metals will be constructed. The use of doped nanomaterials and new QAC will improve the immobilization and hydrophobic character of the sensing material resulting in more stable membrane composition with better analytical characteristics for applications in real systems.

Objectives:

- Synthesize and characterize new cationic quaternary alkyl ammonium compounds (QAC) based on imidazolium and triazolium groups.
- Synthesize and characterize PVC sensor membranes with new QAC-based ionophores.
- Synthesize and characterize composite sensor membranes with the addition of doped carbon nanomaterials.
- Utilize computational support for selecting the most suitable ionophores through quantum-chemical calculations and molecular dynamic simulations.
- Construct potentiometric sensors for surfactants and determine their analytical properties.
- Test potentiometric sensors for surfactants in model and real samples.

Hypothesis:

- New cationic quaternary alkyl ammonium compounds (QAC) based on imidazolium and triazolium groups can improve the properties of potentiometric sensors for surfactants.
- Doped carbon nanomaterials as electroactive materials can enhance the analytical properties and lifespan of potentiometric sensors for surfactants.

- Using computational modeling to interpret the obtained results can facilitate faster and more efficient selection and optimization of the most suitable ionophore for potentiometric surfactant sensors.
- New potentiometric sensors will be applicable for determining surfactants in real systems.

Expected Scientific contribution:

- Development of novel QAC surfactants with enhanced properties for potentiometric surfactant sensor applications.
- Utilization of doped carbon-based materials in the development of potentiometric surfactant sensors.
- Understanding the response mechanisms and behavior of ionophores in membranes and solutions.
- Developed new surfactant sensors for analyzing a broad spectrum of real samples, ranging from commercial products and wastewater to quality control of products and raw materials.

2. SCIENTIFIC PAPERS

Paper I

Glumac, N.; Fizer, M.; Sakač, N.; Marković, D.; Vrban, L.; Vianello, R.; Šarkanj, B.; Kraševac Sakač, M.; Jozanović, M. Study of a 1,3-Dioctadecyl-1*H*-1,2,3-triazol-3-ium Cation for Potentiometric Surfactants Sensing Applications. *J. Mol. Liq.* 2025, *432*, 127831. https://doi.org/10.1016/j.molliq.2025.127831.

Journal of Molecular Liquids 432 (2025) 127831

Contents lists available at ScienceDirect

Journal of Molecular Liquids

journal homepage: www.elsevier.com/locate/molliq

Study of a 1,3-dioctadecyl-1*H*-1,2,3-triazol-3-ium cation for potentiometric surfactants sensing applications

Nada Glumac [a], Maksym Fizer [b,c], Nikola Sakač [d,*], Dean Marković [e], Lucija Vrban [f], Robert Vianello [f], Bojan Šarkanj [g], Marija Kraševac Sakač [d], Marija Jozanović [h]

[a] Medimurske vode d.o.o., Ul. Matice hrvatske 10, Čakovec 40000, Croatia
[b] Department of Organic Chemistry, Uzhhorod National University, 46 Pidhirna Street, Uzhhorod 88000, Ukraine
[c] Department of Chemistry, University of Nevada, Reno, 1664 N. Virginia Street, Reno, NV 89557-0216, USA
[d] Faculty of Geotechnical Engineering, University of Zagreb, Hallerova 7, Varaždin 42000, Croatia
[e] Department of Biotechnology, University of Rijeka, Ul. Radmile Matejčić, Rijeka 51000, Croatia
[f] Laboratory for the Computational Design and Synthesis of Functional Materials, Division of Organic Chemistry and Biochemistry, Ruđer Bošković Institute, Bijenička Cesta 54, Zagreb 10000, Croatia
[g] Department of Food Technology, University North, Trg dr. Žarka Dolinara 1, Koprivnica 48000, Croatia
[h] Department of Chemistry, University of Osijek, Ulica Cara Hadrijana 8, Osijek 31000, Croatia

ARTICLE INFO

Keywords:
Cationic surfactant
Potentiometric sensor
Triazole
DFT

ABSTRACT

Potentiometric surfactants sensors usually consist of a PVC-membrane with plasticizer and an ion pair. PVC and a plasticizer ensure the lipophilic matrix for a low-solubility ion pair. Ion pair usually consists of a cationic surfactant and an oppositely charged anionic surfactant. To increase the properties of ion pair, and enhance the analytical properties of the surfactant sensor, new molecules have to be synthesized. In this research a 1,3-dioctadecyl-1*H*-1,2,3-triazol-3-ium cationic surfactant (DODTA) was successfully synthesized and characterized. Tetraphenylborate (TPB) was used as a counter ion to synthesize the DODTA-TPB ion pair. To analyze and understand the behavior of the DODTA and DODTA-TPB ion pair in the sensing membrane, a series of computational simulations using density functional theory (DFT) were performed. The electronic structure of the DODTA-TPB ion pair was studied through the analysis of frontier molecular orbitals. Electrostatic interactions were examined via electrostatic potential isosurfaces and partial charge redistribution, while weak dispersion interactions were investigated using van der Waals potential and reduced density gradient (RDG) isosurfaces. DODTA-TPB surfactant sensor showed excellent potentiometric response to cationic surfactants hexadecyltrimethylammonium (CTAB) and cetylpyridinium (CPC), 56.2 and 58.5 mV/ decade of activity, respectively. DODTA-TPB surfactant sensor was used as an end-point indicator in potentiometric titrations of CTAB and technical grade Hyamine 1622 with recoveries from 98.80 to 99.92 %.

1. Introduction

Surfactants are widely used compounds for cleaning, washing, and disinfecting. Cationic surfactants are used as disinfectants and detergents, anionic for washing, while nonionic surfactants improve the washing and cleaning properties of primarily used surfactants. Population growth and extensive urbanization have led to the increased production of surfactants. Apart from their positive properties, they also have some negative effects, such as skin irritation, prevention of oxygen exchange at the air/water interface, etc. The older generation of surfactants, which are usually branched, were replaced by linear surfactants, which led to a reduction in heavy foaming and eutrophication. However, they still end up in water bodies and have a negative impact on the environment. Classical methods for quantifying surfactants are, usually time consuming and complicated such as the two-phase titration or the MBAS method. Their major drawbacks also include the use of toxic chemicals such as chloroform, lack of reproducibility, and the need for professional and trained analysts. Ion-selective electrodes [1] for surfactants are their interesting potential substitute. These sensors can be solid-state sensors or liquid membrane sensors. [2,3] The biggest challenge in developing surfactant sensors is finding of right combination of ionophores (ion pairs) and a membrane

* Corresponding author.
E-mail address: nsakac@gfv.unizg.hr (N. Sakač).

https://doi.org/10.1016/j.molliq.2025.127831
Received 26 February 2025; Received in revised form 29 April 2025; Accepted 22 May 2025
Available online 23 May 2025

medium in which to dissolve them. Ion pairs usually consist of two oppositely charged surfactants, and their main properties should be low water solubility and a high molar mass. [1].

Researchers have begun to synthesize new cationic surfactants and new ion pairs to reduce leaching, extend sensor lifetime, and lower the detection limit. [4–7] It is also important that the synthesis and procedures are effective to reduce the environmental impact and lower the price.[8] The other part of the sensor is the membrane medium in which the ion pair is dissolved. This is usually a mixture of high molecular weight PVC with a lipophilic plasticizer. The choice of the plasticizer affects the final response of the sensor. [9] The plasticizer should also prevent water penetration into the membrane and by improving the flexibility of PVC, also increase the solubility of the ionophore in the final sensing membrane matrix. Surfactant sensors are used as end-point indicators in potentiometric titrations. [2] The goal of optimizing the sensor membrane is to achieve well-defined target breakpoints and inflections with high electromotive signal change for reproducible endpoint indication over a wide concentration range. To reach this target, there is a need to synthesize new ion pair complexes and to model the interaction of anionic and cationic parts of the ion pair complex to speed up the process and select the best-matched parts of ion pairs. [10].

There were several attempts to use the experimental and model data on ion pair formulations and interactions in potentiometric surfactant sensor ion pairs and membranes, i.e. experimental and theoretical study on cetylpyridinium dipicrylamide to calculate the ion-exchanger for cetylpyridinium selective electrodes [11], or development of PVC-based cetylpyridinium-selective electrode to investigate the mechanism of interaction between the cetylpyridinium cation and hydrophobic and lipophilic anions through the association reaction [12]. However, cetylpyridinium and related alkylammonium surfactants are known for their significant toxicity [13]. This motivates the search for alternative cationic surfactants with lower toxicity profiles. In our previous research, we demonstrated that triazole-based surfactants represent a promising class of functional materials with various potential applications [14,15]. Importantly, the 1,2,3-triazole moiety is associated with relatively low toxicity, making triazolium-based cations attractive candidates compared to conventional quaternary ammonium surfactants.

Building upon this background, the goal of the present work was to design and synthesize a new cationic surfactant, 1,3-dioctadecyl-1*H*-1,2,3-triazol-3-ium bromide (DODTA-Br), using a one-pot synthetic route. Its structure was fully characterized and evaluated for potential application in sensor development. Quantum chemical calculations on the DODTA-TPB associate allowed us to gain further insights into interionic interactions. A simultaneous slight decrease of the highest occupied molecular orbital (HOMO) energy and increase of the lowest unoccupied molecular orbital (LUMO) energy were observed during the association of 1,3-dioctadecyl-1*H*-1,2,3-triazol-3-ium (DODTA) and tetraphenylborate (TPB) ions. Relatively small values of electron donations between the ions testified to the presence of negligible covalent components in the interionic interactions and predominant electrostatic interactions. Various types of Fukui function reactivity descriptors indicated that the associate's most reactive sites matched well with the localization of frontier molecular orbital isosurfaces. The ionophore DODTA-TPB was used to prepare a highly stable and fast-responding cationic surfactant sensor, which was characterized in terms of reaction properties and perturbation.

2. Materials and methods

2.1. Chemicals

Organic synthesis was performed with all analytical grade chemicals: 1,2,3-1*H*-triazole, 1-bromooctadecane, $NaHCO_3$ (Sigma Aldrich, Darmstadt, Germany), and sodium tetraphenylborate (TPB) (Fluka, Buchs, Switzerland). Organic solvents used for the synthesis and extractions were anhydrous acetonitrile (ACN), dichloromethane (DCM), methanol, and hexane (Kemika, Zagreb, Croatia). For sensor membrane production and sensor fabrication; hydrophobic plasticizer o-nitrophenyloctylether (o-NPOE) (Merck, Darmstadt, Germany), high molecular weight PVC (Sigma-Aldrich, Hamburg, Germany), tetrahydrofuran (THF) (Merck, Darmstadt, Germany) and NaCl (Sigma-Aldrich, Hamburg, Germany) as an inner solution; were used.

Potentiometric measurements were carried out with technical grade benzethonium chloride (Hyamine 1622), and analytical grades cationic surfactants hexadecyltrimethylammonium bromide (CTAB) and cetylpyridinium chloride (CPC) (Merck, Munich, Germany) and analytical grade anionic surfactant sodium dodecylsulfate (SDS). Salts for interfering measurements were purchased from Kemika, Zagreb, Croatia.

2.2. Synthesis of 1,3-dioctadecyl-1H-1,2,3-triazol-3-ium bromide DODTA-Br (1)

The alkylation of 1,2,3-1*H*-triazole (0.365 g, 5.28 mmol) was performed under basic conditions by the addition of $NaHCO_3$ (607 mg, 7.22 mmol) in anhydrous ACN (5 mL) and an excess of 1-bromooctadecane (4 g, 12 mmol). The progress of the reaction was followed by TLC (DCM/methanol – 10:0.1) and the reaction was carried out under reflux for 2 days in an inert nitrogen atmosphere. NaBr salt was precipitated with hexane and the crude product 1 was obtained by filtration. Further purification by flash chromatography (DCM/methanol – 10:0.1) gave the desired bisalkylated ionic salt 1 (2.818 g, 4.30 mmol) in an 81.5 % yield.

2.3. DODTA ionophore synthesis

New cationic surfactant DODTA-Br was used for the synthesis of DODTA-TPB ionophore. The sensing ion pair DODTA–TPB (2) was synthesized by mixing 2 mmol of DODTA-Br (1) with 2 mmol of sodium tetraphenylborate, for 4 h in ACN. Next, after filtration, the filtrate was washed with DCM and stored in a freezer for 24 h at −18 °C. After filtration, DCM was removed by rotary evaporation. DODTA–TPB ion pair was dried at 80 °C to reach the constant mass. Prepared DODTA-TPB ion pair was stored dry and ready for analysis and surfactant sensor preparation.

2.4. DODTA–TPB surfactant sensor fabrication

To prepare the DODTA-TPB surfactant sensor membrane a high molecular weight PVC was sonicated with a plasticizer o-NPOE (1:2) and 1 % of the ion pair was added after 10 min. After adding 2 mL of THF and sonication, the cocktail was poured into the glass mold. After drying, a layer was incorporated into the electrode body containing 3 M NaCl as an inner electrolyte.

2.5. Instrumentation

IR spectra were recorded in the KBr salt matrix using a Shimadzu FTIR – 8400 S infrared spectrophotometer with IRsolution ver. 1.30 software. The ^{1}H and ^{13}C NMR spectra were recorded by a Varian 400 instrument in $CDCl_3$ as solvent.

Spectroscopic information on the molecular ions was obtained through the API 2000 LC-ESI-MS/MS (Applied Biosystems, Foster City, CA, USA) in q1 ms scan mode.

For the elemental analysis, PerkinElmer 2400 CHNS/O Series II System was used (PerkinElmer Inc., Waltham, MA, USA).

For response measurement, Metrohm 794 Basic Titrino with the Metrohm 781 pH meter (Metrohm, Herisau, Switzerland) was used. For titrations, Metrohm 808 Titrando was employed. All measurements were carried out with an Ag/AgCl reference electrode.

2.6. Computational methods and software

Total energies, optimized geometries, vibrational frequencies, thermochemical parameters including Gibbs free energies, and electron densities were calculated at the B3LYP/6-31G(d) level of theory [16,17]. The Grimme's D3 model employing Becke-Johnson dumping was applied to increase the density functional theory (DFT) method's accuracy in the description of weak interactions [18,19]. A conductor-like polarizable continuum model (CPCM) was utilized to include water solvation effects [20]. Moreover, the CPCM solvation model enables the screening of ion charges, preventing unphysical charge delocalization and artifacts such as undesired covalent bond formation between DODTA and TPB ions. The DFT calculations were performed with the ORCA 5.0.3 code [21,22] with the SHARK fast-math module [23]. Analyses of electrostatic potential, molecular orbitals, charge decomposition, and Fukui function isosurfaces were based on the electron density obtained with the above-mentioned method using the Multiwfn 3.8 program [24]. The average reduced density gradient method was used to analyze weak interionic interactions during the molecular dynamics simulation [10,25]. The trajectory was obtained at the COSMO-PM7 level of theory [26,27] using the MOPAC2016 and Cuby 4 codes [28,29]. Visualization was performed in the VMD 1.9.3 software [30]. The calculated vibrational modes were assigned to specific bond vibrations with the vibAnalysis code [31].

3. Results

3.1. Syntesis and characterization of 1,3-dioctadecyl-1H-1,2,3-triazol-3-ium bromide DODTA-Br (1)

Heating of 1,2,3-1*H*-triazole with 1-bromooctadecane under reflux with $NaHCO_3$ as a base in acetonitrile under N_2 atmosphere afforded bisalkylated ionic salt DODTA-Br (**1**) in 81.5 % of yield (Scheme 1). After the isolation by flash chromatography (DCM/methanol – 10:0.1), the DODTA-Br (**1**) was fully characterized by ^{1}H and ^{13}C NMR, mass spectrometry, ATR-FTIR spectroscopy, and elemental analysis.

3.1.1. NMR analysis

The ^{1}H NMR and ^{13}C NMR spectra of DODTA-Br (**1**) are shown in Figs. S1 and S2, respectively. As shown S1, in the ^{1}H NMR spectrum, the ring protons H-C(4) and H-C(5) appeared as broad singlets at 11.86 and 8.67 ppm, respectively. The H-C(1′) and H-C(1″) of two octadecyl chains were assigned as quartets with coupling constant J – 7.8 Hz at 4.45 ppm. Protons H-C(2′) and H-C(2″) were identified in the identical chemical region of 2.08 and 1.93. Due to the similar chemical environment, all protons of the two chains from H-C(3′) to H-C(17′) and from H-C(3″) to H-C(17″) appeared together in the NMR region between 1.68 and 1.41 ppm. The terminal methyl groups H-C(18′) and H-C(18″) of both chains were identified at 0.86 ppm as triplets with coupling constant J – 7.0 Hz.

The signals of carbon atoms in ^{13}C NMR of DODTA-Br (**1**) were found at 143.2, 143.0, 53.0 (2C atoms), 48.9 (2C atoms), 31.9 (2C atoms), 30.1 (2C atoms), 29.7 (12C atoms), 29.6 (4C atoms), 29.5, 29.4, 29.3 (2C atoms), 28.9 (2C atoms), 26.2, 26.1, 22.7 (2C atoms), 14.1 (2C atoms) (Fig. S2).

3.1.2. IR analysis

The IR characterization of DODTA-Br (**1**) was performed by comparison with literature data of similar compounds [32] and its IR spectra is presented in Fig. 1.

The strong absorptions at 2950, 2915, and 2850 cm^{-1} could be assigned to C–H alkenyl and alkyl stretching, and the strong bands at 1580 1470, and 1160 cm^{-1} to C=C and C-N stretching. The ring torsion motions give specific bands at 720, and 640 cm^{-1} in fingerprint region.

The ESI-MS/MS spectrum in a positive and negative mode of DODTA-Br (**1**) are shown in Figs. S3 and S4. As expected, the peak of the DODTA cation appeared at m/z value 574.6 in the positive ion mode at a concentration of 2.5 ng μL^{-1}.

The latter was also confirmed with the data of the elemental analysis of DODTA-Br (**1**), since the experimentally determined and the calculated values for the C, H, and N contents for the expected molecular formula $C_{38}H_{76}BrN_3$ were in complete agreement: (exp.): C, 65.31; H, 11.38; Br N/A; N, 6.27; (calc.): C, 69.69; H, 11.70; Br, 12.20; N, 6.42.

3.2. Modeling the DODTA-TPB ion pair structure (Associate structure modeling)

The theoretical study presented here focused on analyzing the formation of ionic associates and interionic interactions between DODTA cations and TPB anions.

The interacting ions considered here are characterized by considerable structural differences. The TPB anions are relatively symmetric and rigid, while the DODTA cations contain long alkyl octadecyl chains which are extremely flexible and predefine the existence of numerous conformational isomers. Calculations of the energies of the optimized geometries of all possible conformers would therefore require enormous computational resources. Thus, we have here considered only four conformational isomers of DODTA, which, in our opinion, represent the

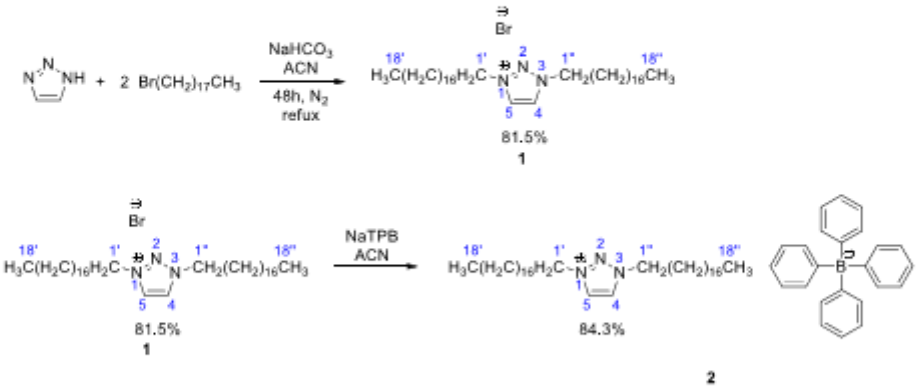

Scheme 1. Reaction scheme of preparation of DODTA–TPB ionophore (**2**) employing bisalkylated ionic salt DODTA –Br 1,3-dioctadecyl-1*H*-1,2,3-triazol-3-ium bromide (**1**).

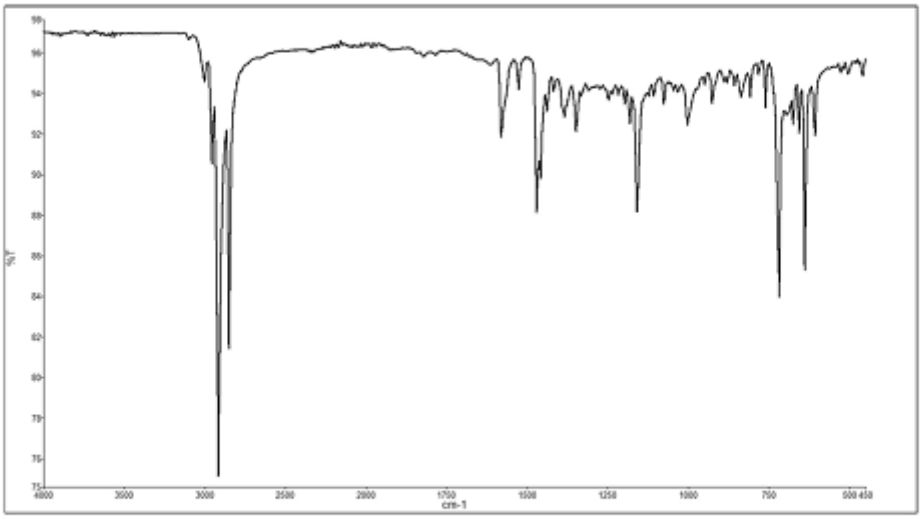

Fig. 1. ATR-FTIR spectra of 1,3-dioctadecyl-1*H*-1,2,3-triazol-3-ium bromide (1).

most considerable structural differences between the conformers. The limited selection of conformers was dictated by the vast number of possible structures arising from free rotation around sigma C–C bonds in the alkyl chains. To significantly reduce the number of isomers considered, we focused on those exhibiting substantial differences in the configuration of the alkyl chains at the points of attachment to the triazolium rings, as this region most significantly influences the electronic structure of the heterocycle. Based on this rationale, we selected conformations that differ in the values of the C5–N1–C1′–C2′ and C4–N3–C1″–C2″ torsional angles, which were chosen to be approximately 90° or 180°. As n-alkanes and straight-chain alkyl groups in their crystalline state typically have all-trans (staggered) conformations, we assumed the same all-trans arrangement for the alkyl chains considered here.

The four DODTA conformers studied here are shown in Fig. 2. The conformers have different torsion angles between the ring and the alkyl chains. It should be highlighted that during the geometry optimization step, conformers 2 and 4 (see Fig. 2c, d) were transformed into conformer 1, which confirmed the higher stability of the latter. The Gibbs free energies of conformer 1 was 3.4 kcal/mol lower than that of conformer 3. Therefore, conformer 1 was considered as a structure of the DODTA cation in our further calculations. The correctness of the

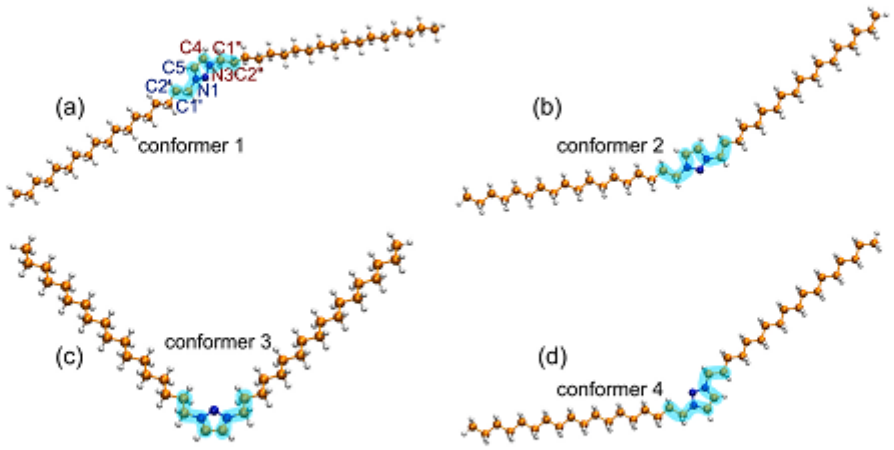

Fig. 2. Four conformers of DODTA considered in this study. The critical torsion angles θ_1(C1′-C2′-N1-C5) and θ_2(C1″-C2″-N3-C4) are highlighted in blue. (a) Conformer 1 is characterized by θ_1 = 82.7° and θ_2 = 88.3°; (b) conformer 2 is characterized by θ_1 = 0.0° and θ_2 = 0.0°; (c) conformer 3 is characterized by θ_1 = 178.8° and θ_2 = 179.0°; and (d) conformer 4 is characterized by θ_1 = 179.0° and θ_2 = 0.0°. (For interpretation of the references to colour in this figure legend, the reader is referred to the web version of this article.)

selected CPCM-B3LYP-D3BJ/6-31G(d) theoretical method was confirmed by the good match of the calculated vibrational modes of the DODTA cation and the experimental infrared (IR) spectrum of DODTA bromide (see Fig. S5 in the electronic supplementary information file). The most significant experimental peaks were assigned to specific vibrations through an automatic vibrational mode relevance determination analysis made with the vibAnalysis code.

The next stage of the study involved modeling the DODTA-TPB ion associate structure. During this step, the most crucial task was to determine the reciprocal locations of the DODTA and TPB ions. An analysis of the ions' electrostatic potential (ESP) isosurfaces was performed to determine the sites with the highest localizations of positive and negative charges (see Fig. 3). The grading of the ESP was done according to the Red-Green-Blue scheme, where the most positive areas of ESP were colored in red and the most negative areas were represented in blue. The areas where the ESP values were close to zero were colored in green. As shown in Fig. 2a, the minima of ESP were located between the phenyl rings (bright blue dots). Thus, minima with ESP values of –4.5 eV were found above the phenyl ring planes and minima with ESP values of –4.9 eV were located closer to the central boron atoms.

On the other hand, in the case of the DODTA cations, ESP maxima were located around the triazolium rings (bright red dots). Maxima above the ring planes were characterized by ESP values of + 5.1 eV, while maxima with higher values of ESP were located around the H–C═C–H fragments of the triazolium rings. The maxima between the two hydrogen atoms were characterized by ESP values of + 5.3 eV; two maxima located closer to the hydrogen atoms had ESP values of + 5.6 eV and two maxima located between the CH ring groups and α-methylene CH_2 group had the highest ESP values of + 5.7 eV. The ESP values monotonically decreased with distance from the positively charged triazolium cycle. For example, starting at the C7 position of the alkyl chain, the ESP values were characterized by almost zero values. An analogous redistribution of positive charges has previously been observed in cetylpyridinium cations [33]. Moreover, the analysis of various types of partial atomic charges also testified to the high concentration of positive charges on the triazolium rings and neighboring methylene groups, whereas the methylene groups that were located further away were almost neutral (see Fig. S6).

To prepare the initial geometry of the DODTA–TPB ion associate, the ions were manually positioned so that their ESP extrema, shown in Fig. 3, were aligned to maximize electrostatic attraction. This prearranged structure was then fully optimized at the CPCM-B3LYP-D3BJ/6-31G(d) level of theory without any symmetry or positional constraints. The optimized geometry of the DODTA–TPB ion associate is shown in Fig. S7. The frontier molecular orbitals were then analyzed to better understand the interionic interactions in the associate (see Fig. 4). The electrostatic attraction between ions does not involve the formation of new covalent bonds or changes in ones existing between the interacting ions; therefore, no significant differences were expected in the molecular orbitals of the associate compared to the molecular orbitals of free ions. It should be highlighted, that the HOMO–1 and HOMO of the associate were identical to the corresponding orbitals of the TPB anion, with marginal differences in energies of –0.15 eV and –0.03 eV, respectively. On the other hand, the LUMO and LUMO + 1 of the associate corresponded to the cation's orbitals, being only slightly higher in energy by + 0.24 eV and + 0.17 eV, respectively. The simultaneous slight decrease of the HOMO energy and increase of the LUMO one supported the favorable association of DODTA and TPB ions.

Frontier molecular orbitals commonly determine the reactivity of DODTA-TPB ion associates. Thus, the analysis of nucleophilic, electrophilic, and radical Fukui functions (see Figs. S8) [34] as local reactivity descriptors clearly indicated that the associate's most reactive sites matched well with the localization of frontier molecular orbital isosurfaces. Fig. 5 shows that the electrophilic Fukui functions, which showed the areas that interacted with the electrophiles most actively, were localized on the carbon atoms at the 1, 2, 4, and 6 positions of the phenyl rings of the TPB anions. On the contrary, the nucleophilic Fukui functions indicated that all five atoms of the DODTA triazolium ring were most reactive under the action of nucleophiles. In the case of radical reagents, the attack was expected to be on carbon atoms in positions 1 and 4 of the TPB phenyl rings and nitrogen atoms of the DODTA triazolium ring.

Another way to analyze interionic interactions involves charge decomposition analysis (CDA), which provides valuable insights into how charges are transferred between the fragments in a complex [35], and in this case, between ions in the associate. The analysis was performed with the Multiwfn software. The donation of electrons from the anions to the cations was equal to only 0.0928e, and the back-donation of electrons from the cations to the anions was equal to 0.0204e. The overlap population between the occupied molecular orbitals was found

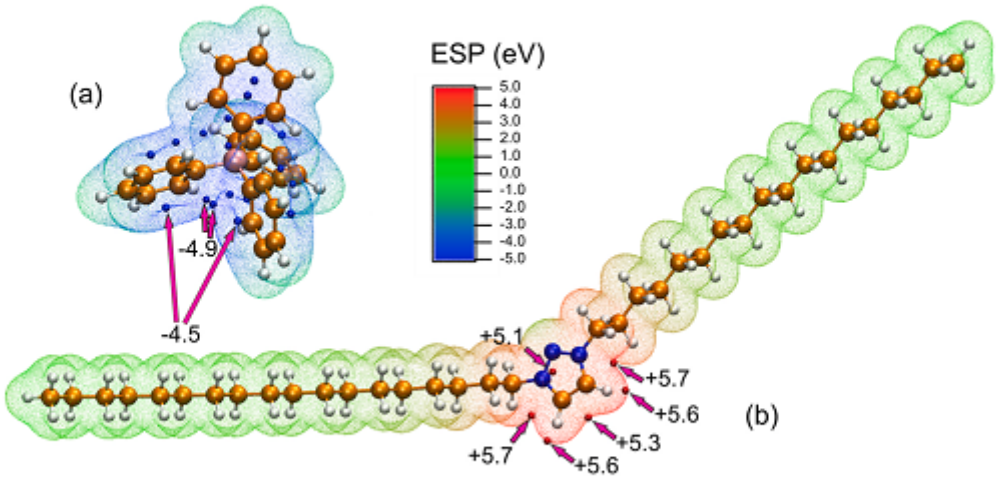

Fig. 3. Electrostatic potential isosurfaces of TPB (a) and DODTA (b). Values are in eV.

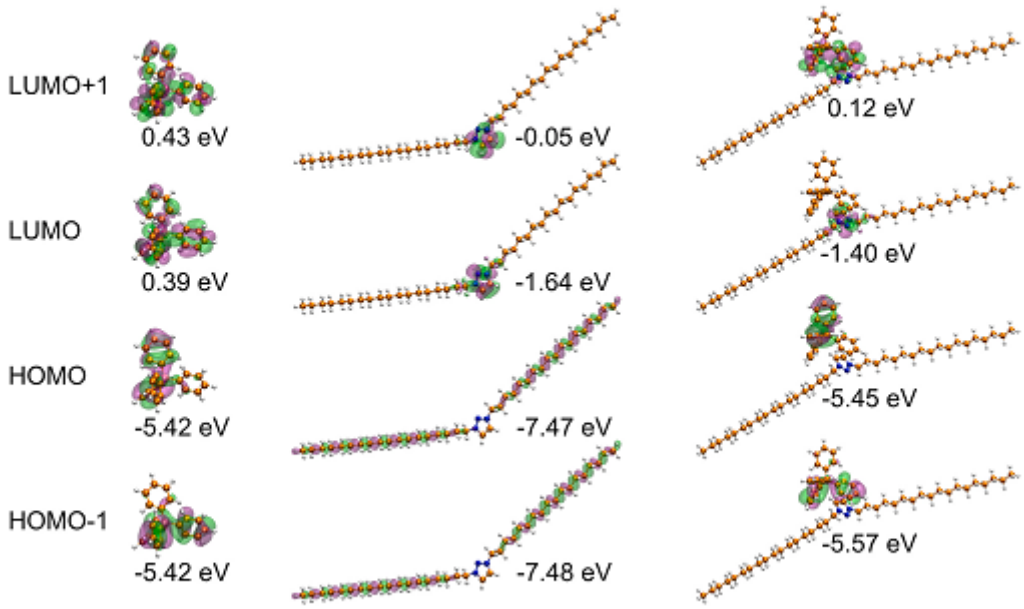

Fig. 4. Frontier (HOMO–1, HOMO, LUMO, and LUMO + 1) molecular orbital isosurfaces of a TPB anion (left), DODTA cation (middle), and the DODTA-TPB associate (right).

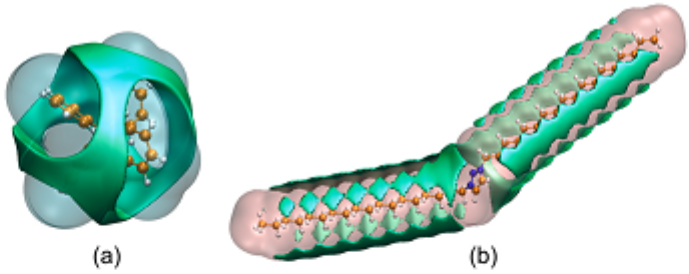

Fig. 5. Van der Waals (vdW) potential isosurfaces (green areas) mapped onto vdW surfaces presented with a 0.001 isovalue of electron density of the TPB anion (blue surface, a) and the DODTA cation (pink surface, b). (For interpretation of the references to colour in this figure legend, the reader is referred to the web version of this article.)

to be equal to –0.1302e; this negative value implies that repulsive effects dominated the overall interaction between the ions' occupied frontier molecular orbitals. Again, relatively small values of electron donations between the ions suggested that the covalent components only played a negligible role in the interionic interactions and that electrostatic interactions were predominant instead.

However, electrostatic interactions are not the only type of interaction that play an important role in the interionic attraction between DODTA and TPB ions. Weak van der Waals (vdW) forces cannot be ignored, especially when analyzing free ions' vdW potentials [36]. The vdW potential isosurfaces of TPB and DODTA are presented in Fig. 5. In the case of the TPB anions, the vdW potential had the most significant impact on the regions between the phenyl rings. In the case of the DODTA cations, the vdW potential had a high impact along the alkyl chains. These findings confirmed that weak interactions would be very structure-dependent since various ion conformations and mutual locations could lead to significant overlaps of regions with high values of vdW potentials.

To analyze the vdW interactions in various associate structures, we generated the molecular dynamics trajectory of the associate in a water solution at 300 K. Modeling was performed at the semiempirical PM7 level of theory combined with the COSMO solvation model. Cuby 4 and MOPAC2016 were used for the simulation. A video of a part of the simulated trajectory can be found in the video supplementary material (VIDEO-S1). Furthermore, the obtained trajectory was analyzed with Multiwfn to generate an average non-covalent interaction isosurface based on promolecular atomic densities (see Fig. 6). The red areas on the isosurface correspond to areas of strong repulsion inside the phenyl rings and between the phenyl rings of the TPB anions. The bright blue areas correspond to regions of strong electrostatic attraction between the

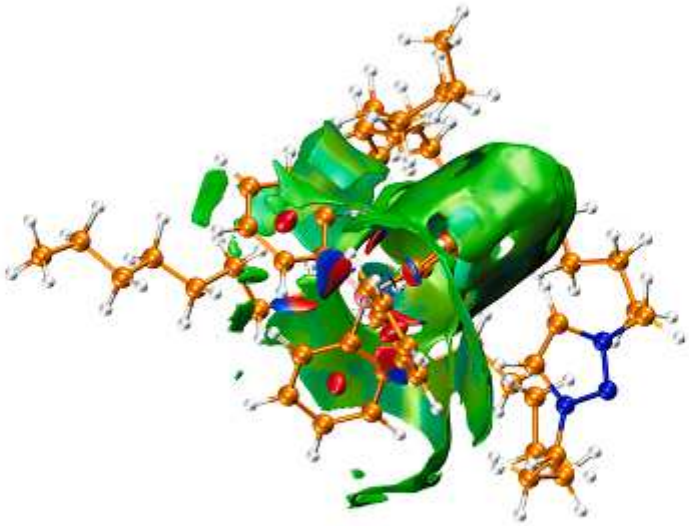

Fig. 6. Average reduced density gradient isosurface based on promolecular atomic densities for the study of non-covalent interionic interactions.

ortho-hydrogen atoms of phenyl rings and the π-system of the neighboring phenyl rings. The largest green area corresponds to weak vdW interionic interactions. This area reproduces the vdW surface of the TPB anions, suggesting that interionic interactions were taking place over the whole surface of the TPB and DODTA ions aided by the various structural conformations of the ions.

3.3. Response characteristics of DODTA-TPB surfactant sensor

To investigate the response properties of the DODTA-TPB surfactant sensor incremental addition of CTAB and CPC in the deionized water was performed. The response mechanism of surfactant sensors based on ionophore and liquid-membrane type membranes to cationic surfactants are described in a modified Nernst equation:

$$E = E^{o} + S \log a_{C.S.}$$

where E represents the electromotive force, E^{o} a constant potential term, S is the slope, and $a_{C.S.}$ is the activity of the selected cationic surfactant.

The response of the surfactant sensor DODTA-TPB to cationic surfactant CTAB and CPC showed high linearity over a wide concentration range. The response results and the statistical calculations including the calculated slope, linear response range, and intercept were shown in Table 1. DODTA-TPB surfactant sensor had a linear response range for CTAB from 7.9×10^{-6} to 7.2×10^{-4} M, with a corresponding slope value of 56.2 mV/ decade of activity, with high linearity ($R2 = 0.9967$), intercept of 312 ± 5 mV and limit of detection (LOD) 7.1×10^{-6} M. The DODTA surfactant sensor showed a linear response range for CPC from 3.2×10^{-6} to 9.2×10^{-4} M, with a corresponding slope value of 58.5 mV/decade of activity, with high linearity ($R^2 = 0.9899$), an intercept of 351 ± 5 mV and LOD 2.9×10^{-6} M.

Table 1
Response characteristics of DODTA-TPB surfactant sensor for cationic surfactants CTAB and CPC.

Parameters	CTAB	CPC
Slope (mV/decade)	56.2 ± 0.3	58.5 ± 0.2
Correlation coefficient (R^2)	0.9967	0.9899
Intercept (mV)	312 ± 5	351 ± 5
Useful linear concentration range (M)	7.9×10^{-6} to 7.2×10^{-4}	3.2×10^{-6} to 9.2×10^{-4}

The interference of common cations was calculated by the fixed interference method (FIM) proposed by IUPAC. The concentrations of solutions of interfering cations were adjusted to 0.01 M. Cationic surfactant CPC was incrementally added to the interfering ion solutions. The calculated K^{Pot}_{Surf} for the response of DODTA-TPB surfactant sensor to Ca^{2+} was 6.1×10^{-4}, for Na^{+}, 4.1×10^{-4} and for Mg^{2+} it was 5.7×10^{-4}. The K^{Pot}_{Surf} values showed a low interfering influence of selected cations on the DODTA-TPB surfactant sensor response.

3.4. Titration of cationic surfactants

A fabricated DODTA-TPB surfactant sensor was used as an end-point indicator for titration of cationic surfactant CPC with the anionic surfactant SDS (4×10^{-3} M) shown in Fig. 7. The response of the DODTA-TPB sensor was a well-defined sigmoidal curve with 357 ± 10 mV signal change. The corresponding first derivative showed a distinguished sharp peak at the expected end-point with a signal dE/dV change of 69.3 ± 1.1 mV/ml.

The standard addition method was used to test recoveries of the prepared DODTA-TPB surfactant sensor. DODTA-TPB surfactant sensor was used as an end-point indicator for the titration of known amounts of cationic surfactants (analytical grade CPC and technical grade Hyamnie 1622), at two concentration levels 50 and 10 μmol, with SDS as a titrant (4×10^{-3} M), shown in Table 2. Calculated recoveries for CPC were 99.92 and 98.80 %, and for Hyamine 1622, 99.84 and 99.50 %, respectively.

DODTA-TPB surfactant sensor was used as an end-point detector of the potentiometric titration of 3 commercial mouth-wash waters containing cationic surfactants. SDS as a titrant (4×10^{-3} M) was used as a counter ion. The results were compared with our previously published and well elaborated DMIC-TPB surfactant sensor. [2] The results were presented in the Table 3.

DODTA-TPB surfactant sensor showed excellent response characteristics and good recoveries for investigated p.a. and technical grade cationic surfactants. With extensive use, it lasted more than 6 months.

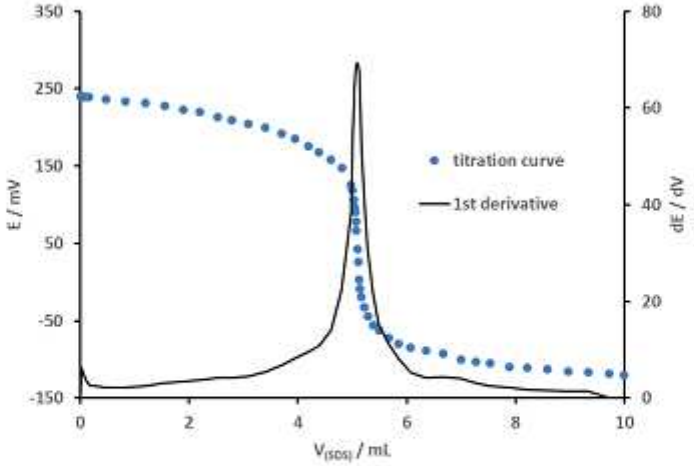

Fig. 7. Potentiometric titration of a cationic surfactant CPC with the anionic surfactant SDS ($4x10^{-3}$ M) and the DODTA-TPB surfactant sensor as an end-point indicator, including the calculated 1st derivative (full line) on secondary y-axis.

Table 2
Potentiometric titration of known amounts of cationic surfactants CPC and technical grade Hyamine 1622 with SDS as a titrant ($4x10^{-3}$ M) with calculated recoveries, with mean values at ± 95 % confidence limits.

Cationic surfactant	Chemical purity	n (Added) / μmol	n (Found)* / μmol	Recovery / %
CTAB	p.a.	50	49.96 ± 0.03	99.92
		10	9.88 ± 0.05	98.80
Hyamine 1622	Technical	50	49.92 ± 0.04	99.84
	grade	10	9.95 ± 0.03	99.50

*five repetitions.

Table 3
Comparison of the DODTA-TPB surfactant sensor and previously published DMIC-TPB surfactant sensors [2] on titration of commercial mouth-wash samples containing cationic surfactant. Potentiometric titrations were performed with SDS as a titrant ($4x10^{-3}$ M).

Sample	DODTA-TPB (%)	DMIC-TPB (%)
1	4.623	4.612
2	4.813	4.812
3	5.015	5.017

4. Conclusions

A new cationic surfactant, 1,3-dioctadecyl-1*H*-1,2,3-triazol-3-ium (DODTA), was synthesized and combined with tetraphenylborate (TPB) to form a functional ion pair. DFT computations confirmed that electrostatic interactions and dispersion forces jointly stabilize the DODTA–TPB associate, without significant charge transfer between the ions. Molecular dynamics simulations reveal that multiple conformations of the DODTA-TPB ion pair remain stable both in aqueous solution and within a modeled PVC-based membrane environment.

The proposed DODTA-TPB surfactant sensor was successfully fabricated and tested on a potentiometric response on two cationic surfactants, CTAB and CPC. DODTA-TPB surfactant sensor showed a linear response range for CTAB from $7.9x10^{-6}$ to $7.2x10^{-4}$ M, with a corresponding slope value of 56.2 mV/ decade of activity; and a linear response range for CPC from $3.2x10^{-6}$ to $9.2x10^{-4}$ M, with a corresponding slope value of 58.5 mV/ decade of activity.

The standard addition method was successfully used to test recoveries of the prepared DODTA-TPB surfactant sensor. DODTA-TPB surfactant sensor was used as an end-point indicator for the titration of analytical grade CPC and technical grade Hyamnie 1622, at two concentration levels 50 and 10 μmol, with SDS as a titrant. Calculated recoveries for CPC were 99.92 and 98.80 %, and for Hyamine 1622 were 99.84 and 99.50 %, respectively.

These results highlight the strong potential of DODTA–TPB as a new standard material for sensitive and accurate quantification of surfactants in liquid samples.

CRediT authorship contribution statement

Nada Glumac: Writing – original draft, Validation, Investigation, Formal analysis, Data curation, Conceptualization. **Maksym Fizer**: Visualization, Software, Formal analysis, Data curation, Conceptualization, Writing – review & editing, Writing – original draft. **Nikola Sakač**: Writing – review & editing, Writing – original draft, Visualization, Validation, Supervision, Resources, Project administration, Methodology, Investigation, Formal analysis, Data curation, Conceptualization. **Dean Marković**: Writing – original draft, Resources, Conceptualization. **Lucija Vrban**: Formal analysis, Data curation. **Robert Vianello**: Writing – original draft, Formal analysis, Data curation. **Bojan Šarkanj**: Writing – original draft, Visualization, Methodology, Investigation, Formal analysis. **Marija Kraševac Sakač**: Writing – original draft, Validation, Methodology, Investigation. **Marija Jozanović**: Writing – review & editing, Writing – original draft, Supervision, Project administration, Methodology, Investigation.

Declaration of competing interest

The authors declare that they have no known competing financial interests or personal relationships that could have appeared to influence the work reported in this paper.

Appendix A. Supplementary data

Supplementary data to this article can be found online at https://doi.org/10.1016/j.molliq.2025.127831.

Data availability

Data will be made available on request.

References

[1] E. Zdrachek, E. Bakker, Potentiometric Sensing, Anal. Chem. 93 (2021) 72–102, https://doi.org/10.1021/acs.analchem.0c04249.

[2] D. Madunić Čačić, M. Sak-Bosnar, O. Galović, N. Sakač, R. Matešić-Puač, Determination of cationic surfactants in pharmaceutical disinfectants using a new sensitive potentiometric sensor, Talanta 76 (2008) 259–264, https://doi.org/10.1016/j.talanta.2008.02.023.

[3] N. Sakač, M. Karnaš, M. Jozanović, M. Medvidović-Kosanović, S. Martinez, J. Macan, M. Sak-Bosnar, Determination of anionic surfactants in real samples using a low-cost and high sensitive solid contact surfactant sensor with MWCNTs as the ion-to-electron transducer, Anal. Methods. 9 (2017) 2305–2314, https://doi.org/10.1039/C7AY00099E.

[4] V. Kumar, R. Suri, S. Mittal, Review on new ionophore species for membrane ion selective electrodes, J. Iran. Chem. Soc. 20 (2023) 509–540, https://doi.org/10.1007/s13738-022-02708-3.

[5] J. Zhai, D. Yuan, X. Xie, Ionophore-based ion-selective electrodes: signal transduction and amplification from potentiometry, Sensors & Diagnostics. 1 (2022) 213–221, https://doi.org/10.1039/D1SD00055A.

[6] M. Cuartero, M. Más-Montoya, M. Soledad García, D. Curiel, J.A. Ortuño, New carbazolo[1,2-a]carbazole derivative as ionophore for anion-selective electrodes: Remarkable recognition towards dicarboxylate anions, Talanta 123 (2014) 200–206, https://doi.org/10.1016/j.talanta.2014.02.022.

[7] N. Sakač, D. Madunić-Čačić, D. Marković, B. Della Ventura, R. Velotta, A. Ptiček Siročić, B. Matasović, N. Sermek, B. Đurin, B. Šarkanj, M. Jozanović, The 1,3-Dioctadecyl-1H-imidazol-3-ium Based Potentiometric Surfactant Sensor for Detecting Cationic Surfactants in Commercial Products, Sensors 22 (2022) 9141, https://doi.org/10.3390/s22239141.

[8] M.K. Abd El-Rahman, H.E. Zaazaa, N.B. Eldin, A.A. Moustafa, Just-Dip-It (Potentiometric Ion-Selective Electrode): An Innovative Way of Greening Analytical Chemistry, ACS Sustain. Chem. Eng. 4 (2016) 3122–3132, https://doi.org/10.1021/acssuschemeng.6b00138.

[9] N. Sakač, D. Madunić-Čačić, M. Karnaš, B. Đurin, I. Kovač, M. Jozanović, The influence of plasticizers on the response characteristics of the surfactant sensor for cationic surfactant determination in disinfectants and antiseptics, Sensors 21 (2021), https://doi.org/10.3390/s21103535.

[10] N. Sakač, D. Madunić-Čačić, D. Marković, L. Hok, R. Vianello, V. Vrček, B. Šarkanj, B. Đurin, B. Della Ventura, R. Velotta, M. Jozanović, Potentiometric Surfactant Sensor for Anionic Surfactants Based on 1,3-dioctadecyl-1H-imidazol-3-ium tetraphenylborate, Chemosensors. 10 (2022), https://doi.org/10.3390/chemosensors10120523.

[11] M. Fizer, O. Fizer, V. Sidey, R. Mariychuk, Y. Studenyak, Experimental and theoretical study on cetylpyridinium dipicrylamide – A promising ion-exchanger for cetylpyridinium selective electrodes, J. Mol. Struct. 1187 (2019) 77–85, https://doi.org/10.1016/j.molstruc.2019.03.067.

[12] O. Fizer, M. Fizer, V. Sidey, Y. Studenyak, Predicting the end point potential break values: A case of potentiometric titration of lipophilic anions with cetylpyridinium chloride, Microchem. J. 160 (2021) 105758, https://doi.org/10.1016/j.microc.2020.105758.

[13] T.C. Hrubec, R.P. Seguin, L. Xu, G.A. Cortopassi, S. Datta, A.L. Hanlon, A.J. Lozano, V.A. McDonald, C.A. Healy, T.C. Anderson, N.A. Musse, R.T. Williams, Altered toxicological endpoints in humans from common quaternary ammonium compound disinfectant exposure, Toxicol. Reports. 8 (2021) 646–656, https://doi.org/10.1016/j.toxrep.2021.03.006.

[14] M.M. Fizer, O.I. Fizer, M.V. Slivka, R.T. Mariychuk, New [1,3]thiazolo[3,2-b][1,2,4]triazol-7-ium cationic surfactant as a stabilizer of silver and gold nanoparticles, Appl. Nanosci. 13 (2023) 5079–5090, https://doi.org/10.1007/s13204-022-02687-0.

[15] M. Fizer, O. Fizer, H. Hryhorka, M. Slivka, M. Šoral, V. Dujnič, M. Kopáčová, V. Puntyo, R. Mariychuk, New 5-alkyl-1,2,4-triazole-3-thione surfactants with antifungal and silver nanoparticles stabilization activity, J. Mol. Liq. 396 (2024) 123943, https://doi.org/10.1016/j.molliq.2023.123943.

[16] A.D. Becke, Density-functional thermochemistry. III. The role of exact exchange, J. Chem. Phys. 98 (1993) 5648–5652, https://doi.org/10.1063/1.464913.

[17] C. Lee, W. Yang, R.G. Parr, Development of the Colle-Salvetti correlation-energy formula into a functional of the electron density, PhysRevB.3 37 (1988) 785–789, https://doi.org/10.1103/PhysRevB.37.785.

[18] S. Grimme, J. Antony, S. Ehrlich, H. Krieg, A consistent and accurate ab initio parametrization of density functional dispersion correction (DFT-D) for the 94 elements H-Pu, J. Chem. Phys. 132 (2010), https://doi.org/10.1063/1.3382344.

[19] S. Grimme, S. Ehrlich, L. Goerigk, Effect of the damping function in dispersion corrected density functional theory, J. Comput. Chem. 32 (2011) 1456–1465, https://doi.org/10.1002/jcc.21759.

[20] M. Garcia-Ratés, F. Neese, Effect of the Solute Cavity on the Solvation Energy and its Derivatives within the Framework of the Gaussian Charge Scheme, J. Comput. Chem. 41 (2020) 922–939, https://doi.org/10.1002/jcc.26139.

[21] F. Neese, F. Wennmohs, U. Becker, C. Riplinger, The ORCA quantum chemistry program package, J. Chem. Phys. 152 (2020), https://doi.org/10.1063/5.0004608.

[22] F. Neese, Software update: The ORCA program system—Version 5.0, WIREs Comput. Mol. Sci. 12 (2022), https://doi.org/10.1002/wcms.1606.

[23] F. Neese, The <scp>SHARK</scp> integral generation and digestion system, J. Comput. Chem. 44 (2023) 381–396, https://doi.org/10.1002/jcc.26942.

[24] T. Lu, F. Chen, Multiwfn: A multifunctional wavefunction analyzer, J. Comput. Chem. 33 (2012) 580–592, https://doi.org/10.1002/jcc.22885.

[25] P. Wu, R. Chaudret, X. Hu, W. Yang, Noncovalent Interaction Analysis in Fluctuating Environments, J. Chem. Theory Comput. 9 (2013) 2226–2234, https://doi.org/10.1021/ct4001087.

[26] J.J.P. Stewart, Optimization of parameters for semiempirical methods VI: more modifications to the NDDO approximations and re-optimization of parameters, J. Mol. Model. 19 (2013) 1–32, https://doi.org/10.1007/s00894-012-1667-x.

[27] A. Klamt, G. Schüürmann, Cosmo,, a new approach to dielectric screening in solvents with explicit expressions for the screening energy and its gradient, J. Chem. Soc., Perkin Trans. 2 (1993) 799–805, https://doi.org/10.1039/P29930000799.

[28] J.J.P. Stewart, MOPAC2016: Stewart Computational Chemistry, Http://Openmopac.Net/. (2016).

[29] J. Rezáč, Cuby: An integrative framework for computational chemistry, J. Comput. Chem. 37 (2016) 1230–1237, https://doi.org/10.1002/jcc.24312.

[30] W. Humphrey, A. Dalke, K. Schulten, VMD: Visual molecular dynamics, J. Mol. Graph. 14 (1996) 33–38, https://doi.org/10.1016/0263-7855(96)00018-5.

[31] F. Teixeira, M.N.D.S. Cordeiro, Improving Vibrational Mode Interpretation Using Bayesian Regression, J. Chem. Theory Comput. 15 (2019) 456–470, https://doi.org/10.1021/acs.jctc.8b00439.

[32] A.A. Jbarah, A. Ihle, K. Banert, R. Holze, The electrosorption of 1,2,3-triazole on gold as studied with surface-enhanced Raman spectroscopy, J. Raman Spectrosc. 37 (2006) 123–131, https://doi.org/10.1002/jrs.1476.

[33] M. Fizer, O. Fizer, Theoretical study on charge distribution in cetylpyridinium cationic surfactant, J. Mol. Model. 27 (2021) 203, https://doi.org/10.1007/s00894-021-04820-2.

[34] R. Pucci, G.G.N. Angilella, Density functional theory, chemical reactivity, and the Fukui functions, Found. Chem. 24 (2022) 59–71, https://doi.org/10.1007/s10698-022-09416-z.

[35] S. Dapprich, G. Frenking, Investigation of Donor-Acceptor Interactions: A Charge Decomposition Analysis Using Fragment Molecular Orbitals, J. Phys. Chem. 99 (1995) 9352–9362, https://doi.org/10.1021/j100023a009.

[36] T. Lu, Q. Chen, van der Waals potential: an important complement to molecular electrostatic potential in studying intermolecular interactions, J. Mol. Model. 26 (2020) 315, https://doi.org/10.1007/s00894-020-04577-0.

Paper II

Glumac, N.; Vrban, L.; Vianello, R.; Jozanović, M.; Fizer, M.; Kraševac Sakač, M.; Velotta, R.; Iannotti, V.; Della Ventura, B.; Cvetnić, M. A DODTA–TPB-Based Potentiometric Sensor for Anionic Surfactants: A Computational Design and Environmental Application. *Chemosensors* 2025, *13*, 321. https://doi.org/10.3390/chemosensors13090321.

chemosensors

MDPI

Article

A DODTA–TPB-Based Potentiometric Sensor for Anionic Surfactants: A Computational Design and Environmental Application

Nada Glumac [1], Lucija Vrban [2], Robert Vianello [2], Marija Jozanović [3,*], Maksym Fizer [4,5], Marija Kraševac Sakač [6], Raffaele Velotta [7], Vincenzo Iannotti [7,8], Bartolomeo Della Ventura [7], Matija Cvetnić [9], Dean Marković [10] and Nikola Sakač [6,*]

1 Međimurske vode d.o.o., 40000 Čakovec, Croatia; nada.glumac@medjimurske-vode.hr
2 Laboratory for the Computational Design and Synthesis of Functional Materials, Division of Organic Chemistry and Biochemistry, Ruđer Bošković Institute, 10000 Zagreb, Croatia; lucija.vrban@irb.hr (L.V.); robert.vianello@irb.hr (R.V.)
3 Department of Chemistry, University of Osijek, 31000 Osijek, Croatia
4 Department of Organic Chemistry, Uzhhorod National University, 88000 Uzhhorod, Ukraine; max.fizer@uzhnu.edu.ua
5 Department of Chemistry, University of Nevada, Reno, NV 89557, USA
6 Faculty of Geotechnical Engineering, University of Zagreb, 42000 Varaždin, Croatia; msakac@gfv.unizg.hr
7 Department of Physics "E. Pancini", Università Di Napoli Federico II, 80126 Napoli, Italy; rvelotta@unina.it (R.V.); viannotti@unina.it (V.I.); bartolomeo.dellaventura@unina.it (B.D.V.)
8 CNR-SPIN, c/o Department of Physics "E. Pancini", Piazzale V. Tecchio 80, 80125 Naples, Italy
9 Faculty of Chemical Engineering and Technology, University of Zagreb, Trg Marka Marulića 19, 10000 Zagreb, Croatia; mcvetnic@fkit.unizg.hr
10 Department of Biotechnology, University of Rijeka, 51000 Rijeka, Croatia; dean.markovic@biotech.uniri.hr
* Correspondence: mjozanovic@kemija.unios.hr (M.J.); nsakac@gfv.unizg.hr (N.S.)

Abstract

Surfactants are used in various washing applications with potential negative environmental and health impacts. The ion-pair 1,3-dioctadecyl-1*H*-1,2,3-triazol-3-ium-tetraphenylborate (DODTA–TPB) was used to fabricate the potentiometric sensor for the quantification of anionic surfactants. The computational analysis of the $DODTA^{+}$–TPB^{-} adduct reveals a dynamic, thermodynamically favorable interaction driven primarily by hydrophobic C–H···π contacts and the flexibility of the C-18 chains, rather than electrostatic or π–π stacking forces. These findings, supported by the MM-PBSA, RDF, and structural analyses, align with broader trends in molecular recognition and provide a foundation for designing advanced ion-pair-based sensors. The sensor showed advanced analytical properties to anionic surfactants with low interfering effects of selected anions. The response of the SDS was investigated in the range from 8.1×10^{-8} M to 1.0×10^{-2} M, with a slope of −59.2 mV and a limit of detection (LOD) of 3.1×10^{-7} M; and DBS was in the range of 8.1×10^{-8} M to 2.5×10^{-3} M with a slope of −57.5 mV and an LOD of 5.9×10^{-7} M. The sensor was tested on potential interfering ions. Potentiometric titrations of technical-grade anionic surfactants had high recovery rates from 100.2 to 100.4%. The recovery test for spiked samples of surface waters was from 94.2 to 96.5%. The sensor was tested on commercial samples containing anionic surfactants, and the results were compared and showed a good agreement with the two-phase titration method.

Keywords: anionic surfactant; potentiometry; sensor; ion-pair; water analysis; DFT

Received: 30 June 2025
Revised: 5 August 2025
Accepted: 11 August 2025
Published: 1 September 2025

Citation: Glumac, N.; Vrban, L.; Vianello, R.; Jozanović, M.; Fizer, M.; Sakač, M.K.; Velotta, R.; Iannotti, V.; Della Ventura, B.; Cvetnić, M.; et al. A DODTA–TPB-Based Potentiometric Sensor for Anionic Surfactants: A Computational Design and Environmental Application. *Chemosensors* 2025, *13*, 321. https://doi.org/10.3390/chemosensors13090321

1. Introduction

Surfactants, or surface-active agents, are amphiphilic compounds that reduce the surface and interfacial tension between different phases (liquid–liquid, liquid–gas, or liquid–solid). They consist of a hydrophilic (water-attracting) head and a hydrophobic (water-repelling) tail, allowing them to interface between polar and non-polar substances. The main properties in physical terms are (i) the critical micelle concentration (CMC)—the concentration at which surfactants self-assemble into micelles, essential for detergency and emulsification; (ii) the surface tension reduction, which enables wetting, foaming, and emulsification; and (iii) self-assembly and micelle formation, where surfactants organize into micelles, bilayers, and vesicles, which is critical for biological membranes and drug delivery. They have a wide range of applications across different industries: detergents such as cleaning and disinfection products, pharmaceuticals and drug delivery, the food industry, the petroleum industry, cosmetics and personal care, nanotechnology and material science, etc. Among them, anionic surfactants dominate global production, making up approximately 70% of the market, with an increasing demand due to their effectiveness in home and personal care products. The expanding consumer market has led to a significant rise in surfactant consumption, with the industry valued at USD 45.57 billion in 2024 and anticipated to reach around USD 76.81 billion by 2034, expanding at a CAGR of 5.36% from 2025 to 2034 [1].

Since they are widely used, surfactants are often emitted into the environment. Classical methods for surfactant analysis are as follows: (1) The two-phase titration method [2], where the titration of an anionic surfactant with a cationic surfactant is performed in the presence of a mixed indicator, like methylene blue/dimidium bromide or tetrabromophenolphthalein ethyl ester, until a color change indicates the end-point. The color of the organic phase will change when the anionic surfactant is completely neutralized by the cationic surfactant. (2) The MBAS (Methylene Blue Active Substances) method [3,4] involves the formation of a colored complex between the anionic surfactant and the cationic dye methylene blue, which is then extracted into an organic solvent, and the blue color intensity is measured by a spectrophotometer. The presented methods are expensive and time-consuming, use toxic chemicals, and produce toxic waste; also, they require skilled personnel [5–9]. On the other hand, chemical sensors for surfactants, especially electrochemical surfactant sensors, are much simpler, cheaper, faster, and easier to operate [10–12]. Usually, the main component of the potentiometric surfactant sensors is the ion-pair, which is incorporated in the polymer (like PVC) enriched with a specific organic plasticizer [13–16]. The ion-pair usually consists of the cationic surfactant and a negatively charged anionic surfactant or some other high-molecular-weight anion, like tetraphenyl borate (TPB)—an organoboron anion consisting of a central boron atom with four phenyl groups [17]. The synthesis and selection of the ion-pair components are of the most importance to the sensing membrane preparation and potentiometric response [18,19]. The ideal ion-pair should have a low water solubility, a low level of leaching from the membrane, and high lipophilicity, and, finally, the sensing membrane itself should have a high resistance [10,20,21]. In this way, the fabricated surfactant sensors could have a high response, extended lifetime, and broad useful concentration range [22–24]. To fulfill all these requirements, new ion-pairs need to be synthesized and investigated through both experiments and chemical modeling [17,25,26].

From a computational perspective, the design and optimization of ion-pairs for potentiometric sensors rely on understanding the molecular interactions that govern their stability and functionality. Computational methods, such as molecular dynamics (MD) simulations and DFT computations, provide detailed insights into the electronic, geometric, and energetic properties of ion-pair adducts. These techniques allow researchers to probe

the dynamic behavior and conformational flexibility of ionophores in condensed phases, while binding free energy estimates provide a thermodynamic basis for assessing the feasibility and reversibility of the ion-pair formation, which are crucial for the sensor performance. By integrating computational modeling with experimental validation, researchers can predict the behavior of ion-pairs under various conditions, guiding the rational design of advanced ionophores with tailored properties for specific analytical applications.

In our recent work, we introduced a novel ion-pair, 1,3-dioctadecyl-1*H*-1,2,3-triazol-3-ium tetraphenylborate (DODTA–TPB), characterized and utilized as the active component in a PVC-based liquid membrane potentiometric sensor for cationic surfactants [27]. The present study extends this research by employing DODTA–TPB as the active molecule in a potentiometric sensor for anionic surfactants, such as sodium dodecyl sulfate (SDS) and sodium dodecyl benzenesulfonate (DBS). Through molecular dynamics (MD) simulations, molecular mechanics Poisson–Boltzmann surface area (MM-PBSA) calculations, and radial distribution function (RDF) analyses, we elucidated the structural and energetic properties of the DODTA–TPB adduct. These computational methods revealed that hydrophobic C–H···π interactions and the flexibility of the C-18 alkyl chains dominate the ion-pair stability, with minimal contributions from electrostatic or π–π stacking forces. These findings guided the design of the sensor by ensuring reversible binding and high lipophilicity, which is critical for the selective detection of anionic surfactants in complex aqueous environments. Compared to traditional methods like the ISO 2271 two-phase titration, which is time-consuming and relies on toxic organic solvents, the DODTA–TPB sensor offers a simpler, faster, and greener alternative, aligning with EU water quality directives (e.g., Directive 2000/60/EC) that emphasize the rapid and sustainable monitoring of pollutants like surfactants. By integrating computational modeling with experimental validation, this study establishes a robust framework for designing next-generation ion-pair-based sensors with an optimized performance for environmental and industrial applications.

2. Materials and Methods

2.1. Chemicals and Materials

Chemicals for organic synthesis were 1,2,3-1*H*-triazole, 1-bromooctadecane, $NaHCO_3$ (Sigma Aldrich, Darmstadt, Germany), and sodium tetraphenylborate (TPB) (Fluka, Buchs, Switzerland). To prepare the sensing membrane, following chemicals were used: o-nitrophenyloctylether (o-NPOE) (Merck, Darmstadt, Germany), high-molecular-weight PVC (Sigma-Aldrich, Hamburg, Germany), and tetrahydrofuran (THF) (Merck, Darmstadt, Germany). Chemicals for potentiometric measurements were anionic surfactants with analytical grade: sodium dodecylsulfate (SDS) and sodium dodecylbenzenesulfonate (DBS) (all from Fluka, Buchs, Switzerland); and anionic surfactants with technical grade were SDS, DBS, and lauryl ether sulfate (LES) (all from Fluka, Buchs, Switzerland). Analytical-grade chemicals for interference measurements were all from Kemika, Zagreb, Croatia. Potentiometric titrations were carried out with titrant 1,3-didecyl-2-methylimidazolium chloride (DMIC) (Merck, Munich, Germany). Anionic surfactant vial test Hach Anionic Surfactants TNTplus Vial Test was purchased from Hach Lange, Berlin, Germany.

Commercial samples were purchased in the local stores. Environmental samples were sampled (500 mL) in spring 2025 at the four locations in north-west Croatia. A lake water sample was taken at Lake Motičnjak, one sample was taken at the hydro accumulation Drava, and two samples of river water were taken at the rivers Mura and Drava. All environmental samples were taken to the lab on the same day and filtered with a standard syringe filter to remove impurities. Next, they were tested on anionic surfactants by a previously published method [9] and fast commercial vial test. No sample pre-treatment of processing was applied, and the samples were spiked and measured on the same day.

Surfactant SDS (50 µmol) was spiked in the environmental samples and titrated with cationic surfactant DMIC in corresponding concentrations.

2.2. Sensor Preparation

The DODA-TPB ion-pair was synthesized according to the fast and green principle procedure described in our previous publication [27]. After the ion-pair synthesis, purification, and characterization, the ion-pair was mixed with a high-molecular-weight PVC, THF, and a plasticizer o-NPOE, as described previously [27]. The sensing membrane was cut into small disk and inserted into the electrode body containing 3 M sodium chloride (Kemika, Zagreb, Croatia). The DODA-TPB surfactant sensor was stored in deionized water after measurements.

2.3. Measuring Setup

The potentiometric response measurements were carried out on dosing device Metrohm 794 Basic Titrino interconnected with Metrohm 781 pH meter (Metrohm, Herisau, Switzerland). Potentiometric titrations were performed by titration device Metrohm 808 Titrando with Tiamo software (Metrohm, Herisau, Switzerland).

2.4. Computational Details

Initial structures of $DODTA^+$, TPB^-, and all model compounds were constructed using MarvinSketch (ChemAxon) [28]. Geometry optimizations were performed using density functional theory (DFT) at the B3LYP/6–31+G(d) level of theory in Gaussian 16 [29]. [REF] Frequency calculations were conducted at the same level to confirm that all optimized structures corresponded to true minima. Electrostatic potential (ESP) calculations were then performed at the HF/6–31G(d) level, and RESP (Restrained Electrostatic Potential) charges were derived for use in molecular mechanics simulations. The General AMBER Force Field (GAFF) was employed for all organic molecules. RESP charges and GAFF atom types were assigned using Antechamber [30]. The resulting input files were processed using ACPYPE to generate GROMACS-compatible topology (.top) and coordinate (.gro) files. Each system was solvated in a truncated octahedral simulation box with a minimum 6 Å buffer between the solute and the box edge, using the TIP3P water model. Counterions were added as needed to maintain charge neutrality. All molecular dynamics simulations were performed using GROMACS 2025.15. Energy minimization was first carried out using the steepest descent algorithm until the maximum force was below 1000 kJ mol^{-1} nm^{-1}. Covalent bonds involving hydrogen atoms were constrained using the LINCS algorithm, allowing a 2 fs integration timestep. Long-range electrostatic interactions were calculated using the particle mesh Ewald (PME) method with a 1.0 nm cutoff. Van der Waals interactions were treated with the same cutoff. Following energy minimization, the systems were equilibrated under NVT and then NPT conditions. Production simulations were performed for 300 ns in the NPT ensemble at 300 K and 1 bar, using the velocity-rescaling thermostat and the c-rescale barostat. Binding free energies were calculated using the Molecular Mechanics Generalized Born Surface Area (MMGBSA) method as implemented in the gmx_MMPBSA package. Representative snapshots were extracted every 1 ns from the final 100 ns of each simulation for statistical averaging. Trajectory analyses included cluster analysis, radial distribution function (RDF) calculations, and interatomic distance measurements, all performed using standard GROMACS tools. Visual inspection and qualitative analysis of key interaction motifs were carried out using PyMOL 3.1.

3. Results and Discussion

3.1. Computational Analysis

The computational analysis was conducted to gain deeper insight into the dynamic behavior of the $DODTA^+$ cation in an aqueous environment and to elucidate the intermolecular interactions that facilitate its adduct formation with the TPB^- anion. This study particularly emphasizes the electronic, geometric, and energetic characteristics that define the DODTA–TPB adduct, employing molecular dynamics (MD) simulations, molecular mechanics Poisson–Boltzmann surface area (MM-PBSA) calculations, and radial distribution function (RDF) analyses. These methods are widely employed in the literature to study ion-pair interactions and molecular recognition processes [31].

Although the $DODTA^+$ molecule possesses a rigid triazole core, it exhibits significant flexibility due to the presence of two unconstrained lipophilic C-18 chains. This inherent molecular flexibility, in contrast to the relatively rigid TPB^- anion, is clearly demonstrated in the calculated root-mean-square deviation (RMSD) analysis (Figure S1). The RMSD, a standard metric in MD simulations, quantifies the structural deviations of $DODTA^+$ over time, reflecting its ability to adopt multiple conformations in the solution. This conformational adaptability is consistent with findings in the literature on amphiphilic molecules, where long alkyl chains enhance flexibility and facilitate interactions with hydrophobic or aromatic partners [32]. As will be detailed in the following discussion, this adaptability of $DODTA^+$ is a key factor in its efficient recognition and interaction with TPB^-, enabling the cation to adjust its geometry to optimize binding.

The adduct formation between $DODTA^+$ and TPB^- is a thermodynamically favorable process; however, the analysis reveals that the adduct is not static and undergoes a continuous association and dissociation over the simulation time. The dynamic nature of the DODTA–TPB ion-pair is evidenced by the fluctuating $B(TPB^-)\cdots N(DODTA^+)$ distances observed during the simulation (Figure S2). These distances exceed 15 Å in some instances, indicating a temporary dissociation, while in approximately 66% of the sampled structures, they remain below 6 Å, suggesting close contact. This behavior aligns with studies on ion-pair dynamics in aqueous media, where weak or reversible interactions lead to a broad distribution of intermolecular distances [33]. Despite this variability, the MM-PBSA calculations indicate that the binding free energy for $DODTA^+$ and TPB^- is exergonic, with a ΔG_{BIND} value of −23.4 kcal mol^{-1}. This negative binding energy confirms the feasibility of the interaction and suggests a delicate balance between adduct stability and reversibility. In the context of sensor applications, this balance is crucial, as it ensures the formation of a stable ion-pair while permitting a reversible dissociation, which is essential for the detection and exchange of other anionic analytes in the solution.

The structural analysis of the representative DODTA–TPB adduct (Figure 1) identifies two predominant types of stabilizing interactions: (1) the π–π stacking between the triazole moiety of $DODTA^+$ and a phenyl ring of TPB^-, and (2) multiple C–H···π interactions between the flexible C-18 chains of $DODTA^+$ and additional phenyl rings in TPB^-. These interactions are consistent with those reported for aromatic systems in aqueous environments, where π–π stacking and C–H···π contacts often drive molecular recognition [34]. The boron–nitrogen separation, measured from the central unsubstituted triazole nitrogen in $DODTA^+$ of 5.2 Å in the representative structure, closely aligns with the radial distribution function (RDF) analysis, which shows a peak at 5.4 Å (Figure 1). The RDF analysis quantifies the probability of finding the boron atom of TPB^- at a given distance from the representative nitrogen atom of $DODTA^+$, confirming the dynamic yet stable nature of the adduct. This consistency supports the validity of the proposed representative structure and highlights the key molecular interactions responsible for the stability and functionality of the DODTA–TPB ion-pair.

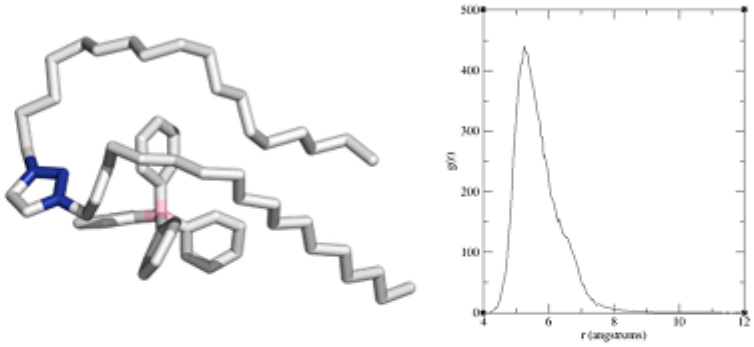

Figure 1. The representative structure of the DODTA–TPB adduct in the aqueous solution (**left**; hydrogen atoms omitted for clarity) as elucidated from the 300 ns molecular dynamics simulations. The corresponding radial distribution function (RDF) graph (**right**) shows the distribution of N(DODTA$^+$)···B(TPB$^-$) distances involving the central unsubstituted triazole nitrogen in the cation, with a peak at 5.4 Å, indicating the preferred intermolecular separation in the adduct.

The close proximity between the boron and nitrogen atoms in the DODTA–TPB ion-pair may initially suggest that electrostatic attraction is the dominant force driving the binding between the opposite charges of DODTA$^+$ and TPB$^-$. However, this hypothesis can be ruled out based on a thorough analysis of atomic charge distributions before and after the adduct formation (Figure S3). The findings indicate that, prior to binding, the triazole unit in DODTA$^+$ only accommodates approximately one-third of the excess positive charge (0.28 |e|), while the remaining charge is distributed within the C-18 alkyl chains. Interestingly, this distribution remains unchanged after the adduct is formed, which suggests that electrostatic interactions do not play a predominant role in stabilizing the adduct. In fact, upon the formation of the DODTA–TPB adduct, only 1% of the total charge density is exchanged between the two components. This is evident from the sum of the atomic charges on DODTA$^+$ and TPB$^-$ within the adduct, which have values of +1.01 |e| and −0.99 |e|, respectively. These results conclusively eliminate electrostatic interactions as a major contributor to the stability of the adduct, suggesting that hydrophobic and dispersion forces dominate the interaction.

Furthermore, we investigated the extent of π···π stacking interactions among the components by analyzing the distances between the center of the mass of the triazole ring in DODTA$^+$ and the phenyl groups in TPB$^-$. Using the commonly accepted 4 Å threshold for π···π interactions [25], we observed that such interactions only occur in 11% of the structures sampled during the molecular dynamics simulations. These relatively low frequencies suggest that π···π interactions between formally charged groups only marginally contribute to the overall adduct formation, further highlighting their limited role in stabilizing the adduct.

In an effort to better understand the contribution of the C–H···π interactions, we examined a series of model cationic components, replacing one or both of the C-18 alkyl chains in DODTA$^+$ with smaller methyl groups (Table 1). This modification allows us to assess the impact of the alkyl chains on the binding affinity. The results revealed that when one C-18 chain was substituted with a methyl group, the binding affinity decreased almost by half (ΔG_{BIND} = −14.9 kcal mol^{-1}). Furthermore, when both C-18 chains were consistently replaced with methyl groups, the binding affinity showed an even more substantial 79% reduction (ΔG_{BIND} = −5.0 kcal mol^{-1}). These findings underscore the critical role of the long alkyl chains in facilitating the binding of TPB$^-$, as their presence significantly enhances

the affinity of the cationic $DODTA^+$ for TPB^-. This observation is further supported by simulations involving a simple alkane, $C_{36}H_{74}$, which is composed of two alkyl chains of equivalent lengths to those in $DODTA^+$. Despite being formally uncharged, $C_{36}H_{74}$ demonstrated a binding affinity for TPB^- that almost surpassed that of the model cationic triazoles, $\Delta G_{BIND} = -12.0$ kcal mol^{-1} (Table 1), thus retaining approximately 51% of the full $DODTA^+$ affinity. This suggests that the hydrophobic interactions provided by the alkyl chains, along with their flexibility, play a dominant role in recognizing and binding TPB^- in the solution.

Table 1. MM-PBSA calculated binding affinities (ΔG_{BIND}, in kcal mol^{-1}) between the TPB^- anion and selected cations following the molecular dynamics simulations in water.

Cation Component	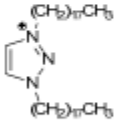	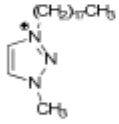	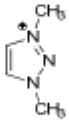	$CH_3(CH_2)_{34}CH_3$
ΔG_{BIND}	−23.4	−14.9	−5.0	−12.0

The dominance of the hydrophobic interactions and the flexibility of the C-18 chains have significant implications for designing potentiometric sensors based on ionophores like $DODTA^+$. The reversible nature of the DODTA–TPB adduct, balanced by a favorable ΔG_{BIND} value, aligns with the requirements for selective ion detection, where stability and exchangeability are key [13]. The limited contribution of electrostatics suggests that future designs could prioritize hydrophobic motifs to enhance the binding affinity, while maintaining a minimal charge dependence to improve selectivity in complex aqueous environments. These insights build on the existing literature, where hydrophobic cavities and flexible alkyl chains are engineered into ionophores to optimize the performance [35].

3.2. Potentiometric Sensor Characterization

The first step in the DODTA-TPB surfactant sensor characterization was to observe the response characteristics of the sensor toward selected anionic surfactants. The sensor response mechanism corresponds to the modified Nernstian equation (Equation (1)):

$$E = E_0 - Sloga_{AS^-} \quad (1)$$

where E is an electrode potential, E_0 is a standard electrode potential, S is the slope of the electrode, and a_{AS^-} is the activity of the investigated surfactant anion.

SDS and DBS were used as model molecules to observe the response characteristics of the DODTA-TPB surfactant sensor to anionic surfactants. The response measurements were carried out in deionized water. The response characteristics of SDS were investigated in the range from 8.1×10^{-8} M to 1.0×10^{-2} M, while the response characteristics of DBS were investigated in the range from 8.1×10^{-8} M to 2.5×10^{-3} M (Figure 2). The potentiometric response for SDS showed a high linear range from 4.1×10^{-7} to 5.1×10^{-3} M, with a slope value of -59.2 ± 0.4 mV/decade of activity and calculated limit of detection (LOD) of 3.1×10^{-7} M. The potentiometric response for DBS had a linear range from 8.1×10^{-7} to 6.1×10^{-4} M, with a slope value of -57.5 ± 0.5 mV/decade of activity and a 5.9×10^{-7} M LOD. Detection limits were estimated according to the IUPAC recommendations [36]. The sensor showed high stability with a signal drift of 3 mV/hour.

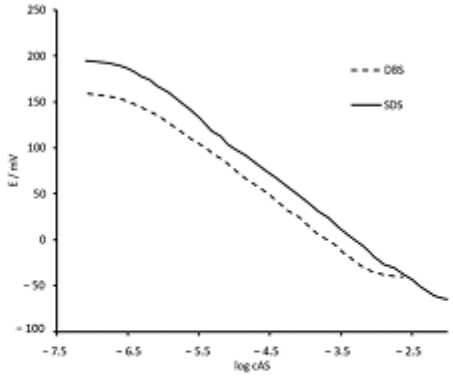

Figure 2. Potentiometric response curves of the DODTA-TPB surfactant sensor to anionic surfactants SDS and DBS in deionized water. The curves were rearranged vertically for clarity.

The comparison with previously published response characteristics of ion-pairs containing TPB as a counter ion showed a good agreement with new DODTA-TPB ion-pair sensing properties to the anionic surfactants DBS and SDS in terms of the linear response range, slope per decade of activity, and LOD (Table 2).

Table 2. Response characteristics of potentiometric surfactants sensors based on different ion-pairs containing anionic TPB counter ion.

AS *	Sensor Characteristic	Ion-Pair				
		New DODTA-TPB	DMIC-TPB [37]	DODI-TPB [25]	DHBI-TPB [38]	DDA-TPB [39]
DBS	LOD (M)	5.9×10^{-7}	6.0×10^{-7}	7.1×10^{-7}	6.1×10^{-7}	2.0×10^{-7}
	Linear response range (M)	8.1×10^{-7}–6.1×10^{-4}	8×10^{-7}–6×10^{-4}	6.3×10^{-7}–3.2×10^{-4}	8.9×10^{-7}–4.1×10^{-3}	2.5×10^{-7}–1.2×10^{-3}
	Slope (mV/decade of activity)	−57.5	−57.8	−59.3	−58.4	−55.3
SDS	LOD (M)	3.1×10^{-7}	3.2×10^{-7}	6.8×10^{-7}	3.2×10^{-7}	2.5×10^{-7}
	Linear response range (M)	4.1×10^{-7}–5.1×10^{-3}	4.0×10^{-7}–5×10^{-3}	5.9×10^{-7}–4.1×10^{-3}	4.6×10^{-7}–5.1×10^{-3}	3.2×10^{-7}–4.6×10^{-3}
	Slope (mV/decade of activity)	−59.2	−59.3	−58.3	−60.1	−58.5

* Anionic Surfactant.

3.3. Interference Study

To observe the influence of potential interfering ions, a series of anions were prepared (Table 3). The concentration of the interfering ion solution was 0.01 M, for each investigated anion. SDS was incrementally added to the interfering ion solution and the DODTA-TPB surfactant sensor potentiometric response was measured. To calculate the interfering influence on potentiometric response, a fixed interference method was used [40]. For all selected anions, the logarithm of the selectivity coefficient was calculated. The DODTA-TPB surfactant sensor showed a high stability and a low influence of investigated interfering anions.

Next, the influence of the pH on the DODTA-TPB surfactant sensor potentiometric response on SDS was investigated. The sensor showed a high stability in the range from pH 3 to 10. Small signal deviations were observed at pH 2 and from pH 11, but still there was no significant influence on the response signal.

Table 3. The calculated selectivity coefficient (logarithm) for selected anions (0.01 M) measured with the DODTA-TPB surfactant sensor for the anionic surfactant SDS.

Interfering Anions	$logK^{pot}_{An^-_L}$
Acetate	−3.72
Benzoat	−3.84
Bromide	−3.21
Borate	−2.98
Chloride	−3.83
Carbonate	−4.14
Dihydrogenphosphate	−4.01
EDTA	−3.84
Fluoride	−3.68
Hydrogen carbonate	−4.02
Hydrogen sulfate	−3.86
Nitrate	−3.93
Sulfate	−4.62

3.4. Potentiometric Titrations of Model and Environmental Samples

For the titration of anionic surfactants SDS (4×10^{-3} M) and DBS (4×10^{-3} M), the cationic surfactant DMIC was used. The chemical reaction is as follows (Equation (2)):

$$An^-_{AS} + Cat^+_{CS} \rightleftarrows An_{AS}Cat_{CS} \quad (2)$$

The An^-_{AS} represents the anionic surfactant (analyte, SDS, or DBS), the Cat^+_{CS} represents the cationic surfactant (titrant, DMIC), and the $An_{AS}Cat_{CS}$ is the low solubility complex, usually manifesting as a white precipitate.

Potentiometric titration curves for the titration of SDS (4×10^{-3} M) and DBS (4×10^{-3} M) with DMIC cationic surfactants (4×10^{-3} M) used as a titrant are presented in Figure 3. The DODTA-TPB surfactant sensor was used as an end-point indicator. The titration curves for the model samples of SDS and DBS had defined and sharp inflection points with a high potential signal change (Figure 3). The end-point could be easily detected.

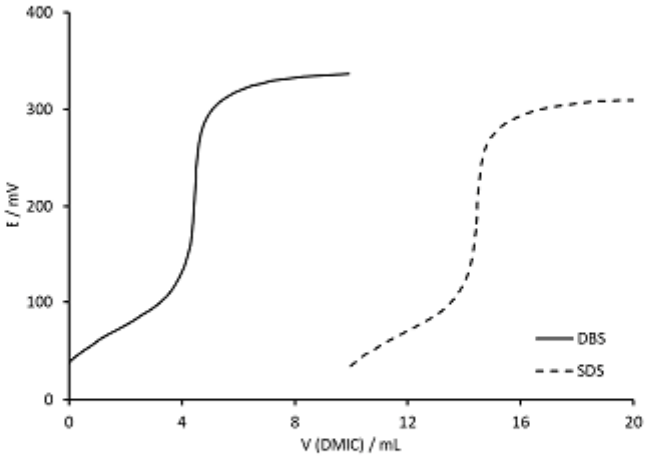

Figure 3. Potentiometric titrations of model samples containing DBS (4×10^{-3} M, full line) and SDS (4×10^{-3} M, dashed line) with DMIC cationic surfactants, DMIC (4×10^{-3} M), and the DODTA-TPB surfactant sensor as the end-point detector. The titration curves were rearranged horizontally for clarity.

To observe the behavior of the DODTA-TPB surfactant sensor in solutions of the technical-grade anionic surfactant, a series of three anionic surfactants (SDS, DBS, and lauryl ether sulfate (LES)) were titrated, with DMIC (4×10^{-3} M) as a titrant. A fixed amount of the technical-grade anionic surfactant was added to the deionized water and titrated by the DODTA-TPB surfactant sensor as an end-point indicator. The titration curves were sigmoidal, with well-defined inflection points. The overall signal change (ΔE) was 301.1 mV for the DBS titration curve and 276.2 mV for the SDS titration curve. Calculated recoveries were from 100.2 to 100.4%, respectively (Table 4).

Table 4. Potentiometric titrations of three technical-grade anionic surfactants with DMIC (4×10^{-3} M) as a titrant and the DODTA-TPB surfactant sensor as an end-point indicator, with mean values at ±95% confidence limits.

Technical-Grade Anionic Surfactant	*w* (Surfactant) */%	*n* (Added)/μmol	*n* (Found) **/μmol	Recovery/%
SDS	91.28 ± 0.31	50	50.21 ± 0.04	100.4
DBS	47.61 ± 0.25	50	50.13 ± 0.09	100.2
LES	28.74 ± 0.12	50	50.11 ± 0.05	100.2

* Average of 5 measurements. ** Average of 5 measurements.

After testing the DODTA-TPB surfactant sensor on model solutions and technical-grade anionic surfactants, six samples of commercial products with declared anionic surfactant contents were used to qualify the amount of anionic surfactants in the samples. Powdered, liquid/gel, and handwashing detergents were purchased from the local store. DMIC (in varying concentrations) was used as a titrant, and the DODTA-TPB surfactant sensor was used as an end-point indicator (Table 5). The titration curves were well defined and sigmoidal, and the end-point could be easily calculated. Calculated values for powdered detergents were 5.83 and 6.74% of anionic surfactants, for handwashing detergents they were 13.85 and 16.41%, and for the liquid/gel detergents they were 2.57 and 2.73% of anionic surfactants. The calculated amounts of anionic surfactants were in agreement with our previous measurements [25]. For the comparison, a two-phase method [2] was used on the same samples. The calculated amounts were in good agreement with the DODTA-TPB sensor.

Table 5. Results for the potentiometric titration of commercial products containing anionic surfactants by the DODTA-TPB surfactant sensor compared with a two-phase titration method. DMIC was used as a titrant.

Commercial Detergents		*w* (ANIONIC SURFACTANT)/%	
		DODTA-TPB	Two-Phase Titration *
Powdered	sample 1	5.83 ± 0.21	5.91
	sample 2	6.74 ± 0.13	7.01
Handwashing	sample 3	13.85 ± 0.56	13.69
	sample 4	16.41 ± 0.06	16.08
Liquid/gel	sample 5	2.57 ± 0.06	2.66
	sample 6	2.72 ± 0.19	2.76

* [2].

The DODTA-TPB surfactant sensor was used as an end-point indicator in the potentiometric titrations of environmental water samples from the following locations in north-west Croatia: one sample of lake water (lake Motičnjak); one sample of hydroaccumulation Drava; and two samples of river water (rivers Mura and Drava). pH values were measured

in all the samples and were in the range from 7.7 to 8.5. All environmental samples were tested on anionic surfactants by a previously published method [37] and fast commercial vial test and showed no anionic surfactants presence in the samples. The anionic surfactant SDS (50 µmol) was spiked in the environmental samples and titrated with DMIC. The recovery results are shown in Table 6. SDS was successfully quantified in all environmental samples, which is a promising result since no matrix interfering effect was observed, and recoveries were in the range from 94.2 to 96.5%.

Table 6. Recoveries for the potentiometric titration of spiked SDS (50 µmol) in environmental samples by the DODTA-TPB surfactant sensor as an end-point indicator. DMIC was used as a titrant.

Sampling Place	Vial Test	Added SDS	Recovery%
River Drava	No A.S. *	50 µmol	96.5%
River Mura	No A.S.	50 µmol	95.8%
Lake Motičnjak	No A.S.	50 µmol	94.2%
Hydro accumulation Drava	No A.S.	50 µmol	94.5%

* A.S.—anionic surfactant.

4. Conclusions

The development of a DODTA-TPB-based potentiometric sensor represents a significant advancement in the detection of anionic surfactants, offering a sensitive, selective, and environmentally friendly alternative to traditional methods. The computational analysis, utilizing molecular dynamics simulations, MM-PBSA calculations, and RDF analyses, elucidated the dynamic and thermodynamically favorable interactions between the $DODTA^+$ cation and TPB^- anion, primarily driven by hydrophobic C–H···π contacts and the flexibility of the C-18 alkyl chains. These findings highlight the limited role of electrostatic and π–π stacking interactions, emphasizing the importance of hydrophobic forces in stabilizing the ion-pair adduct, which is critical for its functionality in sensor applications, thus ensuring stable yet reversible binding with target analytes. The sensor demonstrated excellent near-Nernstian responses for SDS and DBS, with low detection limits and a broad linear response range, making it suitable for both trace-level and high-concentration measurements. Its reliability was further confirmed through the minimal interference from common anions and the consistent performance across a wide pH range.

Practical applications highlighted the sensor's accuracy, with near-quantitative recoveries in technical-grade surfactants and a strong agreement with standard methods in commercial product testing. The environmental analyses of spiked water samples yielded high recovery rates, proving its effectiveness in real water samples. The sensor's simplicity, cost-efficiency, and reduced need for toxic reagents align with the growing demand for sustainable analytical tools. Using the computational insights and practical potentiometric measurements, this work provides a blueprint for designing advanced ion-selective sensors. Future research could expand its use to other surfactant classes or integrate it into portable systems for on-site monitoring, further enhancing its impact on environmental and industrial applications.

Supplementary Materials: The following supporting information can be downloaded at https://www.mdpi.com/article/10.3390/chemosensors13090321/s1: Figure S1: RMSD graphs from the molecular dynamics simulation of the DODTA+ cation (in black) and the TPB– anion (in red) in aqueous solution, showing significantly higher flexibility of the former; Figure S2: Evolution of the distance between the boron atom in TPB– and the nitrogen atoms in DODTA+ during the molecular dynamics simulation, indicating that the DODTA–TPB adduct formation is reversible and in equilibrium with the dissociated components; Figure S3: Charge distribution within the DODTA+ cation and the TPB– anion, either isolated or within the elucidated representative structure of the DODTA–TPB adduct,

as obtained from the NBO analysis at the (SMD)/M06–2X/6–31+G(d) level of theory in water. The specific set of atoms considered for the analysis is denoted by color (red for the cation, blue for the anion) and includes the attached hydrogen atoms. The results reveal that only 1% of the charge density is transferred between the overall components following DODTA–TPB adduct formation.

Author Contributions: Conceptualization, R.V. (Robert Vianello), L.V., N.G., M.J. and N.S.; methodology, M.J., N.S., N.G., R.V. (Robert Vianello), L.V. and M.F.; software, R.V. (Robert Vianello), L.V. and M.F.; validation, N.S., M.J. and N.G.; formal analysis, N.G., R.V. (Robert Vianello), L.V., M.F., M.C., D.M. and M.K.S.; investigation, N.G., M.K.S., N.S. and M.J.; resources, N.G., M.J., N.S., D.M., R.V. (Raffaele Velotta), B.D.V. and V.I.; data curation, N.G., R.V. (Raffaele Velotta), B.D.V.:, V.I. and M.C.; writing—original draft preparation, R.V. (Robert Vianello), L.V., N.G., M.J. and N.S.; writing—review and editing, N.G., M.J., N.S., R.V. (Robert Vianello), M.F., L.V., R.V. (Raffaele Velotta) and V.I.; visualization, N.G., M.K.S., N.S. and M.J.; supervision, N.S. and M.J.; project administration, N.G., M.K.S., N.S. and M.J.; funding acquisition, M.J., N.S., R.V. (Raffaele Velotta), B.D.V., V.I. and D.M. All authors have read and agreed to the published version of the manuscript.

Funding: Part of this work was supported by the Croatian Science Foundation [grant number IP-2020-02-8090].

Institutional Review Board Statement: Not applicable.

Informed Consent Statement: Not applicable.

Data Availability Statement: The data presented in this study are available on request.

Acknowledgments: L.V. and R. Vianello thank the Zagreb University Computing Centre (SRCE) for granting computational resources on the SUPEK supercomputer.

Conflicts of Interest: Nada Glumac was employed by the company Međimurske vode d.o.o. The remaining authors declare that the research was conducted in the absence of any commercial or financial relationships that could be construed as a potential conflict of interest.

References

1. Presedence Research Surfactants Market Size, Share and Trends 2025 to 2034. Available online: https://www.precedenceresearch.com/surfactants-market#:~:text=Report%20Code%20%3A%201728-,Surfactants%20Market%20Size%20and%20Forecast%202025%20to%202034,5.36%25%20from%202025%20to%202034 (accessed on 10 May 2025).
2. *ISO 2271:1989*; Surface Active Agents, Detergents, Determination of Anionic-Active Matter by Manual or Mechanical Direct Two-phase Titration Procedure. ISO: Geneva, Switzerland, 1989.
3. *ISO 7875-1:1996*; Water Quality-Determination of Surfactant-Part 1: Determination of Anionic Surfactants by Measurement of the Methylene Blue Index (MBAS). ISO: Geneva, Switzerland, 1996. Available online: https://www.iso.org/standard/24784.html (accessed on 7 August 2018).
4. Wyrwas, B.; Zgoła-Grześkowiak, A. Continuous flow methylene blue active substances method for the determination of anionic surfactants in river water and biodegradation test samples. *J. Surfactants Deterg.* **2014**, *17*, 191–198. [CrossRef] [PubMed]
5. Yoon, J.H.; Shin, Y.G.; Kirkham, M.B.; Jeong, S.S.; Lee, J.G.; Kim, H.S.; Yang, J.E. A Simplified Method for Anionic Surfactant Analysis in Water Using a New Solvent. *Toxics* **2022**, *10*, 162. [CrossRef] [PubMed]
6. Yoon, J.H.; Shin, Y.G.; Kim, H.S.; Kirkham, M.B.; Yang, J.E. Screening of a Novel Solvent for Optimum Extraction of Anionic Surfactants in Water. *Toxics* **2022**, *10*, 1–13. [CrossRef] [PubMed]
7. Ródenas-Torralba, E.; Reis, B.F.; Morales-Rubio, Á.; De La Guardia, M. An environmentally friendly multicommutated alternative to the reference method for anionic surfactant determination in water. *Talanta* **2005**, *66*, 591–599. [CrossRef]
8. Lengyel, J.; Krtil, J. Radiometric determination of anionic surfactants by two-phase titration method with the use of131I-Rose Bengal as indicator. *J. Radioanal. Nucl. Chem. Lett.* **1986**, *103*, 51–61. [CrossRef]
9. Miller, C.; Bageri, B.S.; Zeng, T.; Patil, S.; Mohanty, K.K. Modified Two-Phase Titration Methods to Quantify Surfactant Concentrations in Chemical-Enhanced Oil Recovery Applications. *J. Surfactants Deterg.* **2020**, 23, 1159–1167. [CrossRef]
10. Zdrachek, E.; Bakker, E. Potentiometric Sensing. *Anal. Chem.* **2021**, 93, 72–102. [CrossRef]
11. Kovács, B.; Csóka, B.; Nagy, G.; Ivaska, A. All-solid-state surfactant sensing electrode using conductive polymer as internal electric contact. *Anal. Chim. Acta* **2001**, *437*, 67–76. [CrossRef]
12. Khedr, A.M.; Abu Shawish, H.M.; Gaber, M.; Abed Almonem, K.I. Potentiometric Determination of Alkyl Dimethyl Hydroxyethyl Ammonium Surfactant by a New Chemically Modified Carbon Past Electrode. *J. Surfactants Deterg.* **2014**, *17*, 183–190. [CrossRef]

13. Bakker, E.; Pretsch, E.; Bühlmann, P. Selectivity of Potentiometric Ion Sensors. *Anal. Chem.* **2000**, *72*, 1127–1133. [CrossRef]
14. Mihali, C.; Vaum, N. Use of Plasticizers for Electrochemical Sensors. In *Recent Advances in Plasticizers*; InTech: London, UK, 2012.
15. Mikhelson, K.N.; Peshkova, M.A. Advances and trends in ionophore-based chemical sensors. *Russ. Chem. Rev.* **2015**, *84*, 555–578. [CrossRef]
16. Kulapina, E.G.; Ovchinskii, V.A. New modified electrodes for the separate determination of anionic surfactants. *J. Anal. Chem.* **2000**, *55*, 169–174. [CrossRef]
17. Sakač, N.; Madunić-Čačić, D.; Marković, D.; Ventura, B.D.; Velotta, R.; Ptiček Siročić, A.; Matasović, B.; Sermek, N.; Đurin, B.; Šarkanj, B.; et al. The 1,3-Dioctadecyl-1H-imidazol-3-ium Based Potentiometric Surfactant Sensor for Detecting Cationic Surfactants in Commercial Products. *Sensors* **2022**, *22*, 9141. [CrossRef]
18. Vladimirova, N.; Puchkova, E.; Dar'in, D.; Turanov, A.; Babain, V.; Kirsanov, D. Predicting the Potentiometric Sensitivity of Membrane Sensors Based on Modified Diphenylphosphoryl Acetamide Ionophores with QSPR Modeling. *Membranes* **2022**, *12*, 953. [CrossRef] [PubMed]
19. Turyshev, E.S.; Kopytin, A.V.; Zhizhin, K.Y.; Kubasov, A.S.; Shpigun, L.K.; Kuznetsov, N.T. Potentiometric quantitation of general local anesthetics with a new highly sensitive membrane sensor. *Talanta* **2022**, *241*, 123239. [CrossRef]
20. Fizer, O.; Fizer, M.; Sidey, V.; Studenyak, Y. Predicting the end point potential break values: A case of potentiometric titration of lipophilic anions with cetylpyridinium chloride. *Microchem. J.* **2021**, *160*, 105758. [CrossRef]
21. Bakker, E.; Bühlmann, P.; Pretsch, E. Carrier-Based Ion-Selective Electrodes and Bulk Optodes. 1. General Characteristics. *Chem. Rev.* **1997**, *97*, 3083–3132. [CrossRef]
22. Kumar, V.; Suri, R.; Mittal, S. Review on new ionophore species for membrane ion selective electrodes. *J. Iran. Chem. Soc.* **2023**, *20*, 509–540. [CrossRef]
23. Cuartero, M.; Más-Montoya, M.; Soledad García, M.; Curiel, D.; Ortuño, J.A. New carbazolo[1,2-a]carbazole derivative as ionophore for anion-selective electrodes: Remarkable recognition towards dicarboxylate anions. *Talanta* **2014**, *123*, 200–206. [CrossRef]
24. Krivačič, S.; Speck, A.; Kassal, P.; Bakker, E. Towards mass-production of ion-selective electrodes by spotting: Optimization of membrane composition and real-time tracking of membrane drying. *Sens. Actuators B Chem.* **2025**, *423*, 136759. [CrossRef]
25. Sakač, N.; Madunić-Čačić, D.; Marković, D.; Hok, L.; Vianello, R.; Vrček, V.; Šarkanj, B.; Đurin, B.; Della Ventura, B.; Velotta, R.; et al. Potentiometric Surfactant Sensor for Anionic Surfactants Based on 1,3-dioctadecyl-1H-imidazol-3-ium tetraphenylborate. *Chemosensors* **2022**, *10*, 523. [CrossRef]
26. Abd El-Rahman, M.K.; Zaazaa, H.E.; Eldin, N.B.; Moustafa, A.A. Just-Dip-It (Potentiometric Ion-Selective Electrode): An Innovative Way of Greening Analytical Chemistry. *ACS Sustain. Chem. Eng.* **2016**, *4*, 3122–3132. [CrossRef]
27. Glumac, N.; Fizer, M.; Sakač, N.; Marković, D.; Vrban, L.; Vianello, R.; Šarkanj, B.; Sakač, M.K.; Jozanović, M. Study of a 1,3-dioctadecyl-1H-1,2,3-triazol-3-ium cation for potentiometric surfactants sensing applications. *J. Mol. Liq.* **2025**, *432*, 127831. [CrossRef]
28. Cherinka, B.; Andrews, B.H.; Sánchez-Gallego, J.; Brownstein, J.; Argudo-Fernández, M.; Blanton, M.; Bundy, K.; Jones, A.; Masters, K.; Law, D.R.; et al. Marvin: A Tool Kit for Streamlined Access and Visualization of the SDSS-IV MaNGA Data Set. *Astron. J.* **2019**, *158*, 74. [CrossRef]
29. Frisch, M.J.; Trucks, G.W.; Schlegel, H.B.; Scuseria, G.E.; Robb, M.A.; Cheeseman, J.R.; Scalmani, G.; Barone, V.; Petersson, G.A.; Nakatsuji, H.; et al. *G16_C01 2016, Gaussian 16, Revision C.01*; Gaussian Inc.: Wallin, UK, 2016.
30. Wang, J.; Wang, W.; Kollman, P.A.; Case, D.A. Automatic atom type and bond type perception in molecular mechanical calculations. *J. Mol. Graph. Model.* **2006**, *25*, 247–260. [CrossRef] [PubMed]
31. Genheden, S.; Ryde, U. The MM/PBSA and MM/GBSA methods to estimate ligand-binding affinities. *Expert Opin. Drug Discov.* **2015**, *10*, 449–461. [CrossRef]
32. Israelachvili, J.N. *Intermolecular and Surface Forces*; Elsevier: Amsterdam, The Netherlands, 2011; ISBN 9780123751829.
33. Marcus, Y.; Hefter, G. Ion Pairing. *Chem. Rev.* **2006**, *106*, 4585–4621. [CrossRef] [PubMed]
34. Meyer, E.A.; Castellano, R.K.; Diederich, F. Interactions with Aromatic Rings in Chemical and Biological Recognition. *Angew. Chem. Int. Ed.* **2003**, *42*, 1210–1250. [CrossRef] [PubMed]
35. Bühlmann, P.; Chen, L.D. Ion-Selective Electrodes With Ionophore-Doped Sensing Membranes. In *Supramolecular Chemistry*; John Wiley and Sons: Hoboken, NJ, USA, 2012.
36. Guilbault, G.G.; Durst, R.A.; Frant, M.S.; Freiser, H.; Hansen, E.H.; Light, T.S.; Pungor, E.; Rechnitz, G.; Rice, N.M.; Rohm, T.J.; et al. Recommendations for nomenclature of ion-selective electrodes. *Pure Appl. Chem.* **1976**, *48*, 127–132. [CrossRef]
37. Madunić-Čačić, D.; Sak-Bosnar, M.; Samardžić, M.; Grabarić, Z. Determination of anionic surfactants in industrial effluents using a new highly sensitive surfactant-selective sensor. *Sens. Lett.* **2009**, *7*, 50–56. [CrossRef]
38. Sakač, N.; Madunić-Čačić, D.; Marković, D.; Hok, L.; Vianello, R.; Šarkanj, B.; Đurin, B.; Hajdek, K.; Smoljan, B.; Milardović, S.; et al. Potentiometric Surfactant Sensor Based on 1,3-Dihexadecyl-1H-benzo[d]imidazol-3-ium for Anionic Surfactants in Detergents and Household Care Products. *Molecules* **2021**, *26*, 3627. [CrossRef] [PubMed]

39. Samardžić, M.; Galović, O.; Petrušić, S.; Sak-Bosnar, M. The Analysis of Anionic Surfactants in Effluents Using a DDA-TPB Potentiometric Sensor. *Int. J. Electrochem. Sci.* **2014**, *9*, 6166–6181. [CrossRef]
40. Buck, R.P.; Lindner, E. Recomendations for nomenclature of ion-selective electrodes (IUPAC recommendations 1994). *Pure Appl. Chem.* **1994**, *66*, 2527–2536. [CrossRef]

Paper III

Glumac, N.; Momčilović, M.; Kramberger, I.; Štraus, D.; Sakač, N.; Kovač-Andrić, E.; Đurin, B.; Kraševac Sakač, M.; Đambić, K.; Jozanović, M. Potentiometric Surfactant Sensor with a Pt-Doped Acid-Activated Multi-Walled Carbon Nanotube-Based Ionophore Nanocomposite. *Sensors* 2024, *24*, 2388. https://doi.org/10.3390/s24082388.

sensors

MDPI

Article

Potentiometric Surfactant Sensor with a Pt-Doped Acid-Activated Multi-Walled Carbon Nanotube-Based Ionophore Nanocomposite

Nada Glumac [1], Milan Momčilović [2], Iztok Kramberger [3], Darko Štraus [3], Nikola Sakač [4,*], Elvira Kovač-Andrić [5], Bojan Đurin [6], Marija Kraševac Sakač [7], Kristina Đambić [5] and Marija Jozanović [5,*]

[1] Međimurske Vode D.O.O., 40000 Čakovec, Croatia; nada.glumac@medjimurske-vode.hr
[2] Faculty of Sciences and Mathematics, University of Niš, 18000 Niš, Serbia; milan.momcilovic@pmf.edu.rs
[3] Faculty of Electrical Engineering and Computer Science, University of Maribor, 2000 Maribor, Slovenia; iztok.kramberger@um.si (I.K.); darko.straus@um.si (D.Š.)
[4] Faculty of Geotechnical Engineering, University of Zagreb, 42000 Varaždin, Croatia
[5] Department of Chemistry, University of Osijek, 31000 Osijek, Croatia; eakovac@kemija.unios.hr (E.K.-A.); kdjambic@gmail.com (K.Đ.)
[6] Department of Civil Engineering, University North, 42000 Varaždin, Croatia; bdjurin@unin.hr
[7] Faculty of Chemical Engineering and Technology, University of Zagreb, 10000 Zagreb, Croatia; mkrasevac@fkit.hr
* Correspondence: nsakac@gfv.unizg.hr (N.S.); mjozanovic@kemija.unios.hr (M.J.)

Abstract: Two new surfactant sensors were developed by synthesizing Pt-doped acid-activated multi-walled carbon nanotubes (Pt@MWCNTs). Two different ionophores using Pt@MWCNTs, a new plasticizer, and (a) cationic surfactant 1,3-dihexadecyl-1H-benzo[d]imidazol-3-ium-DHBI (Pt@MWCNT-DHBI ionophore) and (b) anionic surfactant dodecylbenzenesulfonate-DBS (Pt@MWCNT-DBS ionophore) composites were successfully synthesized and characterized. Both surfactant sensors showed a response to anionic surfactants (dodecylsulfate (SDS) and DBS) and cationic surfactants (cetylpyridinium chloride (CPC) and hexadecyltrimethylammonium bromide (CTAB)). The Pt@MWCNT-DBS sensor showed lower sensitivity than expected with the sub-Nernstian response of ≈23 mV/decade of activity for CPC and CTAB and ≈33 mV/decade of activity for SDS and DBS. The Pt@MWCNT-DHBI surfactant sensor had superior response properties, including a Nernstian response to SDS (59.1 mV/decade) and a near-Nernstian response to DBS (57.5 mV/decade), with linear response regions for both anionic surfactants down to ≈2×10^{-6} M. The Pt@MWCNT-DHBI was also useful in critical micellar concentration (CMC) detection. Common anions showed very low interferences with the sensor. The sensor was successfully employed for the potentiometric titration of a technical grade cationic surfactant with good recoveries. The content of cationic surfactants was measured in six samples of complex commercial detergents. The Pt@MWCNT-DHBI surfactant sensor showed good agreement with the ISE surfactant sensor and classical two-phase titration and could be used as an analytical tool in quality control.

Keywords: potentiometric surfactant sensor; metal-doped MWCNT; surfactants; carbon nanocomposite; sensor

Citation: Glumac, N.; Momčilović, M.; Kramberger, I.; Štraus, D.; Sakač, N.; Kovač-Andrić, E.; Đurin, B.; Kraševac Sakač, M.; Đambić, K.; Jozanović, M. Potentiometric Surfactant Sensor with a Pt-Doped Acid-Activated Multi-Walled Carbon Nanotube-Based Ionophore Nanocomposite. *Sensors* 2024, *24*, 2388. https://doi.org/10.3390/s24082388

Academic Editor: Antonios Kelarakis

Received: 10 March 2024
Revised: 27 March 2024
Accepted: 8 April 2024
Published: 9 April 2024

1. Introduction

Surfactants are organic molecules with the properties of lowering the surface tension of water. Usually, they consist of hydrophilic heads and hydrophobic tails rich in carbohydrates. There are four main types of surfactants: anionic, cationic, amphoteric, and nonionic [1]. They are usually used in everyday life and the industry as detergents for washing, cleaning (anionic), and disinfection (cationic). The global surfactant market is constantly growing. From a medical point of view and life standard, this is positive, but from

an environmental and health standpoint, this is a challenge. Surfactants have a negative influence on the environment since they disintegrate cells, prevent oxygen exchange, etc.; they irritate the skin and can cause other health issues. For this reason, it is important to monitor the water constantly and increase quality control during detergent production. Classical methods of surfactant detection include two-phase titration and the MBAS method [2,3]. Both methods are time-consuming, require skilled experts, have a lack of reproducibility, and are in contrast to the principles of green chemistry (since they require toxic organic solvents for extraction). Other more common instrumental methods are chromatography methods like Size-Exclusion Chromatography [4], Ion-Exchange Chromatography [5], HPLC [6], and Gas Chromatography [7]. These methods offer reproducibility but require skilled personnel and are expensive to perform and operate.

To overcome all these issues in surfactant analysis, chemical sensors could be a fast, reliable, and easy-to-use strategy. Surfactant sensors based on liquid-type membranes are the most common. PVC is mixed with the selected plasticizer in a ratio of 1:2 [8]. This composition acts like a solvent for the ionophore (usually 1%). The ionophore is an ion pair usually made of a large cationic surfactant and an oppositely charged lipophilic ion. The most important part of the sensor membrane is the ionophore. Recent advances in liquid membrane-type ion-selective electrodes (ISE) for surfactants offer the use of new molecules for ion-pair synthesis and the use of nanomaterials to improve sensor characteristics [9–11]. Nanomaterials can be chemically bound to the ion pair. On the other hand, an inclusion complex with an ion pair or charged surfactant can also act as an ionophore [12–14]. An example of the latter is surfactant-selective electrochemical sensors based on single-walled carbon nanotubes (SWCNTs), where CTAB and SDS, adsorbed to the SWCNTs, act as ionophores [15]. In this study, two electrodes were fabricated: CTAB-SWCNT and SWCNT-SDS. The proposed sensors exhibited a Nernstian response of 59.5 mV/decade of activity for SDS and a near-Nernstian response of 57.2 mV/decade of activity for CTAB over a wide concentration range.

The electrochemical characteristics of electrodes depend significantly on their surface properties. The rate of electron transfer can be notably enhanced by the surface functional groups which contain oxygen. Carbon nanotubes (CNTs) exhibit two distinct surface regions due to their specific structures: sidewalls and ends. The defect-free structure of intact nanotubes is similar to the basal planes of pyrolytic graphite. However, cap regions may be potentially more reactive due to a higher curve strain compared to the sidewall. The treatment of carbon nanotubes by physical or chemical means to open their ends generates various oxygen-containing groups, resembling the properties of edge sites on basal planes of pyrolytic graphite [16]. Electrochemical sensors containing multi-walled CNTs have shown superior properties in terms of functional surfaces, small dimensions, great chemical stability, good conductivity, a modifiable sidewall and great mechanical strength, sensitivity, a broad potential window, and low background current [17].

The use of carbon-based nanomaterials in electrochemical sensor development was improved by metal-doped nanomaterials, like metal-doped carbon nanotubes (CNTs) [10,18,19]. This resulted in a conductivity increase, which caused a faster response time and extended operating range [20]. When used in potentiometric sensors, metal-doped nanomaterials offer several advantages as follows: enhanced sensitivity, improved selectivity, a wider detection range, faster response time, improved stability, reduced fouling, and could result in better miniaturization and integration [10,21–25]. The MWCNTs/Fe-Co doped nanocomposite was used for the potentiometric determination of sulpiride in real water samples. Using the metal-doped MWCNTs resulted in many advantages, such as enhanced charge transfer and sensitivity, fast response time, and increased selectivity; the detection limits were 7.6×10^{-7} M [21]. The combined presence of carbon nanotubes with their excellent electron-transfer capacity and platinum Pt, which possesses the best catalytic activity among all pure metals and remains the most frequently used catalyst in a variety of applications, can lead to remarkable synergistic effects. For instance, MWCNTs decorated with Pt nanoparticles showed excellent features in the sensor for monitoring hydrogen peroxide

concentrations [17]. Platinum nanoparticles are more often employed and supported onto carriers rather than being used separately. This is because they can easily agglomerate or deactivate while supporting them onto carriers enhances their stability and durability [26]. Also, in the hybrid version, the surface area available for electrochemical reactions is much higher; the dispersion of nanoparticles is uniform and supports MWCNTs, which can facilitate the adsorption of reactant molecules onto the electrode's surface. MWCNTs can alter the electronic structure and chemical environment of Pt nanoparticles, thereby allowing for the tuning of their activity and selectivity, which is the case in numerous reports dealing with this matter [27].

In this paper, we synthesized Pt-doped MWCNTs, which were used for the fabrication of two ionophores, (a) Pt@MWCNT-DHBI and (b) Pt@MWCNT-DBS ionophores. These ionophores were used, together with a new Elvaloy 742 plasticizer, to fabricate two sensing membrane nanocomposites for potentiometric applications in surfactant analysis. Platinum was selected since it offers high conductivity and chemical stability. The sensors were characterized, and the selected sensor was successfully tested on technical grade and commercial product samples. The presented sensing platform featured advantages like fast and low-cost preparation, high stability and sensitivity, and a wide linear dynamic range. Also, this electrochemical setup for the effective determination of surfactant concentrations can be employed as a part of portable devices for on-site use. In addition to the technical improvement of the prepared composite material, there is a significant saving in the costs of applying platinum in such a highly dispersed version instead of pure metal.

2. Materials and Methods

2.1. Chemicals

Potentiometric measurements were carried out for the following anionic surfactants: sodium salts SDS—dodecylsulfate and DBS—dodecylbenzenesulfonate (Fluka, Buchs, Switzerland), cationic surfactants Hyamine 1622—benzethonium chloride, CPC—cetylpyridinium chloride, and CTAB—hexadecyltrimethylammonium bromide (Merck, Munich, Germany). The pH was adjusted using corresponding amounts of NaOH and HCl (all from Kemika, Zagreb, Croatia). HNO_3, H_2SO_4, H_2PtCl_6, and $NaBH_4$ were used for the doping process (all from Kemika, Zagreb, Croatia).

For the preparation of the sensing membrane nanocomposite, a high molecular weight PVC (Sigma Aldrich, Taufkirchen, Germany) and plasticizer Elvaloy 742 (DuPont, Wilmington, DE, USA) were used.

For interference measurements, the most common interfering cations were used, such as NH_4^+, Ca^{2+}, Na^+, Mg^{2+}, and $C_8H_{20}N^+$ (Merck, Munich, Germany).

2.2. Pt-Doped MWCNT Synthesis

For the sake of doping with platinum, 150 mg of the activated MWCNTs were suspended in the mixture containing 10 mL of ethanol and 10 mL of deionized water and sonicated for 10 min. Then, 0.5 mL of the aqueous solution of H_2PtCl_6 (160 g/L) was introduced and sonicated for another 5 min. The reduction in Pt ions to their elemental state was performed by the addition of 60 mg of $NaBH_4$ previously dissolved in 20 mL of deionized water. Platinum doping effects were confirmed by our previous study [28]. After 24 h, probes were filtrated on the Buchner funnel with copious amounts of deionized water, dried, and Pt-doped acid-activated MWCNTs were produced according to the following procedure. For the purpose of chemical activation, 500 mg of MWCNTs (Merck, Munich, Germany) was heated at 50 °C with 20 mL of the mixture of concentrated acids (HNO_3:H_2SO_4 = 1:3) under reflux for 210 min. Activated MWCNTs were rinsed at the Buchner funnel with at least 1 L of deionized water, then dried for a couple of hours, homogenized, and kept in a glass cuvette for further procedure. This step is crucial for the introduction of hydroxyl functional groups in the structure of MWCNT.

2.3. Pt@MWCNT-DHBI Ionophore Production

The 1,3-dihexadecyl-1H-benzo[d]imidazol-3-ium (DHBI) cationic surfactant synthesis was described in our previous paper [29]. The synthesis of the ionophore based on carbon nanotubes' complex with a cationic surfactant was presented for the first time recently [15]. This ionophore was used for surfactant selective electrochemical sensor fabrication. In this work, we performed a modification of this protocol to enhance the Pt@MWCNT and cationic surfactant interaction and the inclusion of complex formation. In total, 5 mL of hexane was added to 0.05 g of MWCNT and stirred for 24 h. This was carried out to increase the hydrophobicity of the inner cavity of the Pt@MWCNT and enhance the inclusion of complex formation. Next, the Pt@MWCNTs were left to dry at room temperature. After this, 2 mL of the 5×10^{-4} M solution of DHBI-Br was added to the Pt-doped MWCNTs and stirred for 24 h. After filtration, the precipitate was washed with ultrapure water. Next, the precipitate dried at 80 °C. The prepared Pt@MWCNT-DHBI ionophore was ready for further processing.

2.4. Pt@MWCNT-DHBI Surfactant Sensor Fabrication

The sensor membrane nanocomposite was fabricated by mixing 3 mg of Pt@MWCNT-DHBI ionophore with 25 mL of THF (Fluka, Buchs, Switzerland) and 120 mg of high molecular weight PVC. Then, 180 mg of the Elvaloy 742 plasticizer was added and stirred by ultrasound for a few minutes. The cocktail was poured into a glass ring mold and left for 24 h to dry. The membrane was cut into small discs and one of these discs was mounted in the Phillips electrode body IS-561 (Glasblaeserei Moeller, Zurich, Switzerland) filled with 3 M of potassium chloride as an inner filling solution. The sensor was prepared and ready to use. The sensor was stored in deionized water between the measuring intervals.

2.5. Instrumentation

The distribution of Pt nanoparticles on the MWCNTs' was examined using high-resolution transmission electron microscopy (HR-TEM) with the JEOL JEM-F200 instrument (JEOL, Tokyo, Japan).

The Pt@MWCNT and Pt@MWCNT-DHBI surfactant sensors were characterized by the Shimadzu IR solution 1.30 FTIR-8400 S infrared spectrophotometer (Shimadzu, Kyoto, Japan). For response, interference, and pH measurement, a Metrohm 794 Basic Titrino with the Metrohm 781 pH meter (Metrohm, Herisau, Switzerland) was used. For titrations, a Metrohm 808 Titrando (Metrohm, Herisau, Switzerland) was employed. The Ag/AgCl reference electrode was used in all measurements. The membrane resistance was measured by the UT15B Max True RMS Digital Multimeter (Uni-Trend Technology EU GmbH, Augsburg, Germany).

2.6. Response Procedure

Potentiometric response measurements were carried out by incrementally adding the selected cationic (CPC, CTAB) or anionic (SDS, DBS) surfactant to the fixed amount of deionized water. To reach the logarithmic activity range from approximately −2 to −7, the selected concentrations were 4×10^{-3} M and 4×10^{-4} M.

In order to investigate the interferences from selected anions, including chlorides, carbonates, nitrates, acetates, sulfates, borates, EDTA, dihydrogenphosphates, hydrogen carbonates, and hydrogen sulfates (all chemicals from Kemika, Zagreb, Croatia), tests were performed by incrementally adding SDS in the 0.01 M interfering ion solution.

2.7. Titration Procedure

During potentiometric titrations, the dynamic equivalent point titration (DET) mode with a signal drift of 5 mV/min was used. At higher concentrations, the waiting time was 15 s. To reach the signal stabilization at lower concentrations, a 30 s waiting time was used.

For titrations of the technical grade cationic surfactant Hyamine 1622 (4×10^{-3} M), a corresponding concentration of SDS was used (4×10^{-3} M).

For titrations of commercial products containing anionic surfactants, variable concentrations of CPC were used.

After each measurement, the surfactant sensor was washed with deionized water.

3. Results

3.1. TEM Characteristics of Pt@MWCNT

The representative structure of the Pt@MWCNTs analyzed by Transition Electron Microscopy is illustrated in Figure 1. An effective dispersion and deposition of Pt nanoparticles onto the CNT support can be seen in Figure 1a without evidence of filling the interior of the MWCNT with Pt. A higher magnification, as obtained on the TEM image in Figure 1b, reveals that Pt nanoparticles tend to agglomerate, forming clusters with an average diameter of approximately 10 nm. It is noteworthy that Pt nanoparticles firmly adhere to the surface of nanotubes, as no detached particles were observed. In the HRTEM image depicted in Figure 1c, a cluster of nanoparticles is visible, with a measured D-space of around 0.225 nm, corresponding to the spacing of (111) planes. The Selected Area Electron Diffraction (SAED) patterns of the Pt nanoparticles (Figure 1d) are indexed to three primary planes, (111), (220), and (222), indicating the random orientation of the Pt nanoparticles.

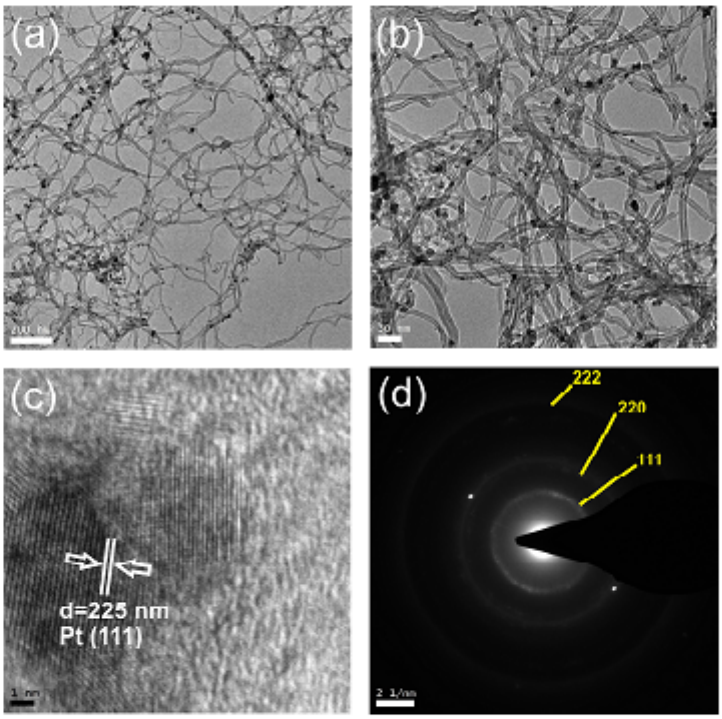

Figure 1. TEM image of Pt-doped MWCNTs: **(a,b)** at different magnifications, **(c)** HRTEM image showing a cluster of Pt nanoparticles and **(d)** Selected Area Electron Diffraction (SAED) patterns.

3.2. IR Characteristics of Pt@MWCNT, Pt@MWCNT-DHBI and Pt@MWCNT-DBS

After the Pt@MWCNT, Pt@MWCNT-DHBI, and Pt@MWCNT-DBS synthesis, the compounds were characterized by FT-IR spectrometer to observe the nanocomposites in the IR spectra and check the stability of the ionophore nanocomposite.

Figure 2 shows the IR spectra of the Pt-doped MWCNTs (PtMWCNT), pure DHBI cationic surfactant, and a doped nanomaterial after the formation of a complex with DHBI (PtMWCNT-DHBI). The spectra of acid-functionalized MWCNT dopped with platinum show several distinctive peaks. The intensive band at 3450 cm^{-1} originates from the stretching vibrations of isolated surface -OH groups, -OH in carboxyl groups, and/or sorbed water in the sample. The weakly expressed stretching peak from the C-O bond can be barely noticed around 1350 cm^{-1}. A slim peak near 2950 cm^{-1} comes from the asymmetric stretching of methyl or methylene groups, usually located at the defect sites on the sidewall surface. The peak at 1560 cm^{-1} is related to the carboxylate anion stretch mode, and this peak is not seen on pristine MWCNT. The characteristic fingerprint regions of the DHBI cationic surfactant, 3025 cm^{-1} and 2960 to 2746 cm^{-1} (ν CH), and aromatic benzene ring shown by signals 1600 and 1465 cm^{-1} (ν CC aromatic stretching) can be also observed at the IR spectra of the PtMWCNT-DHBI complex. In this way, the synthesis was successful, and the complex was formed and ready to use for membrane fabrication and PtMWCNT-DHBI sensor characterization.

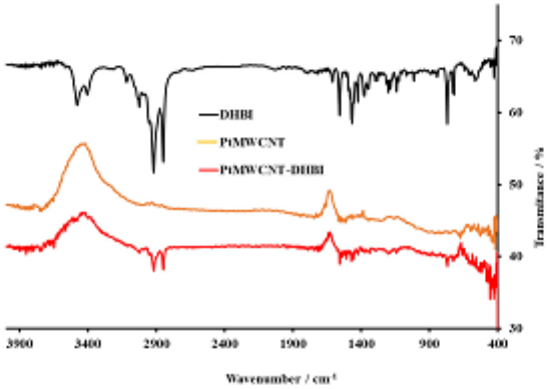

Figure 2. The FT-IR spectra of the DHBI cationic surfactants, the Pt@MWCNT nanomaterial, and the complex of Pt@MWCNT-DHBI in KBr. The DHBI values were adapted to fit the other spectra.

Figure 3 shows the IR spectra of the Pt-doped MWCNTs (PtMWCNTs), pure anionic surfactant DBS, and a doped nanomaterial after the formation of a complex with DBS (PtMWCNT-DBS). As far as the DBS spectrum is concerned, the broadband in the region 3200–3600 cm^{-1} is attributed to O-H bond stretching and indicates the presence of humidity in the solid surfactant sample. The band around 3100 cm^{-1} is related to C-H aromatic stretching, while the bands slightly below 3000 cm^{-1} are attributed to the vibration of the axial deformation of C-H for the CH_2 group of the surfactant tail. In this region, the band may be located from the aromatic stretching vibrations of C-H. The rest of the DBS surfactant spectrum can be considered through the characteristic fingerprint regions, including the widened band around 3038 cm^{-1}, peaks from 2875 to 3005 cm^{-1}, from 1533 to 1690 cm^{-1}, peaks at 1405 cm^{-1}, 1457 cm^{-1} and from 1060 to 1273 cm^{-1}. These regions can generally be attributed to the OH groups, C-H_2 groups, C-O-C groups, and to the aromatic structure of DBS. The characteristic fingerprint regions of two major spectral regions corresponding to the hydrophobic tail, 3005 to 2875 cm^{-1} (ν CH), and the hydrophilic sulfonate region from 1270 to 900 cm^{-1} (ν_{as} S=O (board, very strong) and vs S=O (sharp, very strong)) of DBS can be also observed at the IR spectra of the PtMWCNT-DBS complex. In this way, the synthesis was successful, and the complex was formed and ready to use for membrane fabrication and PtMWCNT-DBS sensor characterization.

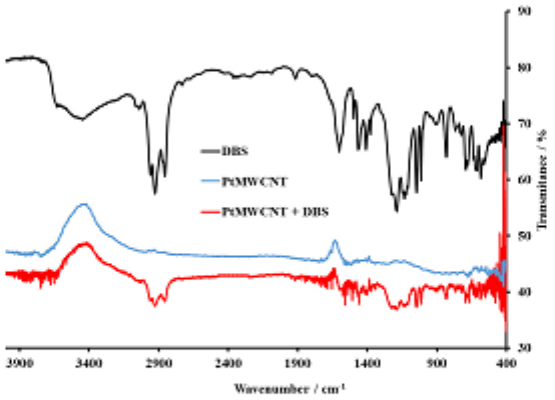

Figure 3. The FT-IR spectra of the DBS anionic surfactants, the Pt@MWCNT nanomaterial, and the Pt@MWCNT-DBS complex in KBr. The DBS values were adapted to fit the other spectra.

3.3. Response Characteristics of Fabricated Surfactant Sensors

The response of the prepared Pt@MWCNT-DHBI surfactant sensor was investigated in deionized water with the incremental addition of cationic surfactants CTAB and CPC, respectively. The increment volumes were calculated according to the achieved concentration of the corresponding cationic surfactant to cover a wide concentration range. The response mechanism of the proposed Pt@MWCNT-DHBI surfactant sensor to cationic surfactants can be described as follows:

$$E = E^o + S\ log\ a_{cat.surf.} \quad (1)$$

The proposed equation is a modified Nernst equation, in which E represents the electromotive force, E^o is a constant potential term, and $a_{cat.surf.}$ is the activity of the corresponding cationic surfactant.

The response mechanism of the proposed Pt@MWCNT-DHBI surfactant sensor to anionic surfactants can be described as follows:

$$E = E^o - S\ log\ a_{an.surf.} \quad (2)$$

The proposed equation is a modified Nernst equation, in which E represents the electromotive force, E^o is a constant potential term, and $a_{an.surf.}$ is the activity of the corresponding anionic surfactant.

Response characteristics were tested in deionized water for both fabricated surfactant sensors, Pt@MWCNT-DHBI and Pt@MWCNT-DBS. Both sensors were tested in the presence of anionic surfactants SDS and DBS and cationic surfactants CPC and CTAB, respectively.

The response characteristics of the proposed surfactant sensor Pt@MWCNT-DHBI for anionic surfactants SDS and DBS are shown in Figure 4. The response calibration curves were linear over a wide concentration range with a distinct inflexion for both anionic surfactants SDS and DBS.

The statistical evaluation of the response of the Pt@MWCNT-DHBI surfactant sensor to SDS and DBS is presented in Table 1. The Pt@MWCNT-DHBI surfactant sensor showed a Nernstian response to SDS (59.1 mV/decade of activity) and a slightly sub-Nernstian response to DBS (57.5 mV/decade of activity). The linear response regions for both anionic surfactants were broad, up to ≈2×10^{-6} M. This was important since it could allow the quantification of anionic surfactants over a broad concentration range, including higher but also lower anionic surfactant concentrations. Additionally, the critical micellar concen-

tration (CMC) for both anionic surfactants was in agreement with the literature [30]. Using the proposed sensor, the CMCs for anionic surfactants could be detected.

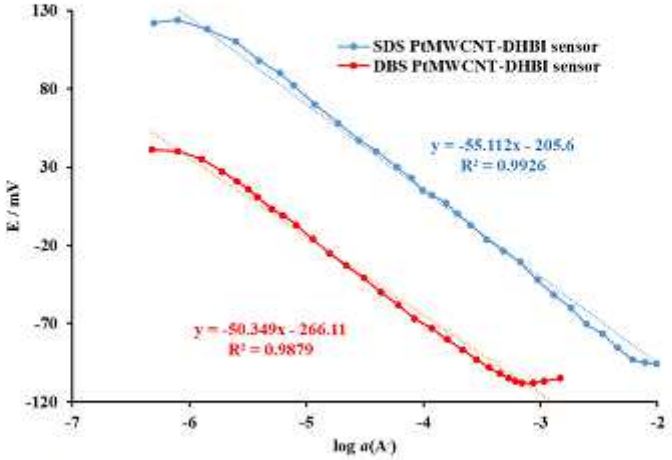

Figure 4. The electromotive force of the Pt@MWCNT-DHBI surfactant sensor as a function of the incremental addition of SDS and DBS anionic surfactants (A^-) in deionized water at 25 °C. The curves were displaced for clarity. The trend lines were added for orientation.

Table 1. Statistical evaluation of response characteristics of the Pt@MWCNT-DHBI surfactant sensor for anionic surfactants SDS and DBS.

Parameters	SDS	DBS
Slope (mV/decade)	59.1 ± 0.2	57.5 ± 0.3
Correlation coefficient (R^2)	0.9993	0.9898
Intercept (mV)	223 ± 2	289 ± 3
Useful linear concentration range (M)	2.5^{-6} to 6.3×10^{-3}	1.8×10^{-6} to 4.5×10^{-4}

The response characteristics of the proposed surfactant sensor Pt@MWCNT-DHBI were also tested for the cationic surfactants CPC and CTAB (Figure 5). The response calibration curves were linear over a wide concentration range with an inflexion for both cationic surfactants CTAB and CPS and CMC concentrations. The statistical evaluation of the response of the Pt@MWCNT-DHBI surfactant sensor to CPC and CTAB showed a sub-Nernstian response in the linear response region, with 49.2 mV/decade of activity for CPC and 44.7 mV/decade of activity for CTAB. The linear response region for CTAB was broader compared to the CPC. Even though the proposed Pt@MWCNT-DHBI surfactant sensor showed good response characteristics, the sub-Nernstian response for both surfactants reduced the sensitivity in cationic surfactant quantification.

The proposed Pt@MWCNT-DBS surfactant sensor was tested in response to the anionic surfactants SDS and DBS (Figure 6). The sensor exhibited a sub-Nernstian response for both anionic surfactants. The useful linear response region for DBS had a slope of 32.1 mV/decade of activity, while the linear response region for SDS could be observed starting from 1×10^{-4} M, with a slope of 33.8 mV/decade of activity. The Pt@MWCNT-DBS surfactant sensor exhibited limited potential usage for anionic surfactant quantification.

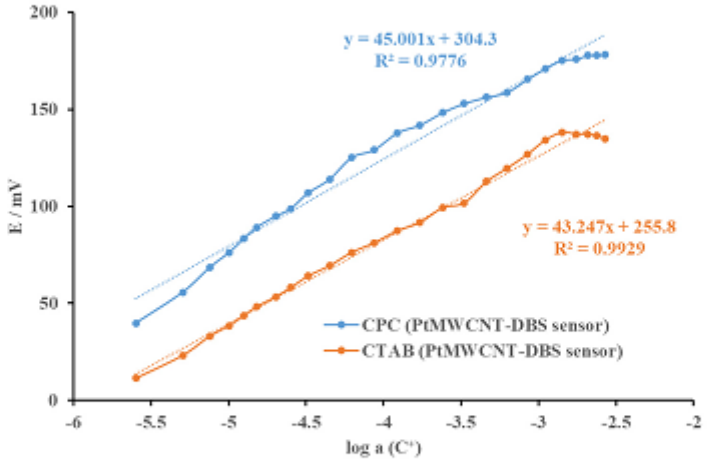

Figure 5. The electromotive force of the Pt@MWCNT-DHBI surfactant sensor as a function of the incremental addition of CPC and CTAB in deionized water at 25 °C. The curves were displaced for clarity. The trend lines were added for orientation.

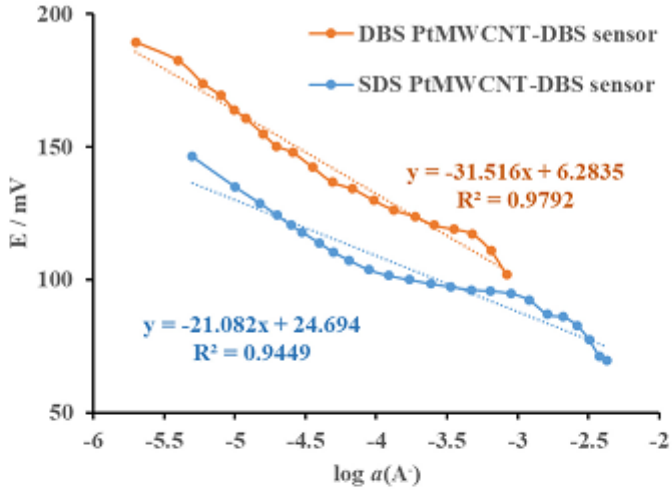

Figure 6. The electromotive force of the Pt@MWCNT-DBS surfactant sensor as a function of the incremental addition of CPC and CTAB cationic surfactants (C^+) in deionized water at 25 °C. The curves were displaced for clarity. The trend lines were added for orientation.

The Pt@MWCNT-DBS surfactant sensor was tested in response to the cationic surfactants CPC and CTAB (Figure 7). The sensor exhibited a sub-Nernstian response for both anionic surfactants. The useful linear response region (1×10^{-4} to 1×10^{-3} M) for CPC had a slope of 23.7 mV/decade of activity, while the linear response region for CTAB (1.6×10^{-4} to 1×10^{-3} M) had a slope of 22.9 mV/decade of activity. The Pt@MWCNT-DBS surfactant sensor exhibited potential usage for the quantification of cationic surfactants in a very narrow region.

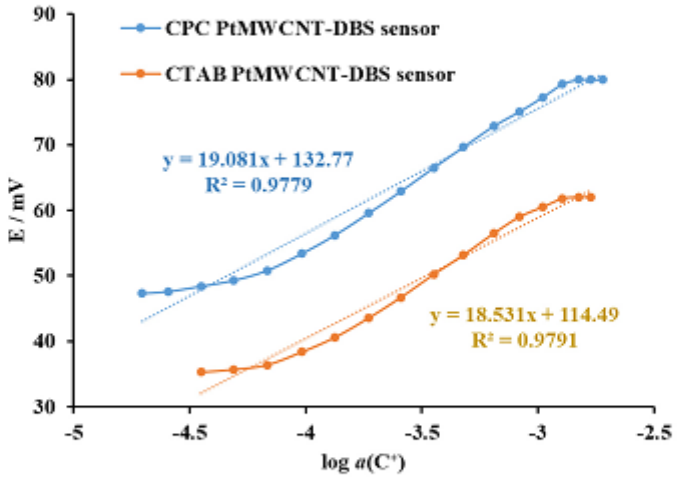

Figure 7. The electromotive force of the Pt@MWCNT-DBS surfactant sensor as a function of the incremental addition of CPC and CTAB cationic surfactants (C^+) in deionized water at 25 °C. The curves were displaced for clarity. The trend lines were added for orientation.

When comparing the two sensors, Pt@MWCNT-DHBI sensors showed superior characteristics compared to Pt@MWCNT-DBS sensors. The sensitivity was two times higher for the same investigated regions, and the useful linear regions were broad, allowing the potential application of the sensor to quantify both anionic and cationic surfactants in water and commercial products. The sensor was further characterized by interferences.

3.4. The Interference Study of Pt@MWCNT-DHBI Sensor

The interference study was performed to observe the response of the Pt@MWCNT-DHBI surfactant sensor to selected interfering anions (Table 2). The solution of the selected interfering cation was used for the incremental addition of SDS. The fixed interference method (FIN) proposed by IUPAC was used to calculate the interfering influence. The calculated $logK_{Surf}^{Pot}$ for selected anions was in the range from −3.2 to 4.7. From the K_{Surf}^{Pot} values, it can be concluded that the usual anions had a minor influence on the response characteristics of the surfactant sensor Pt@MWCNT-DHBI.

Table 2. Calculated logarithm of selectivity coefficient for most common inorganic and organic anions (0.01 M) measured by the Pt@MWCNT-DHBI surfactant sensor and adding SDS.

Interfering Anions	$logK_{An_x^-}^{pot}$
Chloride	−3.2
Carbonate	−4.8
Nitrate	−3.3
Acetate	−4.5
Sulfate	−3.9
Borate	−4.4
EDTA	−4.7
Dihydrogenphosphate	−3.9
Hydrogen carbonate	−3.2
Xylensulfonate	−3.6
Fluoride	−4.3
Bromide	−4.5
Hydrogen sulfate	−3.9

A low influence of potentially interfering anions was also achieved using the membrane composition proposed recently [15]. The selected plasticizer, Elvaloy 742, is a terpolymer of ethylene, vinyl acetate, and carbon monoxide; it contributed to the stability and response of the sensing membrane because it is a permanent, non-migrating plasticizer (with a molecular weight of about 250,000) that provides toughness and flexibility that are locked into the PVC. In essence, membranes could be considered compatible polyblends rather than flexible PVC [31]. The measured sensor drift was ≈6 mV per hour. The combination of the proposed sensor membrane composition with the selected plasticizer and Pt-doped MWCNT-based ionophore allowed the high lipophilicity of the membrane, lower noise, a higher surface area, higher stability, and better charge transfer. The use of a Pt-MWCNTs-based ionophore and a new plasticizer had a positive influence on leaching since the ionophore is more bound inside the sensor membrane matrix.

Before each use, the sensor was conditioned in a solution of the cationic surfactant CTAB (4×10^{-3} M). If the sensor was not used for several weeks, it was stored dry. Before each new series of measurements, the sensor was conditioned using the same procedure. In this way, it was possible to maintain the reproducibility and stability of the electrode. In addition, the use of Pt-doped MWCNTs extended the lifetime by more than six months.

3.5. Titration of Technical Grade Cationic Surfactant with Pt@MWCNT-DHBI Sensor

The titration of charged surfactants, both anionic (A^-) and cationic (C^+), is described by the formation of the low-solubility ion pair (CA):

$$A^- + C^+ \Leftrightarrow CA \quad (3)$$

Finally, the proposed surfactant sensor Pt@MWCNT-DHBI was tested as an end-point indicator in titrations with the cationic surfactant Hyamine 1622. The titration curve was sigmoidal and smooth, with a total signal change of 222.7 ± 9.2 mV (Figure 8). The inflexion point was well-defined and exhibited a sharp signal drop. The first derivative curve showed a sharp peak at the end-point, and the value was well-defined.

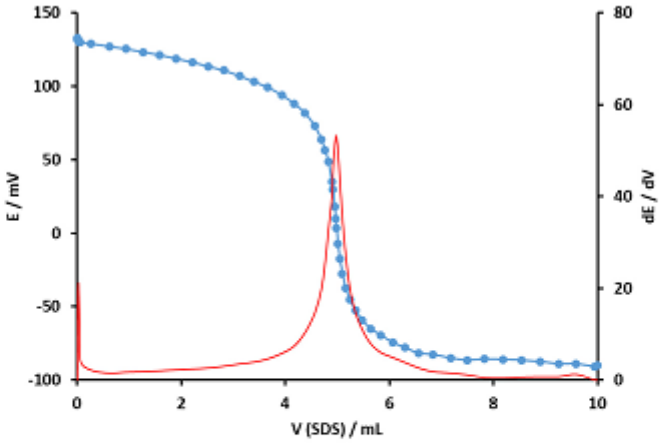

Figure 8. Potentiometric titration (blue) and 1st derivative (red) of a technical grade cationic surfactant Hyamine 1622 titration with anionic surfactant SDS (4×10^{-3} M) and the Pt@MWCNT-DHBI surfactant sensor as an end-point indicator.

The surfactant sensor Pt@MWCNT-DHBI was also used as an end-point indicator for potentiometric titrations of solutions with defined amounts of cationic surfactant added, i.e., by the standard addition method. The added amounts were 50 and 10 µmol of the

selected cationic surfactants CTAB and Hyamnie 1622, respectively (Table 3). The results exhibited recoveries ranging from 98.2 to 99.2%.

Table 3. Results for potentiometric titration of technical grade cationic surfactants CTAB and Hyamine 1622 by the standard addition method. The Pt@MWCNT-DHBI sensor was used as an end-point indicator, and SDS was used as a titrant (4×10^{-3} M), with mean values at ±95% confidence limits.

Cationic Surfactant	*n* (Added)/μmol	*n* (Found)/μmol	Recovery/%
CTAB	50	49.93 ± 0.06	99.8
	10	9.82 ± 0.04	98.2
Hyamine 1622	50	49.96 ± 0.03	99.9
	10	9.92 ± 0.07	99.2

3.6. Titration of Commercial Products with Pt@MWCNT-DHBI Sensor

Six samples of detergents for various applications were purchased in local stores. All of them had declared the content of anionic surfactants. The samples were tested, and the amount of anionic surfactant was calculated based on the end-point potentiometric titration results. As a titrant, a CPC in various concentrations was used. The results presented in Table 4 show the amounts of anionic surfactants measured by the Pt@MWCNT-DHBI surfactant sensor and compared with the ISE surfactant sensor previously published by our group. The results were also compared with the classical two-phase titration method. The results showed good agreement with other methods.

Table 4. Comparison of anionic surfactant content in commercial products measured by potentiometric titration with the Pt@MWCNT-DHBI surfactant sensor, ISE surfactant sensor, and a two-phase titration.

Commercial Detergents		% Anionic Surfactant		
		Pt@MWCNT-DHBI	ISE Surfactant Sensor *	Two-Phase Titration **
Powder	sample 1	6.3 ± 0.1	6.3	6.15
	sample 2	6.1 ± 0.1	6.0	6.09
Liquid gel	sample 3	2.1 ± 0.1	2.1	2.01
	sample 4	2.1 ± 0.1	2.2	2.09
Handwashing	sample 5	13.2 ± 0.1	13.2	13.5
	sample 6	15.1 ± 0.1	15.1	15.3

* surfactant sensor presented in [32]; ** referent method presented in [2].

The Pt@MWCNT-DHBI surfactant sensor was successfully exploited for several months on a daily basis. After checking the response signals from the first days of use with the data from six months of use, there was no significant signal change. This lack of leaching and extended lifetime could be explained by the formation of a strong complex between the acid-activated and Pt-doped MWCNTs with the positively charged DHBI surfactant and the use of a new plasticizer.

4. Conclusions

Two different ionophores using Pt-doped acid-activated MWCNTs in combination with the cationic surfactant DHBI (Pt@MWCNT-DHBI ionophore) and anionic surfactant DBS (Pt@MWCNT-DBS ionophore) were successfully produced and characterized. The use of the new plasticizer Elvaloy 742 in combination with Pt-doped MWCNT-based ionophores was successfully employed in sensing membrane nanocomposite synthesis.

The potentiometric response of both sensors, Pt@MWCNT-DHBI and Pt@MWCNT, to anionic surfactants (SDS and DBS) and cationic surfactants (CPC and CTAB) showed that the Pt@MWCNT-DHBI surfactant sensor revealed superior response properties to SDS

(59.1 mV/decade of activity) and to DBS (57.5 mV/decade of activity), with linear response regions for both anionic surfactants (up to ≈2×10^{-6} M).

The Pt@MWCNT-DHBI surfactant sensor was selected for further analysis. The interference tests showed the low interference influence of common anions and SDS response measurements. The sensor was successfully employed in the potentiometric titration of a technical grade cationic surfactant with recoveries ranging from 98.2 to 99.9%. The sensor was successfully used for the quantification of anionic surfactants in six samples of different commercial detergents. The results were compared with the ISE surfactant sensor and the classical two-phase titration method and showed good agreement.

The use of a Pt@MWCNT-based ionophore and a new plasticizer prevented the leaching, which resulted in an extended lifetime. For these reasons, the Pt@MWCNT-DHBI surfactant sensor is a promising tool for surfactant quantification in product formulations but also in other aqueous samples, like wastewater.

Author Contributions: Conceptualization, N.G., M.M., I.K., D.Š., N.S., M.K.S. and M.J.; methodology, N.G., M.M., D.Š., N.S. and M.J.; software, I.K. and D.Š.; validation, N.G., N.S. and M.J.; formal analysis, N.G., M.M., I.K., D.Š., N.S., M.K.S., B.Đ., K.Đ. and M.J.; investigation, N.G., N.S., D.Š., M.M., M.K.S. and M.J.; resources, N.S., B.Đ., M.J. and E.K.-A.; data curation, M.M., N.S., M.K.S. and M.J.; writing—N.G., N.S. and M.J.; writing—review and editing, M.M., N.S. and M.J.; visualization, M.K.S., I.K., E.K.-A. and B.Đ.; supervision, N.S. and M.J.; project administration, N.G., K.Đ. and M.K.S.; funding acquisition, M.M., N.S. and M.J. All authors have read and agreed to the published version of the manuscript.

Funding: This study was financially supported of the Ministry of Science, Technological Development and Innovations of the Republic of Serbia (Agreement number PMF = 451-03-66/2024-03/200124).

Institutional Review Board Statement: Not applicable.

Informed Consent Statement: Not applicable.

Data Availability Statement: Data are contained within the article.

Conflicts of Interest: Author Nada Glumac was employed by the company Međimurske Vode d.o.o. The remaining authors declare that the research was conducted in the absence of any commercial or financial relationships that could be construed as a potential conflict of interest.

References

1. Sánchez, J.; del Valle, M. Determination of anionic surfactants employing potentiometric sensors—A review. *Crit. Rev. Anal. Chem.* **2005**, *35*, 15–29. [CrossRef]
2. *ISO2271:1989*; Surface Active Agents, Detergents, Determination of Anionic-Active Matter by Manual or Mechanical Direct Two-Phase Titration Procedure. ISO: Geneva, Switzerland, 1989.
3. *ISO16265:2009*; Water Quality—Determination of the Methylene Blue Active Substances (MBAS) Index—Method Using Continuous Flow Analysis (CFA). ISO: Geneva, Switzerland, 2009. Available online: https://www.iso.org/standard/52130.html (accessed on 9 August 2018).
4. Ysambertt, F.; Cabrera, W.; Marquez, N.; Salager, J.L. Analysis of Ethoxylated Nonylphenol Surfactants by High Performance Size Exclusion Chromatography (HPSEC). *J. Liq. Chromatogr.* **1995**, *18*, 1157–1171. [CrossRef]
5. Ripoll-Seguer, L.; Beneito-Cambra, M.; Herrero-Martinez, J.M.; Simó-Alfonso, E.F.; Ramis-Ramos, G. Determination of non-ionic and anionic surfactants in industrial products by separation on a weak ion-exchanger, derivatization and liquid chromatography. *J. Chromatogr. A* **2013**, *1320*, 66–71. [CrossRef] [PubMed]
6. Haefliger, O.P. Universal Two-Dimensional HPLC Technique for the Chemical Analysis of Complex Surfactant Mixtures. *Anal. Chem.* **2003**, *75*, 371–378. [CrossRef] [PubMed]
7. Wulf, V.; Wienand, N.; Wirtz, M.; Kling, H.-W.; Gäb, S.; Schmitz, O.J. Analysis of special surfactants by comprehensive two-dimensional gas chromatography coupled to time-of-flight mass spectrometry. *J. Chromatogr. A* **2010**, *1217*, 749–754. [CrossRef] [PubMed]
8. Sakač, N.; Madunić-Čačić, D.; Marković, D.; Jozanović, M. Study of Cationic Surfactants Raw Materials for COVID-19 Disinfecting Formulations by Potentiometric Surfactant Sensor. *Sensors* **2023**, *23*, 2126. [CrossRef] [PubMed]
9. Yin, T.; Qin, W. Applications of nanomaterials in potentiometric sensors. *TrAC-Trends Anal. Chem.* **2013**, *51*, 79–86. [CrossRef]
10. Cho, G.; Azzouzi, S.; Zucchi, G.; Lebental, B. Electrical and Electrochemical Sensors Based on Carbon Nanotubes for the Monitoring of Chemicals in Water—A Review. *Sensors* **2021**, *22*, 218. [CrossRef]

11. Ahammad, A.J.S.; Lee, J.-J.; Rahman, M.A. Electrochemical Sensors Based on Carbon Nanotubes. *Sensors* **2009**, *9*, 2289–2319. [CrossRef]
12. Galović, O.; Samardžić, M.; Hajduković, M.; Sak-Bosnar, M. A new graphene-based surfactant sensor for the determination of anionic surfactants in real samples. *Sens. Actuators B Chem.* **2016**, *236*, 257–267. [CrossRef]
13. Sakač, N.; Jozanović, M.; Karnaš, M.; Sak-Bosnar, M. A New Sensor for Determination of Anionic Surfactants in Detergent Products with Carbon Nanotubes as Solid Contact. *J. Surfactants Deterg.* **2017**, *20*, 881–889. [CrossRef]
14. Ponnamma, D.; Sung, S.H.; Hong, J.S.; Ahn, K.H.; Varughese, K.T.; Thomas, S. Influence of non-covalent functionalization of carbon nanotubes on the rheological behavior of natural rubber latex nanocomposites. *Eur. Polym. J.* **2014**, *53*, 147–159. [CrossRef]
15. Najafi, M.; Maleki, L.; Rafati, A.A. Novel surfactant selective electrochemical sensors based on single walled carbon nanotubes. *J. Mol. Liq.* **2011**, *159*, 226–229. [CrossRef]
16. Hu, C.; Hu, S. Carbon Nanotube-Based Electrochemical Sensors: Principles and Applications in Biomedical Systems. *J. Sens.* **2009**, *2009*, 1–40. [CrossRef]
17. Yousefi, A.; Babaei, A.; Delavar, M. Application of modified screen-printed carbon electrode with MWCNTs-Pt-doped CdS nanocomposite as a sensitive sensor for determination of natamycin in yoghurt drink and cheese. *J. Electroanal. Chem.* **2018**, *822*, 1–9. [CrossRef]
18. Tsierkezos, N.G.; Othman, S.H.; Ritter, U.; Hafermann, L.; Knauer, A.; Köhler, J.M.; Downing, C.; McCarthy, E.K. Electrochemical analysis of ascorbic acid, dopamine, and uric acid on nobel metal modified nitrogen-doped carbon nanotubes. *Sens. Actuators B Chem.* **2016**, *231*, 218–229. [CrossRef]
19. Xie, J.; Wang, S.; Aryasomayajula, L.; Varadan, V.K. Platinum decorated carbon nanotubes for highly sensitive amperometric glucose sensing. *Nanotechnology* **2007**, *18*, 065503. [CrossRef]
20. Afkhami, A.; Madrakian, T.; Shirzadmehr, A.; Tabatabaee, M.; Bagheri, H. New Schiff base-carbon nanotube–nanosilica–ionic liquid as a high performance sensing material of a potentiometric sensor for nanomolar determination of cerium(III) ions. *Sens. Actuators B Chem.* **2012**, *174*, 237–244. [CrossRef]
21. Khalil, M.M.; Farghali, A.A.; El Rouby, W.M.A.; Abd-Elgawad, I.H. Preparation and characterization of novel MWCNTs/Fe-Co doped TNTs nanocomposite for potentiometric determination of sulpiride in real water samples. *Sci. Rep.* **2020**, *10*, 8607. [CrossRef]
22. Mishra, D.; Krause, A.; Sahni, H.S.; Chatterjee, S. Multi-walled carbon nanotube-functional ionophore based composite potentiometric sensor for selective detection of lead in water. *Diam. Relat. Mater.* **2023**, *137*, 110156. [CrossRef]
23. Abdel-Haleem, F.M.; Gamal, E.; Rizk, M.S.; El Nashar, R.M.; Anis, B.; Elnabawy, H.M.; Khalil, A.S.G.; Barhoum, A. t-Butyl calixarene/Fe2O3@MWCNTs composite-based potentiometric sensor for determination of ivabradine hydrochloride in pharmaceutical formulations. *Mater. Sci. Eng. C* **2020**, *116*, 111110. [CrossRef] [PubMed]
24. Oliveira, T.; Morais, S. New Generation of Electrochemical Sensors Based on Multi-Walled Carbon Nanotubes. *Appl. Sci.* **2018**, *8*, 1925. [CrossRef]
25. Praphakar, R.A.; Jeyaraj, M.; Mehnath, S.; Higuchi, A.; Ponnamma, D.; Sadasivuni, K.K.; Rajan, M. A pH-sensitive guar gum-grafted -lysine-β-cyclodextrin drug carrier for the controlled release of 5-flourouracil into cancer cells. *J. Mater. Chem. B* **2018**, *6*, 1519–1530. [CrossRef] [PubMed]
26. Stamatin, S.N.; Borghei, M.; Dhiman, R.; Andersen, S.M.; Ruiz, V.; Kauppinen, E.; Skou, E.M. Activity and stability studies of platinized multi-walled carbon nanotubes as fuel cell electrocatalysts. *Appl. Catal. B Environ.* **2015**, *162*, 289–299. [CrossRef]
27. Ma, W.; Wan, J.; Fu, W.; Wu, Y.; Wang, Y.; Zhang, H.; Wang, Y. Heterostructures induced between platinum nanoparticles and vanadium carbide boosting hydrogen evolution reaction. *Appl. Catal. A Gen.* **2022**, *633*, 118512. [CrossRef]
28. Ranđelović, M.S.; Momčilović, M.Z.; Miličević, J.S.; Đurović-Pejčev, R.D.; Mofarah, S.S.; Sorrel, C.C. Voltammetric sensor based on Pt nanoparticles suported MWCNT for determination of pesticide clomazone in water samples. *J. Taiwan Inst. Chem. Eng.* **2019**, *105*, 115–123. [CrossRef]
29. Sakač, N.; Marković, D.; Šarkanj, B.; Madunić-Čačić, D.; Hajdek, K.; Smoljan, B.; Jozanović, M. Direct Potentiometric Study of Cationic and Nonionic Surfactants in Disinfectants and Personal Care Products by New Surfactant Sensor Based on 1,3-Dihexadecyl−1H-benzo[d]imidazol−3-ium. *Molecules* **2021**, *26*, 1366. [CrossRef] [PubMed]
30. Sakač, N.; Madunić-Čačić, D.; Marković, D.; Hok, L.; Vianello, R.; Vrček, V.; Šarkanj, B.; Đurin, B.; Della Ventura, B.; Velotta, R.; et al. Potentiometric Surfactant Sensor for Anionic Surfactants Based on 1,3-dioctadecyl-1H-imidazol-3-ium tetraphenylborate. *Chemosensors* **2022**, *10*, 523. [CrossRef]
31. Davidson, C.J.; Meares, P.; Hall, D.G. A polymeric electrode for ionic surfactants. *J. Memb. Sci.* **1988**, *36*, 511–524. [CrossRef]
32. Sakač, N.; Madunić-Čačić, D.; Marković, D.; Hok, L.; Vianello, R.; Šarkanj, B.; Đurin, B.; Hajdek, K.; Smoljan, B.; Milardović, S.; et al. Potentiometric Surfactant Sensor Based on 1,3-Dihexadecyl-1H-benzo[d]imidazol-3-ium for Anionic Surfactants in Detergents and Household Care Products. *Molecules* **2021**, *26*, 3627. [CrossRef]

3. DISCUSSION

Hypothesis #1: New cationic quaternary alkyl ammonium compounds (QAC) based on imidazolium and triazolium groups can improve the properties of potentiometric sensors for surfactants.

The development of potentiometric sensors for surfactants is fundamentally based on the incorporation of an ionophore within a sensitive membrane. [15] The classic and most widely used ionophores are ion-pairs (ionophores) formed between a bulky lipophilic cation and the analyte anionic surfactant.

Potentiometric sensors for surfactants were first reported in the 1970s. These sensors had ion-pairs, plasticizer and a polymer, like PVC. [59–61] The 1990s marked the start of synthesizing PVC membranes for anionic surfactants. This was achieved by incorporating a tetradodecylammonium (TDA) - dodecylbenzenesulfonate (DBS) ion pair into a PVC matrix plasticized with o-nitrophenyl octyl ether (NPOE). [62] A major advantage of the resulting solid-state ion-selective electrodes (ISEs) is their design, which places the membrane directly on a conductive epoxy/graphite support, removing the need for an internal liquid reference. [63] In the early 2000s, cyclic ionophores were developed as an alternative to the quaternary ammonium salts traditionally used in surfactant electrodes. [64,65]

Further advancements in ion-pair-based potentiometric sensors have been extensively explored. In 2006 a PVC membrane electrode that utilized the ion-pair tetrahexadecylammonium-dodecyl sulfate (THA-SDS) as the active sensing material was introduced. [66] This sensor enabled the quantification of anionic surfactants at low concentrations, down to 10^{-5} M. Subsequently, the same research group developed another PVC membrane electrode employing the ion-pair 1,3-didecyl-2-methylimidazolium-tetraphenylborate (DMI-TPB) with o-nitrophenyloctyl ether (NPOE) as the plasticizer. [67] The resulting sensor exhibited a Nernstian response for SDS and a near-Nernstian response for DBS. In 2011, PVC-plasticized liquid membrane electrode based on a hexadecyltrioctadecylammonium-tetraphenylborate (HDTA-TPB) ion pair was introduced. [68] There were many other types of ion-pairs used for surfactant sensor fabrication, like cetyltrimethylammonium-dodecylsulfate (CTA-SDS) [69,70],

dodecyltrimethylammonium-dodecylbenzenesulphonate (DTA-DBS) [71], cetyltrimethylammonium-tetraphenylborate (CTA-TPB) [30], etc.

The introduction of a PVC matrix [72,73] enabled the immobilization of these ion-pairs, leading to a rapid expansion in sensor development. The most prevalent cationic components in these ion-pairs are various quaternary ammonium compounds (QACs). The review paper on potentiometric sensors for anionic surfactatns, by Jozanović et al. [74], highlights numerous examples of published ionophores, including cetyltrimethylammonium (CTA) with dodecylbenzenesulfonate (DBS) [75], dimethyldioctadecylammonium (DDA) with tetraphenylborate (TPB) [47,76], tetraoctadecylammonium (TODA) with TPB [77], etc.

Although classical QACs have been widely applied, their inherent limited selectivity and susceptibility to leaching have driven the search for novel materials with enhanced performance. [15] Recently, attention has turned towards the development of new cationic quaternary alkyl ammonium compounds, particularly those containing imidazole and triazole groups. [78–82]

It is anticipated that the incorporation of these heterocyclic rings could further enhance the properties of potentiometric sensors, such as selectivity, sensitivity, and membrane stability, paving the way for more effective analysis of surfactant in complex samples.

Building upon this background, the goal of the present work was to design and synthesize a new cationic surfactant, 1,3-dioctadecyl-1*H*-1,2,3-triazol-3-ium bromide (DODTA-Br), using a green, one-pot synthetic route. The synthesis was achieved via the bisalkylation of 1*H*-1,2,3-triazole with 1-bromooctadecane under reflux in acetonitrile, with $NaHCO_3$ serving as a base and an inert N_2 atmosphere, yielding the desired ionic product at 81.5% (Scheme 1). Following purification by flash chromatography using a dichloromethane/methanol gradient (10:0.1, v/v), the structure of compound 1 was comprehensively characterized by ^{1}H and ^{13}C NMR spectroscopy, mass spectrometry, ATR-FTIR spectroscopy, and elemental analysis to confirm its identity and purity for subsequent application in sensor development.

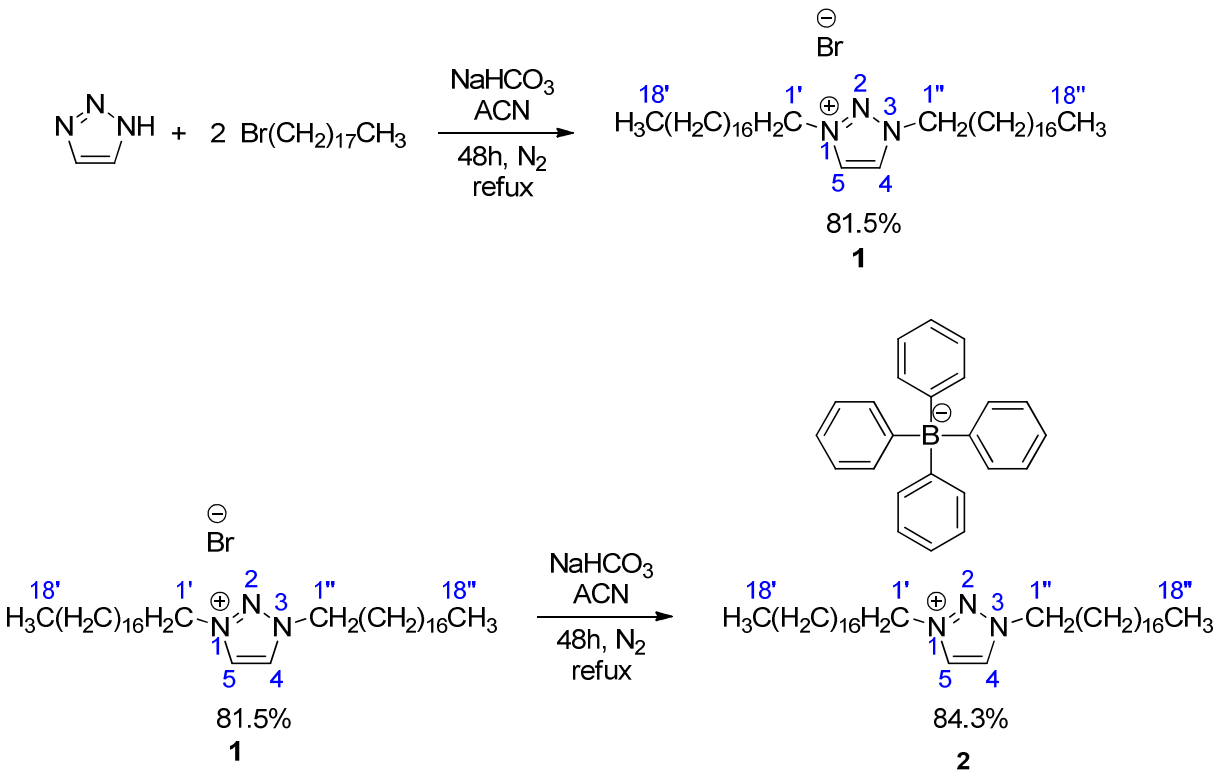

Scheme 1. Syntesis of DODTA–TPB ionophore (**2**) employing bisalkylated ionic salt DODTA -Br 1,3-dioctadecyl-1*H*-1,2,3-triazol-3-ium bromide (**1**).

DODTA–TPB ionophore was then incorporated in the PVC/plasticizer matrix to form a liquid membrane type of surfactant sensor. [83] The PVC-based liquid membrane type was mounted in the Phillips electrode body with 3M KCl as an inner electrolyte.

Surfactant sensor response mechanism

The response of the surfactant sensor to cationic surfactants can be explaind using the following Equation:

$$E = E_0 + Sloga_{CS^+} \qquad (16)$$

where E represents the electromotive force, E^o a constant potential term, S is the slope, and a_{CS^+} is the activity of the selected cationic surfactant.

The response of the surfactant sensor to anionic surfactants can be explaind using the following Equation:

$$E = E_0 - Sloga_{AS^-} \qquad (17)$$

where E represents the electromotive force, E^o a constant potential term, S is the slope, and a_{AS^-} is the activity of the selected anionic surfactant.

The formation of ionophore is based on the precipitation reaction:

$$CS^+ + AS^- \rightleftarrows CSAS \quad (18),$$

where CS^+ = cationic surfactant, AS^- = anionic surfactant, $CSAS$ = ion pair.

The ion pair dissociates as follows:

$$CSAS \rightleftarrows CS^+ + AS^- \quad (19)$$

with a solubility product constant:

$$K_{sp} = a_{CS^+} \cdot a_{AS^-} - \quad (20),$$

where a_{CS^+} and a_{AS^-} represent the activities of ion pair anions and cations.

Prior to the equivalence point, the decrease in sensor potential followed the variation in the concentration of the cationic surfactant, as described by Eq. (16). Once the equivalence point was reached, indicating complete precipitation of the cationic surfactant, a rise in the concentration of the anionic surfactant in the solution became apparent. [84]

From Eq. (20) the relation $a_{CS^+} = K_{sp} / a_{AS^-}$ can be inserted into Eq. 16:

$$E = E_0 + S \log \frac{K_{sp}}{a_{AS^-}} \quad (21),$$

that after rearrangements:

$$E = Const - S \log a_{AS^-} \quad (22)$$

where $Const = E^0 + S \log K_{sp}$.

Cationic surfactants

The response characteristics of the DODTA-TPB surfactant sensor to cationic surfactants were investigated by incrementally adding cetyltrimethylammonium bromide (CTAB) and cetylpyridinium chloride (CPC) in deionized water. The response mechanism of such liquid-membrane sensors follows a modified Nernst equation described in Eq. 16.

The DODTA-TPB sensor exhibited a highly linear response to both CTAB and CPC across a wide concentration range (Paper I, Table 1). For CTAB, the linear range was 7.9 x 10^{-6} to 7.2 x 10^{-4} M, with a slope of 56.2 mV/decade (R2= 0.9967) and limit of detection (LOD) 7.1 x 10^{-6} M. For CPC, the linear range extended from 3.2 x 10^{-6} to 9.2 x 10^{-4} M, with a slope of 58.5 mV/decade (R^2= 0.9899), and LOD 2.9 x 10^{-6} M.

Selectivity against common cations was evaluated using the fixed interference method (FIM) at 0.01 M. The potentiometric selectivity coefficients ($log\ K_{Cat_i^+}^{pot}$) for Ca^{2+} was 6.1 x 10^{-4}, for Na^+, 4.1 x 10^{-4} and for Mg^{2+} it was 5.7 x 10^{-4}., indicating negligible interference.

The utility of the DODTA-TPB sensor as an end-point indicator was demonstrated in titrations of cationic surfactants with sodium dodecyl sulfate (SDS, 4x10^{-3} M). As shown in Figure 1 (Paper I, Figure 7), titration of CPC produced a well-defined sigmoidal curve with a signal change of 357 ± 10 mV. The first derivative exhibited a sharp peak at the equivalence point, with expected signal change (dE/dV) of 69.3 ± 1.1 mV/mL.

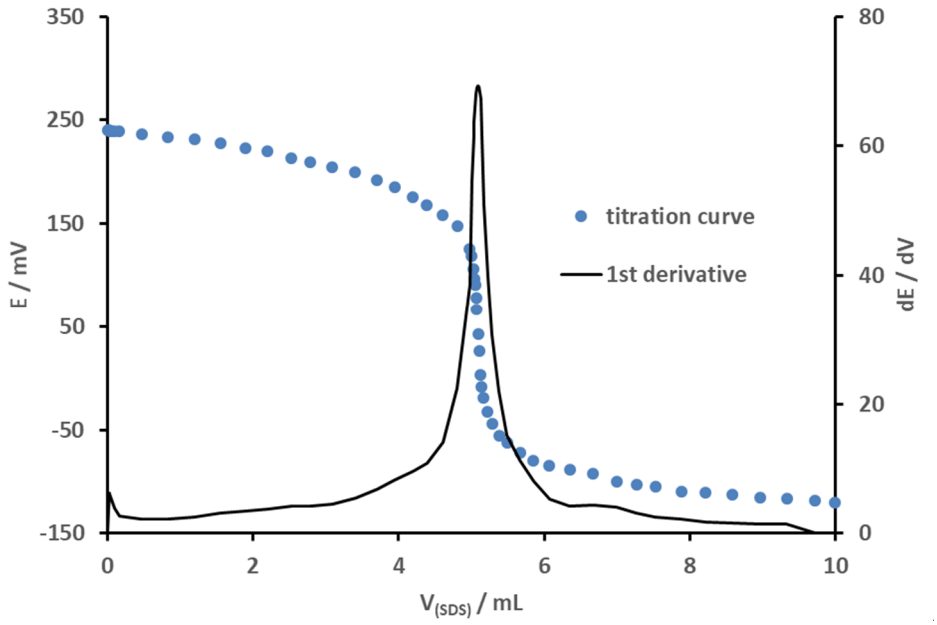

Figure 1. Results for potentiometric titration of a CPC with the SDS (4x10^{-3} M) including calculated 1st derivative (full line) on secondary y-axis. DODTA-TPB surfactant sensor was used as an end-point indicator. (from Paper I, Figure 7)

The standard addition method was used to test recoveries of the prepared DODTA-TPB surfactant sensor (Paper I, Table 2). DODTA-TPB surfactant sensor was used as an end-point indicator for the titration of known amounts of cationic surfactants at two concentration levels

50 and 10 µmol, with SDS as a titrant ($4x10^{-3}$ M). Sensor was tested on analytical grade CPC and technical grade Hyamine 1622. The sensor showed excellent properties with high recoveries: for CPC were 99.92 and 98.80 %, and for Hyamine 1622, 99.84 and 99.50 %. All values are reported at the 95% confidence limit.

Anionic surfactants

DODTA-TPB surfactant sensor was tested on response characteristics toward selected anionic surfactants. The sensor response mechanism corresponds to the modified Nernstian equation described in Eq. 17.

Sodium dodecyl sulfate (SDS) and dodecylbenzene sulfonate (DBS) were used as model anionic surfactants to evaluate the response of the DODTA–TPB surfactant sensor. Measurements were performed in deionized water (Paper II, Figure 7). SDS was investigated in the concentration range 8.1×10^{-8}–1.0×10^{-2} M, while DBS was studied between 8.1×10^{-8} and 2.5×10^{-3} M. For SDS, the sensor showed a linear response from 4.1×10^{-7} to 5.1×10^{-3} M with a slope of −59.2 ± 0.4 mV/decade and a limit of detection (LOD) of 3.1×10^{-7} M (Paper II, Table 2). In the case of DBS, the linear range was 8.1×10^{-7}– 6.1×10^{-4} M with a slope of −57.5 ± 0.5 mV/decade and an LOD of 5.9×10^{-7} M (Paper II, Table 2). Detection limits were calculated according to IUPAC recommendations. [85] The response characteristics of the DODTA–TPB ion-pair sensor toward DBS and SDS showed good agreement with previously reported TPB-based ion-pair sensors, particularly regarding the linear response range, slope per decade of activity, and limit of detection (Paper II, Table 2). The sensor exhibited good stability with a signal drift of about 3 mV h^{-1}.

The effect of potential interfering ions was evaluated using a series of anions (Paper II, Table 3). Interfering ion solutions (0.01 M) were prepared and SDS was gradually added while monitoring the potentiometric response of the DODTA–TPB sensor. Selectivity coefficients ($log\ K_{An_i^-}^{pot}$) were determined using the fixed interference method. [85] The calculated logarithmic selectivity coefficients indicated low interference from the tested anions and good sensor stability. For example, $log\ K_{An_i^-}^{pot}$ for acetate was –3.72, benzoate –3.84, bromide –3.21, chloride –3.83, carbonate –4.14, dihydrogenphosphate –4.01, EDTA –3.84, fluoride –3.68, nitrate –3.93, sulfate –4.62. The sensor showed high stability and pH resistance in the range from pH 3 to 10, and in this way it could be used for different sample applications.

The results presented in this chapter confirm Hypothesis #1, demonstrating that newly designed cationic quaternary alkyl ammonium compounds based on triazolium groups can improve the analytical performance of potentiometric surfactant sensors. The successfully synthesized compound 1,3-dioctadecyl-1*H*-1,2,3-triazol-3-ium bromide (DODTA-Br) enabled the preparation of the DODTA–TPB ionophore, which was effectively incorporated into a PVC-based sensing membrane. QAC based on imidazolium was used with doped carbon nanomaterials to prepared new ionophore and test the hypothesis #2.

Hypothesis#2: Doped carbon nanomaterials as electroactive materials can enhance the analytical properties and lifespan of potentiometric sensors for surfactants.

Pt-doped multiwalled carbon nanotubes (Pt@MWCNT) were synthesized and employed as nanostructured platforms for the preparation of two ionophore materials, Pt@MWCNT– DHBI (based on cationic surfactant 1,3-dihexadecyl-1*H*-benzo[d]imidazol-3-ium – (DHBI) and Pt@MWCNT–DBS. These ionophores were incorporated into sensing membranes plasticized with Elvaloy 742 to fabricate nanocomposite potentiometric sensors for surfactant determination. Platinum was selected due to its high electrical conductivity and chemical stability, which contribute to improved signal transduction.

The fabricated sensors were characterized and subsequently applied to the analysis of technical-grade and commercial surfactant samples. The developed sensing platform demonstrates several advantages, including simple and low-cost preparation, high sensitivity and stability, and a broad linear dynamic range. Furthermore, the electrochemical configuration enables potential integration into portable devices for on-site surfactant monitoring. The use of highly dispersed Pt nanoparticles significantly reduces material consumption compared with bulk platinum, thereby lowering overall sensor cost.

Pt@MWCNT nanomaterial was sussesfuly syntesized and characterised. The morphology and dispersion of Pt nanoparticles on MWCNT were investigated by transmission electron microscopy (TEM) (Paper III, Figure 1). TEM images reveal uniform deposition of Pt nanoparticles on the external surface of the nanotubes, with no evidence of nanoparticle incorporation inside the nanotube channels. Higher magnification images indicate partial nanoparticle agglomeration, forming clusters with an average diameter of approximately *10 nm*. The nanoparticles appear firmly attached to the nanotube surface, as no detached particles were observed.

The synthesized nanocomposites were further characterized by FTIR spectroscopy to confirm ionophore formation and structural stability. The spectra of Pt@MWCNT exhibits a broad band around 3450 cm^{-1}, attributed to O–H stretching vibrations of surface hydroxyl and carboxyl groups as well as adsorbed water (Paper III, Figure 2). A weak band near 1350 cm^{-1} corresponds to C–O stretching vibrations, while the signal at approximately 2950 cm^{-1} is associated with

asymmetric stretching of methyl or methylene groups located at defect sites of the nanotube sidewalls. The band at 1560 cm^{-1} is assigned to the carboxylate stretching mode, confirming the presence of oxygen-containing functional groups introduced during acid functionalization. The spectra of the Pt@MWCNT–DHBI nanocomposite contains characteristic bands of the DHBI surfactant, including C–H stretching vibrations at 3025 cm^{-1} and 2960–2746 cm^{-1}, together with aromatic ring vibrations at 1600 and 1465 cm^{-1} (Paper III, Figure 2). The presence of these features in the composite spectrum confirms the successful formation of the Pt@MWCNT–DHBI ionophore. Similarly, the Pt@MWCNT–DBS spectrum shows characteristic absorption bands of DBS. A broad band in the 3200–3600 cm^{-1} region is assigned to O–H stretching vibrations, while bands around 3100 cm^{-1} and below 3000 cm^{-1} correspond to aromatic and aliphatic C–H stretching modes (Paper III, Figure 3). Additional bands observed in the regions 1533–1690 cm^{-1}, 1457–1405 cm^{-1}, and 1270–900 cm^{-1} are associated with aromatic ring vibrations and sulfonate functional groups. In particular, strong asymmetric and symmetric S=O stretching bands confirm the incorporation of DBS within the nanocomposite structure.

These spectral features confirm the successful synthesis of both ionophore nanocomposites, which were subsequently employed for membrane preparation and potentiometric sensor characterization.

Response characteristics

The potentiometric response of the Pt@MWCNT–DHBI surfactant sensor was investigated in deionized water by incremental addition of the cationic surfactants CTAB and CPC. The added volumes were adjusted to cover a broad concentration range. The response of the sensor toward cationic surfactants follows a previously described modified Nernst equation in Eq. 16; and for anionic surfactants, the response was described by Eq. 17.

Response characteristics of both fabricated sensors, Pt@MWCNT–DHBI and Pt@MWCNT–DBS, were evaluated in deionized water toward anionic surfactants (SDS, DBS) and cationic surfactants (CPC, CTAB).

The Pt@MWCNT–DHBI sensor exhibited linear calibration curves with clear inflection points for SDS and DBS (Paper III, Figure 4). The statistical evaluation (Paper III, Table 1) showed a Nernstian slope for SDS (59.1 mV $decade^{-1}$) and a slightly sub-Nernstian response for DBS (57.5 mV $decade^{-1}$). Both surfactants exhibited broad linear response ranges down to

approximately 2×10^{-6} M, enabling quantification across a wide concentration interval. The detected critical micelle concentrations (CMC) were consistent with literature values. [86]

The response toward cationic surfactants (CPC and CTAB) is shown in Paper III, Figure 5. Linear calibration curves with inflection points corresponding to CMC values were observed. However, the slopes were sub-Nernstian, with 49.2 mV decade^{-1} for CPC and 44.7 mV decade^{-1} for CTAB. The linear region for CTAB was broader than for CPC. Although the sensor demonstrated good response characteristics, the reduced slopes indicate lower sensitivity for cationic surfactant quantification.

The Pt@MWCNT–DBS sensor was also evaluated toward SDS and DBS (Paper III, Figure 6). In both cases, sub-Nernstian responses were obtained. The linear response region for DBS showed a slope of 32.1 mV decade^{-1}, while SDS exhibited a slope of 33.8 mV decade^{-1}, with the linear region starting at approximately 1×10^{-4} M. These characteristics indicate limited applicability of this sensor for anionic surfactant determination.

Similarly, when tested toward CPC and CTAB (Paper III, Figure 7), the Pt@MWCNT–DBS sensor exhibited weak responses with narrow linear regions. For CPC, the useful range (1×10^{-4} – 1×10^{-3} M) showed a slope of 23.7 mV decade^{-1}, while CTAB displayed a slope of 22.9 mV decade^{-1} within 1.6×10^{-4} – 1×10^{-3} M.

Overall, the Pt@MWCNT–DHBI sensor demonstrated significantly superior performance compared to the Pt@MWCNT–DBS sensor. The sensitivity was approximately twofold higher, and the linear response ranges were considerably broader, enabling potential application for the determination of both anionic and cationic surfactants in aqueous solutions and commercial products. Based on these results, the Pt@MWCNT–DHBI sensor was selected for further interference studies.

The interference study was performed to observe the response of the Pt@MWCNT-DHBI surfactant sensor to selected interfering anions. The solution of the selected interfering cation was used for the incremental addition of SDS. The fixed interference method (FIN) proposed by IUPAC was used to calculate the interfering influence. The calculated $log\ K_{An_{i.}^-}^{pot}$ for selected anions were in the range from -3.2 to 4.7 (Paper III, Table 2). From the $log\ K_{An_{i.}^-}^{pot}$ values, it can be concluded that the usual anions have a minor influence on the response characteristics of the surfactant sensor Pt@MWCNT-DHBI.

The low interference from common anions can be attributed to the membrane composition proposed previously. The selected plasticizer, Elvaloy 742, a terpolymer of ethylene, vinyl acetate, and carbon monoxide, contributes to membrane stability due to its non-migrating nature and high molecular weight. This permanent plasticizer enhances membrane toughness and flexibility within the PVC matrix, resulting in membranes that behave as compatible polyblends rather than conventional flexible PVC systems. [87]

The prepared sensor exhibited a potential drift of approximately 6 mV h^{-1}. The combination of the optimized membrane composition, Elvaloy 742 plasticizer, and Pt-doped MWCNT-based ionophore provided increased lipophilicity, reduced noise, improved charge transfer, high surface area, and enhanced stability. Furthermore, the strong incorporation of the ionophore within the membrane matrix reduced leaching effects.

Prior to measurements, the sensor was conditioned in 4×10^{-3} M CTAB solution. When not in use for extended periods, the electrode was stored dry and reconditioned before subsequent measurements. This procedure ensured stable and reproducible responses. The incorporation of Pt-doped MWCNTs also extended the operational lifetime of the sensor to more than six months.

Titration of technical grade cationic surfactant

The Pt@MWCNT–DHBI surfactant sensor was evaluated as an end-point indicator in potentiometric titrations using the cationic surfactant Hyamine 1622. The obtained titration curve was smooth and sigmoidal, showing a total potential change of 222.7 ± 9.2 mV (Paper III, Figure 8). A well-defined inflection point with a sharp potential drop was observed, while the corresponding first derivative curve exhibited a distinct peak at the equivalence point.

The sensor was further applied as an end-point indicator in potentiometric titrations of technical grade surfactants using the standard addition method. Defined amounts of CTAB (50 µmol) and Hyamine 1622 (10 µmol) were added to the sample solutions (Paper III, Table 3). The obtained results showed recoveries between 98.2 and 99.2%, demonstrating good accuracy of the proposed method.

The obtained results confirm Hypothesis #2, demonstrating that doped carbon nanomaterials can improve the analytical performance and operational stability of potentiometric surfactant sensors. The successfully synthesized Pt@MWCNT nanomaterial enabled the preparation of

nanocomposite ionophores and sensing membranes with enhanced conductivity and stability. Among the fabricated sensors, Pt@MWCNT–DHBI exhibited superior performance, including near-Nernstian response, broad linear range, low interference from common ions, and stable operation for more than six months. The sensor was also successfully applied as an end-point indicator in potentiometric titrations of technical surfactants with recoveries close to 100%. These results confirm that Pt-doped MWCNT nanomaterials significantly enhance both the analytical characteristics and durability of potentiometric surfactant sensors, thereby validating the proposed hypothesis.

Hypothesis #3: Using computational modeling to interpret the obtained results can facilitate faster and more efficient selection and optimization of the most suitable ionophore for potentiometric surfactant sensors.

Computational modeling was applied to investigate the formation and stability of the DODTA–TPB ionic associate and to evaluate its suitability as an ionophore for potentiometric surfactant sensors. Previous studies have demonstrated that theoretical analysis of ion-pair formation can provide valuable insight into ion-exchanger behavior in surfactant-selective electrodes. [19,34,88,89] However, commonly used quaternary ammonium surfactants such as cetylpyridinium exhibit significant toxicity [90], motivating the search for alternative cationic structures with improved safety profiles. In this context, triazolium-based surfactants [88,91] represent a promising class of compounds due to their relatively low toxicity and favorable physicochemical properties.

Conformational analysis of the DODTA cation

The DODTA cation contains two long octadecyl chains attached to a triazolium ring, which introduces considerable conformational flexibility. Since exhaustive conformational sampling would require substantial computational resources, four representative conformers were selected based on differences in the torsion angles between the triazolium ring and the alkyl chains (Paper I, Figure 2). Geometry optimization revealed that two of the examined conformers converged toward the same minimum-energy structure (conformer 1), confirming its higher thermodynamic stability. The Gibbs free energy of conformer 1 was 3.4 kcal mol^{-1} lower than that of conformer 3, indicating that conformer 1 represents the most stable structure under the applied theoretical conditions. Consequently, this conformer was used for further calculations. The reliability of the CPCM-B3LYP-D3BJ/6-31G(d) [92,93] computational approach was verified through good agreement between calculated vibrational frequencies and the experimental IR spectrum of DODTA bromide. The Grimme D3 dispersion correction with Becke–Johnson damping was employed to enhance the accuracy of density functional theory (DFT) calculations in describing weak intermolecular interactions Electrostatic potential analysis and ion-pair formation. [94,95]

Electrostatic potential (ESP) mapping was used to identify the most reactive regions of both ions. In the DODTA cation, the highest positive charge density was localized around the triazolium ring, while the TPB anion exhibited the most negative ESP regions between the

phenyl rings and near the central boron atom. This complementary distribution of electrostatic potential indicates that the primary driving force for ion-pair formation is electrostatic attraction between the triazolium head group and the π-electron system of the tetraphenylborate anion. Based on this analysis, the initial geometry of the DODTA–TPB associate was constructed by aligning the regions of opposite electrostatic potential, followed by full geometry optimization. The optimized structure confirmed the formation of a stable ionic associate without the formation of new covalent bonds (Paper I, Figure 3).

Frontier molecular orbital and charge-transfer analysis

Frontier molecular orbital analysis revealed that the HOMO orbitals remained localized on the TPB anion, whereas the LUMO orbitals were primarily associated with the DODTA cation (Paper I, Figure 4). Only minor shifts in orbital energies were observed upon ion association. Specifically, the HOMO energy slightly decreased while the LUMO energy slightly increased, indicating stabilization of the ionic associate. These results demonstrate that the interaction between the ions is predominantly electrostatic rather than covalent.

Charge decomposition analysis (CDA) [96] further supported this conclusion. The calculated electron donation from TPB to DODTA was 0.0928 e, while the back-donation from DODTA to TPB was 0.0204 e, indicating limited charge transfer between the ions. The negative overlap population between occupied orbitals suggested that repulsive interactions between electron clouds prevent significant orbital mixing, again confirming that the ionic associate is stabilized mainly by electrostatic interactions.

Contribution of non-covalent interactions

In addition to electrostatic attraction, van der Waals (vdW) interactions were found to contribute significantly to the stabilization of the ion pair (Paper I, Figure 5). vdW potential analysis indicated that attractive regions are distributed along the phenyl rings of the TPB anion and the hydrophobic alkyl chains of the DODTA cation. These interactions are particularly important in membrane environments, where hydrophobic interactions can enhance the stability of ion pairs within the polymer matrix.

To further examine the role of conformational flexibility, molecular dynamics simulations of the DODTA–TPB associate were performed in aqueous solution at 300 K using the PM7 semiempirical method with the COSMO solvation model. [97,98] Analysis of the trajectory revealed that the alkyl chains of the DODTA cation adapt dynamically to maximize non-covalent interactions with the TPB anion. Reduced density gradient analysis confirmed the

presence of extended regions of weak non-covalent interactions across the surfaces of both ions, indicating that the ionic associate is stabilized by a combination of electrostatic attraction and distributed van der Waals interactions.

Implications for potentiometric surfactant sensors

The theoretical results provide important insight into the suitability of the DODTA–TPB ion pair as an ionophore in potentiometric surfactant sensors. The dominance of electrostatic interactions ensures efficient ion pairing while maintaining reversible ion exchange, which is essential for potentiometric sensing. At the same time, the contribution of hydrophobic and van der Waals interactions enhances the stability of the ion pair within the membrane phase, reducing ionophore leaching and improving sensor lifetime.

These findings demonstrate that computational modeling can significantly assist in the rational design and optimization of ionophores for surfactant-selective sensors. By identifying favorable interaction motifs, stable conformations, and key intermolecular interactions prior to experimental testing, theoretical modeling enables faster screening of potential ionophores and reduces the need for extensive experimental trial-and-error.

Therefore, the integration of quantum chemical calculations and molecular dynamics simulations with experimental sensor development supports Hypothesis #3, which states that the application of computational modeling in the interpretation of experimental results enables faster and more efficient selection and optimization of suitable ionophores for potentiometric surfactant sensors.

Hypothesis #4: New potentiometric sensors will be applicable for determining surfactants in real systems.

DODTA–TPB surfactant sensor

Commercial samples

The DODTA–TPB surfactant sensor was applied as an end-point indicator in potentiometric titrations of three commercial mouthwash samples containing cationic surfactants. Sodium dodecyl sulfate (SDS, 4×10^{-3} M) was used as the titrant acting as the counter ion. The obtained results were compared with those previously reported using the well-established DMIC–TPB surfactant sensor. [84,99] The comparative data are summarized in Table 1 (Paper I, Table 3).

Table 1. Results for the titration of commercial mouth-wash samples containing cationic surfactant for DODTA-TPB sensor and previously published DMIC-TPB surfactant sensors. SDS was used as a titrant ($4x10^{-3}$ M). (Paper I, Table 3).

Sample	DODTA-TPB (%)	DMIC-TPB (%)*
1	4.623	4.612
2	4.813	4.812
3	5.015	5.017

*[84]

To evaluate the performance of the DODTA–TPB surfactant sensor in solutions containing technical-grade anionic surfactants, three representative surfactants – SDS, DBS, and lauryl ether sulfate (LES) – were analyzed by potentiometric titration using DMIC (4×10^{-3} M) as the titrant. Known amounts of the anionic surfactants were dissolved in deionized water, and the titrations were performed with the DODTA–TPB sensor acting as the end-point indicator. The obtained titration curves exhibited typical sigmoidal shapes with well-defined inflection points. The total potential changes (ΔE) were 301.1 mV for DBS and 276.2 mV for SDS, while the calculated recoveries ranged from 100.2 to 100.4% (Paper II, Table 4).

Following validation on model solutions and technical-grade surfactants, the sensor was applied to the determination of anionic surfactants in six commercial detergent samples with declared surfactant content. The analyzed products included powdered, liquid/gel, and handwashing detergents obtained from local retail stores. Potentiometric titrations were performed using DMIC solutions of appropriate concentrations as the titrant, while the DODTA–TPB sensor served as the end-point indicator (Paper II, Table 5). The titration curves were well defined and

sigmoidal, enabling reliable determination of the equivalence point. The calculated anionic surfactant contents were 5.83 and 6.74% for powdered detergents,13.85 and 16.41% for handwashing detergents, and 2.57 and 2.73% for liquid/gel detergents. These results were consistent with our previously reported measurements. [86] For comparison, the same samples were also analyzed using the two-phase titration method. [4] The obtained values showed good agreement with those determined using the DODTA–TPB surfactant sensor.

Environmental samples

The applicability of the DODTA–TPB surfactant sensor as an end-point indicator was further evaluated in potentiometric titrations of environmental water samples collected in north-west Croatia. The analyzed samples included lake water from Lake Motičnjak, hydroaccumulation water from the Drava reservoir, and river water samples from the Drava and Mura rivers.The measured pH values ranged from 7.7 to 8.5. Prior to analysis, all samples were examined for the presence of anionic surfactants using a previously reported analytical method [100] and a commercial vial test. Both approaches confirmed the absence of detectable anionic surfactants. To evaluate potential matrix effects, the samples were spiked with SDS (50 µmol) and subsequently titrated with DMIC as the titrant, using the DODTA–TPB sensor as the end-point indicator. The recovery results are summarized in Paper II, Table 6. Quantification of SDS was successfully achieved in all tested samples, with recoveries ranging from 94.2 to 96.5%. These results indicate that no significant matrix interference was observed, demonstrating the suitability of the proposed sensor for the determination of anionic surfactants in environmental water samples.

Pt@MWCNT–DHBI surfactant sensor

Commercial samples

Six detergent samples intended for different applications were purchased from local retail stores. All products declared the presence of anionic surfactants in their composition. The samples were analyzed by potentiometric titration, and the anionic surfactant content was determined from the calculated end-point values. CPC solutions of appropriate concentrations were used as titrants. The obtained results are summarized in Paper III, Table 4, where the surfactant contents determined using the Pt@MWCNT–DHBI surfactant sensor are compared with values obtained using a previously reported ISE surfactant sensor developed [78] by our group and with the classical two-phase titration method. [4] The calculated surfactant contents ranged in Table 2 from 6.1–6.3% for powdered detergents, 2.1% for liquid/gel detergents, and 13.2–15.1% for handwashing detergents. (adapted from Paper III, Table 4) The results obtained

with the Pt@MWCNT–DHBI sensor are in good agreement with both reference methods, confirming the reliability of the proposed sensing approach.

Table 2. Comparison of Pt@MWCNT-DHBI surfactant sensor, ISE surfactant sensor, and a two-phase titration for results on anionic surfactants content in commercial products. (adapted from Paper III, Table 4)

Commercial detergents		**% ANIONIC SURFACTANT**		
Type	**Sample**	**Pt@MWCNT-DHBI**	**ISE surfactant sensor***	**Two-phase titration****
Powder	1	6.3 ± 0.1	6.3	6.15
	2	6.1 ± 0.1	6.0	6.09
Liquid-gel	3	2.1 ± 0.1	2.1	2.01
	4	2.1 ± 0.1	2.2	2.09
Handwashing	5	13.2 ± 0.1	13.2	13.5
	6	15.1 ± 0.1	15.1	15.3

*[78]

**[4]

The operational stability of the Pt@MWCNT–DHBI surfactant sensor was also evaluated during prolonged use. The sensor was employed in routine measurements for several months without noticeable deterioration of the response signal. Comparison of the signals recorded at the beginning of the testing period with those obtained after six months of use revealed no significant changes. The absence of signal drift and ionophore leaching can be attributed to the strong interaction between the acid-functionalized Pt-doped MWCNT support and the positively charged DHBI surfactant, as well as to the stabilizing effect of the selected plasticizer within the membrane matrix.

The obtained results confirm Hypothesis #4, showing that the newly developed potentiometric sensors are suitable for determining surfactants in real samples. Both the DODTA–TPB and Pt@MWCNT–DHBI sensors were successfully applied to commercial products and environmental water samples, providing results in good agreement with established analytical

methods. Accurate recoveries and well-defined titration curves confirmed reliable quantification without significant matrix interference. Additionally, the Pt@MWCNT–DHBI sensor demonstrated good operational stability over prolonged use. These results confirm the applicability of the developed sensors for surfactant determination in real systems.

4. CONCLUSIONS

Presented work successfully achieved the main research objective, which was the development of new potentiometric sensors for surfactants based on newly synthesized quaternary alkyl ammonium compounds and platinum-doped carbon nanocomposite sensing materials. The study combined organic synthesis, membrane preparation, electrochemical characterization, computational modeling, and application in real samples, providing a comprehensive scientific contribution to the field of potentiometric surfactant sensing.

Main findings are:

- New heterocyclic quaternary alkyl ammonium compound triazolium surfactant 1,3-dioctadecyl-1*H*-1,2,3-triazol-3-ium bromide (DODTA-Br) was successfully synthesized and structurally characterized.
- The DODTA- TPB ion-pair was successfully synthesized, structurally characterized and used as a sensing material to fabricate DODTA–TPB liquid membrane-type surfactant sensor.
- The DODTA-TPB sensor exhibited a highly linear response to a) cationic surfactants CTAB, the linear range was 7.9 x 10^{-6} to 7.2 x 10^{-4} M, with a slope of 56.2 mV/decade and CPC, the linear range extended from 3.2 x 10^{-6} to 9.2 x 10^{-4} M, with a slope of 58.5 mV/decade; and b) anionic surfactants SDS, the linear response range from 4.1 x 10^{-7} to 5.1 x 10^{-3} M with a slope of −59.2 ± 0.4 mV/decade and DBS, the linear range was 8.1 x 10^{-7}– 6.1 x 10^{-4} M with a slope of −57.5 ± 0.5 mV/decade.
- The DODTA-TPB sensor showed high stability towards typical anionic and cationic interfering ions, fast response time (<10 s), with potential drift typically below 1–3 mV and stable potentiometric response over extended use, demonstrating good reproducibility and long-term operational performance.
- The DODTA–TPB surfactant sensor was successfully applied as an end-point indicator in potentiometric titrations of commercial mouthwash samples containing cationic surfactants, showing results comparable to the established DMIC–TPB sensor.
- Potentiometric titrations of technical anionic surfactants (SDS, DBS) produced well-defined sigmoidal curves with large potential changes (ΔE = 276.2 mV for SDS and 301.1 mV for DBS) and recoveries of 100.2–100.4%.

- The sensor was successfully applied to the determination of anionic surfactants in commercial detergents, yielding contents of 5.83–6.74% (powdered), 13.85–16.41% (handwashing), and 2.57–2.73% (liquid/gel detergents), in good agreement with the two-phase titration method.
- The applicability of the sensor was confirmed for environmental water samples, where SDS-spiked lake and river samples showed recoveries of 94.2–96.5%, indicating negligible matrix interference.
- Pt-doped multi-walled carbon nanotubes (Pt@MWCNT) were successfully synthesized and characterized.
- The nanocomposite ionophore system Pt@MWCNT–DHBI (based on cationic surfactant 1,3-dihexadecyl-1*H*-benzo[d]imidazol-3-ium and Pt@MWCNT) was successfully synthesized, characterized and used as a sensing material to fabricate Pt@MWCNT–DHBI liquid membrane-type surfactant sensor.
- The Pt@MWCNT–DHBI sensor exhibited linear calibration curves with Nernstian slope for SDS (59.1 mV/decade) and a slightly sub-Nernstian response for DBS (57.5 mV/decade*)*. Both surfactants exhibited broad linear response ranges down to approximately 2×10^{-6} M.
- The Pt@MWCNT–DHBI sensor showed sub-Nernstian slope, with 49.2 mV/decade for CPC and 44.7 mV/ decade for CTAB. Although the sensor demonstrated good response characteristics, the reduced slopes indicate lower sensitivity for cationic surfactant quantification.
- The Pt@MWCNT–DHBI sensor showed low interference from common anions which can be attributed to the nanocomposite ionophore membrane composition. The optimized membrane composition containing Elvaloy 742 plasticizer and Pt-doped MWCNT ionophore exhibited low potential drift (~6 mV/h), improved charge transfer, reduced noise, enhanced membrane stability, and minimized ionophore leaching.
- The Pt@MWCNT–DHBI surfactant sensor was successfully applied as an end-point indicator in potentiometric titrations with Hyamine 1622, producing a well-defined sigmoidal titration curve with a total potential change of 222.7 mV and a sharp equivalence point.
- Application to technical surfactant samples (CTAB and Hyamine 1622) using the standard addition method yielded recoveries of 98.2–99.2%, confirming the high accuracy of the proposed method.

- The Pt@MWCNT–DHBI surfactant sensor was successfully applied for potentiometric titration of six commercial detergent samples, showing surfactant contents of 6.1–6.3% (powdered), 2.1% (liquid/gel), and 13.2–15.1% (handwashing detergents). The obtained results showed good agreement with both the previously developed ISE surfactant sensor and the classical two-phase titration method, confirming the reliability of the proposed sensing approach.
- Quantum-chemical calculations and molecular dynamics simulations confirmed the formation of a stable DODTA–TPB ionic associate, primarily stabilized by electrostatic attraction between the triazolium head group and the tetraphenylborate anion.
- Non-covalent interactions, particularly van der Waals and hydrophobic interactions between TPB phenyl rings and DODTA alkyl chains, significantly contribute to ion-pair stability, supporting its effective incorporation into the membrane phase of potentiometric surfactant sensors.
- Computational modeling proved to be a valuable tool for understanding ion-pair interactions and guiding ionophore design, enabling more efficient selection and optimization of sensing materials for potentiometric surfactant sensors.

The obtained results open further possibilities for the development of stable, sensitive, selective, and low-cost potentiometric sensors suitable for routine laboratory analysis as well as portable on-site monitoring of surfactants in environmental and industrial systems.

5. REFERENCES

1. Sánchez, J.; del Valle, M. Determination of anionic surfactants employing potentiometric sensors - A review. *Crit. Rev. Anal. Chem.* **2005**, *35*, 15–29, doi:10.1080/10408340590947899.

2. Krogh, K.A.; Halling-Sørensen, B.; Mogensen, B.B.; Vejrup, K. V. Environmental properties and effects of nonionic surfactant adjuvants in pesticides: A review. *Chemosphere* **2003**, *50*, 871–901, doi:10.1016/S0045-6535(02)00648-3.

3. Presedence Research *Surfactants Market Size, Share and Trends 2025 to 2034*; 2025; accessed on Aug 9, 2025).

4. ISO2271:1989 *Surface active agents, Detergents, Determination of anionic-active matter by manual or mechanical direct two-phase titration procedure, ISO 2271, Geneva, Switzerland 1989.*; 1989;

5. ISO16265:2009 Water quality - Determination of the methylene blue active substances (MBAS) index - Method using continuous flow analysis (CFA) Available online: https://www.iso.org/standard/52130.html (accessed on Aug 9, 2025).

6. Haefliger, O.P. Universal Two-Dimensional HPLC Technique for the Chemical Analysis of Complex Surfactant Mixtures. *Anal. Chem.* **2003**, *75*, 371–378, doi:10.1021/ac020534d.

7. Wulf, V.; Wienand, N.; Wirtz, M.; Kling, H.-W.; Gäb, S.; Schmitz, O.J. Analysis of special surfactants by comprehensive two-dimensional gas chromatography coupled to time-of-flight mass spectrometry. *J. Chromatogr. A* **2010**, *1217*, 749–754, doi:10.1016/j.chroma.2009.11.093.

8. Ripoll-Seguer, L.; Beneito-Cambra, M.; Herrero-Martínez, J.M.; Simó-Alfonso, E.F.; Ramis-Ramos, G. Determination of non-ionic and anionic surfactants in industrial products by separation on a weak ion-exchanger, derivatization and liquid chromatography. *J. Chromatogr. A* **2013**, *1320*, 66–71, doi:10.1016/j.chroma.2013.10.046.

9. Ysambertt, F.; Cabrera, W.; Marquez, N.; Salager, J.L. Analysis of Ethoxylated Nonylphenol Surfactants by High Performance Size Exclusion Chromatography

(HPSEC). *J. Liq. Chromatogr.* **1995**, *18*, 1157–1171, doi:10.1080/10826079508009282.

10. Martínez-Barrachina, S.; Alonso, J.; Matia, L.; Prats, R.; Del Valle, M. All-solid-state potentiometric sensors sensitive to nonionic surfactants based on ionophores containing ethoxylate units. *Talanta* **2001**, *54*, 811–820, doi:10.1016/S0039-9140(01)00332-0.

11. Olkowska, E.; Polkowska, Z.; Namieśnik, J. Analytical procedures for the determination of surfactants in environmental samples. *Talanta* **2012**, *88*, 1–13, doi:10.1016/j.talanta.2011.10.034.

12. Olkowska, E.; Polkowska, Z.; Namieśnik, J. Analytics of surfactants in the environment: Problems and challenges. *Chem. Rev.* **2011**, *111*, 5667–5700, doi:10.1021/cr100107g.

13. Yang, D.; Wang, Y.; Wang, Y.; Li, H. A simple and effective luminescence sensor distinguishing cationic surfactants from other type of surfactants. *Sensors Actuators B Chem.* **2016**, *235*, 206–212, doi:10.1016/j.snb.2016.04.115.

14. Wardak, C.; Morawska, K.; Pietrzak, K. New Materials Used for the Development of Anion-Selective Electrodes—A Review. *Materials (Basel).* **2023**, *16*, 5779, doi:10.3390/ma16175779.

15. Zdrachek, E.; Bakker, E. Potentiometric Sensing. *Anal. Chem.* **2021**, *93*, 72–102, doi:10.1021/acs.analchem.0c04249.

16. Mao, C.; Robinson, K.J.; Yuan, D.; Bakker, E. Ion–ionophore interactions in polymeric membranes studied by thin layer voltammetry. *Sensors Actuators B Chem.* **2022**, *358*, 131428, doi:10.1016/j.snb.2022.131428.

17. Sakač, N.; Madunić-Čačić, D.; Marković, D.; Ventura, B. Della; Velotta, R.; Ptiček Siročić, A.; Matasović, B.; Sermek, N.; Đurin, B.; Šarkanj, B.; et al. The 1,3-Dioctadecyl-1*H*-imidazol-3-ium Based Potentiometric Surfactant Sensor for Detecting Cationic Surfactants in Commercial Products. *Sensors* **2022**, *22*, 9141, doi:10.3390/s22239141.

18. Karnaš, M.; Sakač, N.; Jozanović, M.; Tsakiri, M.; Kopriva, M. The Influence of Plasticisers on Response Characteristics of Anionic Surfactant Potentiometric Sensor. *Int. J. Electrochem. Sci.* **2017**, *12*.

19. Fizer, M.; Fizer, O.; Sidey, V.; Mariychuk, R.; Studenyak, Y. Experimental and theoretical study on cetylpyridinium dipicrylamide – A promising ion-exchanger for

cetylpyridinium selective electrodes. *J. Mol. Struct.* **2019**, *1187*, 77–85, doi:10.1016/j.molstruc.2019.03.067.

20. Sorvin, M.; Belyakova, S.; Stoikov, I.; Shamagsumova, R.; Evtugyn, G. Solid-Contact potentiometric sensors and multisensors based on polyaniline and thiacalixarene receptors for the analysis of some beverages and alcoholic drinks. *Front. Chem.* **2018**, *6*, 1–16, doi:10.3389/fchem.2018.00134.

21. Cuartero, M.; Ortuño, J.A.; García, M.S.; Sánchez, G.; Más-Montoya, M.; Curiel, D. Benzodipyrrole derivates as new ionophores for anion-selective electrodes: Improving potentiometric selectivity towards divalent anions. *Talanta* **2011**, *85*, 1876–1881, doi:10.1016/j.talanta.2011.07.027.

22. Cuartero, M.; Más-Montoya, M.; Soledad García, M.; Curiel, D.; Ortuño, J.A. New carbazolo[1,2-a]carbazole derivative as ionophore for anion-selective electrodes: Remarkable recognition towards dicarboxylate anions. *Talanta* **2014**, *123*, 200–206, doi:10.1016/j.talanta.2014.02.022.

23. Zhai, J.; Yuan, D.; Xie, X. Ionophore-based ion-selective electrodes: signal transduction and amplification from potentiometry. *Sensors & Diagnostics* **2022**, *1*, 213–221, doi:10.1039/D1SD00055A.

24. Kumar, V.; Suri, R.; Mittal, S. Review on new ionophore species for membrane ion selective electrodes. *J. Iran. Chem. Soc.* **2023**, *20*, 509–540, doi:10.1007/s13738-022-02708-3.

25. Madunic-Cacic, D.; Sak-Bosnar, M.; Samardzic, M.; Grabaric, Z. Determination of Anionic Surfactants in Industrial Effluents Using a New Highly Sensitive Surfactant-Selective Sensor. *Sens. Lett.* **2009**, *7*, 50–56, doi:10.1166/sl.2009.1009.

26. Madunić-Čačić, D.; Sak-Bosnar, M.; Matešić-Puač, R.; Grabarić, Z. Determination of anionic surfactants in real systems using 1,3-didecyl-2-methyl-imidazolium-tetraphenylborate as sensing material. *Sens. Lett.* **2008**, *6*, 339–346, doi:10.1166/sl.2008.040.

27. Madunić-Čačić, D.; Sak-Bosnar, M.; Matešić-Puač, R. A New Anionic Surfactant-Sensitive Potentiometric Sensor with a Highly Lipophilic Electroactive Material. *Int. J. Electrochem. Sci.* **2011**, *6*, 240–253, doi:10.1016/S1452-3981(23)14990-X.

28. Mostafa, G.A.E. PVC matrix membrane sensor for potentiometric determination of dodecylsulfate. *Int. J. Environ. Anal. Chem.* **2008**, *88*, 435–446, doi:10.1080/03067310701717735.

29. Mahajan, R.K.; Shaheen, A. Effect of various additives on the performance of a newly developed PVC based potentiometric sensor for anionic surfactants. *J. Colloid Interface Sci.* **2008**, *326*, 191–195, doi:10.1016/j.jcis.2008.07.043.

30. Devi, S.; Chattopadhyaya, M.C. Determination of Sodium Dodecyl Sulfate in Toothpastes by a PVC Matrix Membrane Sensor. *J. Surfactants Deterg.* **2012**, 1–6, doi:10.1007/s11743-012-1419-z.

31. Issa, Y.M.; Mohamed, S.H.; Baset, M.A. El Chemically modified carbon paste and membrane sensors for the determination of benzethonium chloride and some anionic surfactants (SLES, SDS, and LABSA): Characterization using SEM and AFM. *Talanta* **2016**, *155*, 158–167, doi:10.1016/j.talanta.2016.04.043.

32. Kowalczyk, I. Synthesis, molecular structure and spectral properties of quaternary ammonium derivatives of 1,1-dimethyl-1,3-propylenediamine. *Molecules* **2008**, *13*, 379–390, doi:10.3390/molecules13020379.

33. Brycki, B.; Kowalczyk, I.; Kozirog, A. Synthesis, molecular structure, spectral properties and antifungal activity of polymethylene-α,ω-bis(n,n-dimethyl-n-dodecyloammonium bromides). *Molecules* **2011**, *16*, 319–335, doi:10.3390/molecules16010319.

34. Fizer, O.; Fizer, M.; Sidey, V.; Studenyak, Y. Predicting the end point potential break values: A case of potentiometric titration of lipophilic anions with cetylpyridinium chloride. *Microchem. J.* **2021**, *160*, 105758, doi:10.1016/j.microc.2020.105758.

35. Bakker, E.; Buehlmann, P.; Pretsch, E. Carrier-Based Ion-Selective Electrodes and Bulk Optodes. 1. General Characteristics. *Chem. Rev. (Washington, D. C.)* **1997**, *97*, 3083–3132, doi:10.1021/CR940394A.

36. Maksymiuk, K.; Stelmach, E.; Michalska, A. Unintended Changes of Ion-Selective Membranes Composition—Origin and Effect on Analytical Performance. *Membranes (Basel).* **2020**, *10*, 266, doi:10.3390/membranes10100266.

37. Hajduković, M.; Samardžić, M.; Galović, O.; Széchenyi, A.; Sak-Bosnar, M. A

functionalized nanomaterial based, new, solid state cationic-surfactant-selective sensor with fast response and low noise. *Sensors Actuators, B Chem.* **2017**, *251*, 795–803, doi:10.1016/j.snb.2017.05.067.

38. Sakač, N.; Madunić-Čačić, D.; Karnaš, M.; Đurin, B.; Kovač, I.; Jozanović, M. The influence of plasticizers on the response characteristics of the surfactant sensor for cationic surfactant determination in disinfectants and antiseptics. *Sensors* **2021**, *21*, 3535.

39. Yin, T.; Qin, W. Applications of nanomaterials in potentiometric sensors. *TrAC - Trends Anal. Chem.* **2013**, *51*, 79–86, doi:10.1016/j.trac.2013.06.009.

40. Crespo, G.A.; Macho, S.; Rius, F.X. Ion-selective electrodes using carbon nanotubes as ion-to-electron transducers. *Anal. Chem.* **2008**, *80*, 1316–22, doi:10.1021/ac071156l.

41. Najafi, M.; Maleki, L.; Rafati, A.A. Novel surfactant selective electrochemical sensors based on single walled carbon nanotubes. *J. Mol. Liq.* **2011**, *159*, 226–229, doi:10.1016/j.molliq.2011.01.013.

42. Cho, G.; Azzouzi, S.; Zucchi, G.; Lebental, B. Electrical and Electrochemical Sensors Based on Carbon Nanotubes for the Monitoring of Chemicals in Water—A Review. *Sensors* **2021**, *22*, 218, doi:10.3390/s22010218.

43. Sakač, N.; Karnaš, M.; Jozanović, M.; Medvidović-Kosanović, M.; Martinez, S.; Macan, J.; Sak-Bosnar, M. Determination of anionic surfactants in real samples using a low-cost and high sensitive solid contact surfactant sensor with MWCNTs as the ion-to-electron transducer. *Anal. methods* **2017**, *9*, 2305–2314.

44. Ghaedi, M.; Naderi, S.; Montazerozohori, M.; Taghizadeh, F.; Asghari, A. Chemically modified multiwalled carbon nanotube carbon paste electrode for copper determination. *Arab. J. Chem.* **2017**, *10*, S2934--S2943, doi:10.1016/j.arabjc.2013.11.029.

45. Sakač, N.; Jozanović, M.; Karnaš, M.; Sak-Bosnar, M. A New Sensor for Determination of Anionic Surfactants in Detergent Products with Carbon Nanotubes as Solid Contact. *J. Surfactants Deterg.* **2017**, *20*, 881–889, doi:10.1007/s11743-017-1978-0.

46. Galović, O.; Samardžić, M.; Hajduković, M.; Sak-Bosnar, M. A new graphene-based surfactant sensor for the determination of anionic surfactants in real samples. *Sensors Actuators B Chem.* **2016**, *236*, 257–267, doi:10.1016/j.snb.2016.05.166.

47. Samardžić, M.; Galović, O.; Hajduković, M.; Sak-Bosnar, M. A novel, fast responding, low noise potentiometric sensor containing a carbon-based polymeric membrane for measuring surfactants in industrial and environmental applications. *Talanta* **2017**, *162*, 316–323, doi:10.1016/j.talanta.2016.10.041.

48. Ponnamma, D.; Sung, S.H.; Hong, J.S.; Ahn, K.H.; Varughese, K.T.; Thomas, S. Influence of non-covalent functionalization of carbon nanotubes on the rheological behavior of natural rubber latex nanocomposites. *Eur. Polym. J.* **2014**, *53*, 147–159, doi:10.1016/j.eurpolymj.2014.01.025.

49. Yousefi, A.; Babaei, A.; Delavar, M. Application of modified screen-printed carbon electrode with MWCNTs-Pt-doped CdS nanocomposite as a sensitive sensor for determination of natamycin in yoghurt drink and cheese. *J. Electroanal. Chem.* **2018**, *822*, 1–9, doi:10.1016/j.jelechem.2018.05.008.

50. Afkhami, A.; Madrakian, T.; Shirzadmehr, A.; Tabatabaee, M.; Bagheri, H. New Schiff base-carbon nanotube–nanosilica–ionic liquid as a high performance sensing material of a potentiometric sensor for nanomolar determination of cerium(III) ions. *Sensors Actuators B Chem.* **2012**, *174*, 237–244, doi:10.1016/j.snb.2012.07.116.

51. Tsierkezos, N.G.; Othman, S.H.; Ritter, U.; Hafermann, L.; Knauer, A.; Köhler, J.M.; Downing, C.; McCarthy, E.K. Electrochemical analysis of ascorbic acid, dopamine, and uric acid on nobel metal modified nitrogen-doped carbon nanotubes. *Sensors Actuators B Chem.* **2016**, *231*, 218–229, doi:10.1016/j.snb.2016.03.032.

52. Mikhelson, K.N. *Ion-Selective Electrodes*; Lecture Notes in Chemistry; Springer Berlin Heidelberg: Berlin, Heidelberg, 2013; Vol. 81; ISBN 978-3-642-36885-1.

53. Umezawa, Y.; Bühlmann, P.; Umezawa, K.; Tohda, K.; Amemiya, S. Potentiometric Selectivity Coefficients of Ion-Selective Electrodes. Part I. Inorganic Cations (Technical Report). *Pure Appl. Chem.* **2000**, *72*, doi:10.1351/pac200072101851.

54. Isildak, Ö.; Özbek, O. Application of Potentiometric Sensors in Real Samples. *Crit. Rev. Anal. Chem.* **2021**, *51*, 218–231, doi:10.1080/10408347.2019.1711013.

55. Sakač, N.; Jozanović, M.; Karnaš, M.; Sak-Bosnar, M. A New Sensor for Determination of Anionic Surfactants in Detergent Products with Carbon Nanotubes as Solid Contact. *J. Surfactants Deterg.* **2017**, *20*, 881–889, doi:10.1007/s11743-017-1978-0.

56. Bakker, E.; Pretsch, E. Modern Potentiometry. *Angew. Chemie Int. Ed.* **2007**, *46*, 5660–5668, doi:10.1002/anie.200605068.

57. Maccà, C. Response time of ion-selective electrodes. *Anal. Chim. Acta* **2004**, *512*, 183–190, doi:10.1016/j.aca.2004.03.010.

58. Frant, M.S. Historical perspective. History of the early commercialization of ion-selective electrodes. *Analyst* **1994**, *119*, 2293, doi:10.1039/an9941902293.

59. Cutler, S.G.; Meares, P.; Hall, D.G. Surfactant-sensitive polymeric membrane electrodes. *J. Electroanal. Chem.* **1977**, *85*, 145–161, doi:10.1016/S0022-0728(77)80160-5.

60. Tanaka, T.; Hiiro, K.; Kawahara, A. Alkylbenzenesulfonate ion selective electrode using ferroin salt in polyvinyl chloride matrix. *Anal. Lett.* **1974**, *7*, 173–176, doi:10.1080/00032717408058753.

61. Nobuhiko, I.; Akinori, J.; Koichiro, M. Some ion selective electrodes based on ion associate impregnated in plastics matrix. *Chem. Lett.* **1973**, *2*, 1297–1298, doi:10.1246/cl.1973.1297.

62. Baró-Romà, J.; Sánchez, J.; del Valle, M.; Alonso, J.; Bartrolí, J. Construction and development of ion-selective electrodes responsive to anionic surfactants. *Sensors Actuators B. Chem.* **1993**, *15*, 179–183, doi:10.1016/0925-4005(93)85046-D.

63. Alegret, S.; Alonso, J.; Bartrolí, J.; Baró-Romà, J.; Sànchez, J.; del Valle, M. Application of an all-solid-state ion-selective electrode for the automated titration of anionic surfactants. *Analyst* **1994**, *119*, 2319–2322, doi:10.1039/AN9941902319.

64. Seguí, M.J.; Lizondo-Sabater, J.; Martínez-Máñez, R.; Pardo, T.; Sancenón, F.; Soto, J. Ion-selective electrodes for anionic surfactants using a new aza-oxa-cycloalkane as active ionophore. *Anal. Chim. Acta* **2004**, *525*, 83–90, doi:10.1016/j.aca.2004.07.032.

65. Seguí, M.A.J.; Lizondo-Sabater, J.; Benito, A.; Martínez-Máñez, R.; Pardo, T.; Sancenón, F.; Soto, J. A new ion-selective electrode for anionic surfactants. *Talanta* **2007**, *71*, 333–8, doi:10.1016/j.talanta.2006.04.005.

66. Sak-Bosnar, M.; Matesic-Puac, R.; Madunic-Cacic, D.; Gmbaric, Z. New potentiometric sensor for determination of low levels of anionic surfactants in industrial effluents. *Tenside, Surfactants, Deterg.* **2006**, *43*, 82–87, doi:10.3139/113.100289.

67. Madunić-Čačić, D.; Sak-Bosnar, M.; Matešić-Puač, R.; Grabarić, Z. Determination of anionic surfactants in real systems using 1,3-Didecyl-2-methyl-imidazolium-tetraphenylborate as sensing material. *Sens. Lett.* **2008**, *6*, 339–346, doi:10.1166/sl.2008.040.

68. Madunič-Čačić, D.; Sak-Bosnar, M.; Matešić-Puač, R. A new anionic surfactant-sensitive potentiometric sensor with a highly lipophilic electroactive material. *Int. J. Electrochem. Sci.* **2011**, *6*, 240–253.

69. Mostafa, G.A.E. PVC matrix membrane sensor for potentiometric determination of dodecylsulfate. *Int. J. Environ. Anal. Chem.* **2008**, *88*, 435–446, doi:10.1080/03067310701717735.

70. Wang, J.; Du, Z.; Wang, W.; Xue, W. Ion-selective electrode for anionic surfactants using hexadecyl trimethyl ammonium bromide-sodium dodecylsulfate as an active ionophore. *Int. J. Electrochem.* **2011**, *2011*, 1–7, doi:10.4061/2011/958647.

71. Mahajan, R.K.; Shaheen, A. Effect of various additives on the performance of a newly developed PVC based potentiometric sensor for anionic surfactants. *J. Colloid Interface Sci.* **2008**, *326*, 191–195, doi:10.1016/j.jcis.2008.07.043.

72. Moody, G.J.; Oke, R.B.; Thomas, J.D.R. A calcium-sensitive electrode based on a liquid ion exchanger in a poly(vinyl chloride) matrix. *Analyst* **1970**, *95*, 910–918, doi:10.1039/AN9709500910.

73. Craggs, A.; Moody, G.; Thomas, J. PVC matrix membrane ion-selective electrodes. *J. Chem. Educ* **1974**, *51*, 541–544, doi:10.1021/ed051p541.

74. Jozanović, M.; Sakač, N.; Karnaš, M.; Medvidović-Kosanović, M. Potentiometric Sensors for the Determination of Anionic Surfactants – A Review. *Crit. Rev. Anal. Chem.* **2021**, *51*, 115–137, doi:10.1080/10408347.2019.1684236.

75. Arvand-Barmchi, M.; Mousavi, M.F.; Zanjanchi, M.A.; Shamsipur, M. A new dodecylsulfate-selective supported liquid membrane electrode based on its N-cetylpyridinium ion-pair. *Microchem. J.* **2003**, *74*, 149–156, doi:10.1016/S0026-265X(02)00182-0.

76. Galović, O.; Samardžić, M.; Sak-Bosnar, M. A new microsensor for the determination of anionic surfactants in commercial products. *Int. J. Electrochem. Sci.* **2015**, *10*, 5176–

5193.

77. Petrušić, S.; Samardžić, M.; Széchenyi, A.; Sak-Bosnar, M. Application of a New Functionalized MWCNTs for the Construction of Surfactant Potentiometric Sensors. *Croat. Chem. Acta* **2017**, *90*, 241–250, doi:10.5562/cca3164.

78. Sakač, N.; Madunić-Čačić, D.; Marković, D.; Hok, L.; Vianello, R.; Šarkanj, B.; Đurin, B.; Hajdek, K.; Smoljan, B.; Milardović, S.; et al. Potentiometric Surfactant Sensor Based on 1,3-Dihexadecyl-1*H*-benzo[d]imidazol-3-ium for Anionic Surfactants in Detergents and Household Care Products. *Molecules* **2021**, *26*, 3627, doi:10.3390/molecules26123627.

79. Badawi, A.M.; Hegazy, M.A.; El-Sawy, A.A.; Ahmed, H.M.; Kamel, W.M. Novel quaternary ammonium hydroxide cationic surfactants as corrosion inhibitors for carbon steel and as biocides for sulfate reducing bacteria (SRB). *Mater. Chem. Phys.* **2010**, *124*, 458–465, doi:10.1016/j.matchemphys.2010.06.066.

80. Yoon, J.; Kim, S.K.; Singh, N.J.; Kim, K.S. Imidazolium receptors for the recognition of anions. *Chem. Soc. Rev.* **2006**, *35*, 355, doi:10.1039/b513733k.

81. Fedorowicz, J.; Sączewski, J. Advances in the Synthesis of Biologically Active Quaternary Ammonium Compounds. *Int. J. Mol. Sci.* **2024**, *25*, 4649, doi:10.3390/ijms25094649.

82. Budetić, M.; Jozanović, M.; Pukleš, I.; Samardžić, M. Review of potentiometric determination of cationic surfactants. *Rev. Anal. Chem.* **2024**, *43*, 20230078, doi:https://doi.org/10.1515/revac-2023-0078.

83. Glumac, N.; Vrban, L.; Vianello, R.; Jozanović, M.; Fizer, M.; Sakač, M.K.; Velotta, R.; Iannotti, V.; Della Ventura, B.; Cvetnić, M.; et al. A DODTA–TPB-Based Potentiometric Sensor for Anionic Surfactants: A Computational Design and Environmental Application. *Chemosensors* **2025**, *13*, 321, doi:10.3390/chemosensors13090321.

84. Madunić Čačić, D.; Sak-Bosnar, M.; Galović, O.; Sakač, N.; Matešić-Puač, R. Determination of cationic surfactants in pharmaceutical disinfectants using a new sensitive potentiometric sensor. *Talanta* **2008**, *76*, 259–264, doi:10.1016/j.talanta.2008.02.023.

85. Buck, R.P.; Lindner, E. Recomendations for nomenclature of ion-selective electrodes (IUPAC recommendations 1994). *Pure Appl. Chem.* **1994**, *66*, 2527–2536, doi:10.1351/pac199466122527.

86. Sakač, N.; Madunić-Čačić, D.; Marković, D.; Hok, L.; Vianello, R.; Vrček, V.; Šarkanj, B.; Đurin, B.; Della Ventura, B.; Velotta, R.; et al. Potentiometric Surfactant Sensor for Anionic Surfactants Based on 1,3-dioctadecyl-1*H*-imidazol-3-ium tetraphenylborate. *Chemosensors* **2022**, *10*, 523, doi:10.3390/chemosensors10120523.

87. Stamatin, S.N.; Borghei, M.; Dhiman, R.; Andersen, S.M.; Ruiz, V.; Kauppinen, E.; Skou, E.M. Activity and stability studies of platinized multi-walled carbon nanotubes as fuel cell electrocatalysts. *Appl. Catal. B Environ.* **2015**, *162*, 289–299, doi:10.1016/j.apcatb.2014.07.005.

88. Fizer, M.M.; Fizer, O.I.; Slivka, M. V; Mariychuk, R.T. New [1,3]thiazolo[3,2-b][1,2,4]triazol-7-ium cationic surfactant as a stabilizer of silver and gold nanoparticles. *Appl. Nanosci.* **2023**, *13*, 5079–5090, doi:10.1007/s13204-022-02687-0.

89. Qu, X.; Persson, K.A. Toward Accurate Modeling of the Effect of Ion-Pair Formation on Solute Redox Potential. *J. Chem. Theory Comput.* **2016**, *12*, 4501–4508, doi:10.1021/acs.jctc.6b00289.

90. Moosavi, S.S.; Zolghadr, A.R. Effect of quaternary ammonium surfactants on biomembranes using molecular dynamics simulation. *RSC Adv.* **2023**, *13*, 33175–33186, doi:10.1039/D3RA05030K.

91. Fizer, M.; Fizer, O.; Hryhorka, H.; Slivka, M.; Šoral, M.; Dujnič, V.; Kopáčová, M.; Pantyo, V.; Mariychuk, R. New 5-alkyl-1,2,4-triazole-3-thione surfactants with antifungal and silver nanoparticles stabilization activity. *J. Mol. Liq.* **2024**, *396*, 123943, doi:https://doi.org/10.1016/j.molliq.2023.123943.

92. Becke, A.D. Density-functional thermochemistry. III. The role of exact exchange. *J. Chem. Phys.* **1993**, *98*, 5648–5652, doi:10.1063/1.464913.

93. Lee, C.; Yang, W.; Parr, R.G. Development of the Colle-Salvetti correlation-energy formula into a functional of the electron density. *Phys. Rev. B* **1988**, *37*, 785–789, doi:10.1103/PhysRevB.37.785.

94. Grimme, S.; Antony, J.; Ehrlich, S.; Krieg, H. A consistent and accurate ab initio

parametrization of density functional dispersion correction (DFT-D) for the 94 elements H-Pu. *J. Chem. Phys.* **2010**, *132*, doi:10.1063/1.3382344.

95. Grimme, S.; Ehrlich, S.; Goerigk, L. Effect of the damping function in dispersion corrected density functional theory. *J. Comput. Chem.* **2011**, *32*, 1456–1465, doi:10.1002/jcc.21759.

96. Dapprich, S.; Frenking, G. Investigation of Donor-Acceptor Interactions: A Charge Decomposition Analysis Using Fragment Molecular Orbitals. *J. Phys. Chem.* **1995**, *99*, 9352–9362, doi:10.1021/j100023a009.

97. Stewart, J.J.P. Optimization of parameters for semiempirical methods VI: more modifications to the NDDO approximations and re-optimization of parameters. *J. Mol. Model.* **2013**, *19*, 1–32, doi:10.1007/s00894-012-1667-x.

98. Klamt, A.; Schüürmann, G. COSMO: a new approach to dielectric screening in solvents with explicit expressions for the screening energy and its gradient. *J. Chem. Soc., Perkin Trans. 2* **1993**, 799–805, doi:10.1039/P29930000799.

99. Madunić-Čačić, D.; Sak-Bosnar, M.; Galović, O.; Sakač, N.; Matešić-Puač, R. Determination of cationic surfactants in pharmaceutical disinfectants using a new sensitive potentiometric sensor. *Talanta* **2008**, *76*, doi:10.1016/j.talanta.2008.02.023.

100. Madunić-Čačić, D.; Sak-Bosnar, M.; Samardžić, M.; Grabarić, Z. Determination of anionic surfactants in industrial effluents using a new highly sensitive surfactant-selective sensor. *Sens. Lett.* **2009**, *7*, 50–56, doi:10.1166/sl.2009.1009.

6. BIOGRAPHY

Nada Glumac was born on 3 March 1966 in Prelog. In 1984, she completed secondary medical school in Varaždin and enrolled at the Faculty of Veterinary Medicine, University of Zagreb. She graduated in 1990, and in 1995 she obtained a master's degree at the same faculty (field: natural sciences; area: veterinary medicine).

After graduation, she worked at Koka Varaždin (1990–1991) and at Bioinstitut (1991–1997). In 1998, she began working at Međimurske vode, where she currently serves as the Head of the Drinking Water and Wastewater Laboratory.

Throughout her career, she has participated in numerous professional trainings and workshops, including: Workshop on Foodborne Bacterial Pathogens, Birmingham (1994); specialization in the water sector at the Croatian Institute of Public Health (1998); Lead Auditor training for ISO 9001:2000; training on the application of HRN EN ISO/IEC 17025 (2002); Internal Auditor for Environmental Protection (2002); toxicology training at the Croatian Institute for Toxicology and Anti-Doping (2025).

She participated as a collaborator in a Croatian Science Foundation project titled *Direct Reuse of Municipal Wastewater for Irrigation Using Membrane Technologies*, in cooperation with the Faculty of Chemical Engineering.

From 2020 to 2022, she participated in the international project Interreg V-A Hungary–Croatia *MonMur – Monitoring of Surface and Groundwater in Međimurje and Zala Counties*. Since 2014, she has been working as an external associate at the Međimurje Polytechnic, where she teaches the courses Environmental Microbiology and Wastewater Treatment in the Environmental Engineering programme. She has also attained the academic title of Senior Lecturer at that institution.

She has presented the results of her doctoral research in three scientific papers published in high-impact (Q1) journals indexed in the Web of Science database. She is also a co-author of seven additional scientific papers and numerous professional publications on topics not related to her doctoral dissertation. She won the gold medal for innovation for the developed potentiometric sensor for surfactants at the innovation fair ARCA 2024.

In addition, she has actively participated in scientific conferences, presenting her research results both orally and through poster presentations.

List of Authors` publications

Scientific Papers in Peer-Reviewed Journals

Glumac, N.; Vrban, L.; Vianello, R.; Jozanović, M.; Fizer, M.; Kraševac Sakač, M.; Velotta, R.; Iannotti, V.; Della Ventura, B.; Cvetnić, M. A DODTA–TPB-Based Potentiometric Sensor for Anionic Surfactants: A Computational Design and Environmental Application. *Chemosensors* **2025**, *13*, 321. https://doi.org/10.3390/chemosensors13090321.

Glumac, N.; Fizer, M.; Sakač, N.; Marković, D.; Vrban, L.; Vianello, R.; Šarkanj, B.; Kraševac Sakač, M.; Jozanović, M. Study of a 1,3-Dioctadecyl-1H-1,2,3-triazol-3-ium Cation for Potentiometric Surfactants Sensing Applications. *J. Mol. Liq.* **2025**, *432*, 127831. https://doi.org/10.1016/j.molliq.2025.127831.

Glumac, N.; Momčilović, M.; Kramberger, I.; Štraus, D.; Sakač, N.; Kovač-Andrić, E.; Đurin, B.; Kraševac Sakač, M.; Đambić, K.; Jozanović, M. Potentiometric Surfactant Sensor with a Pt-Doped Acid-Activated Multi-Walled Carbon Nanotube-Based Ionophore Nanocomposite. *Sensors* **2024**, *24*, 2388. https://doi.org/10.3390/s24082388.

Dolar, D.; Ćurić, I.; Glumac, N. Oporaba komunalne vode za navodnjavanje površina membranskim procesima. *Hrvatske vode*. **2022**, *120*, 73.

Racar, M.; Dolar, D.; Karadakić, K.; Čavarović, N.; Glumac, N.; Ašperger, D.; Košutić, K. Challenges of Municipal Wastewater Reclamation for Irrigation by MBR and NF/RO: Physicochemical and Microbiological Parameters, and Emerging Contaminants. *Sci. Total Environ.* **2020**, *722*, 137959. https://doi.org/10.1016/j.scitotenv.2020.137959.

Ptiček-Siročić, A.; Fujs, N.: Glumac, N. Ispitivanje fizikalno-kemijskih pokazatelja kvalitete voda. *Kem. u ind*. **2016**, *65*, 509. 10.15255/KUI.2015.045.

Scientific Conference Papers and Presentations

Jozanović, M.; Miloš, M.; Čož-Rakovac, R.; Ivančan, P.; Šarkanj, B.; Glumac, N.; Drenjančević, D.; Filipović, N.; Sakač, N.; Marković, D. Influence of Alkyl Chain Length on Antibacterial and Antifungal Activities of Vinylimidazolium Quaternary Ammonium Compounds. In *29th Croatian Meeting of Chemists and Chemical Engineers and 7th Symposium Vladimir Prelog: Book of Abstracts*; Vrsalović Presečki, A., Ed.; Croatian Chemical Society: Split, Croatia, **2025**; p 184.

Jozanović, M.; Ivančan, P.; Šarkanj, B.; Glumac, N.; Drenjančević, D.; Filipović, N.; Sakač, N.; Matasović, B.; Marković, D. Antifungal Activity of Selected N-Substituted Imidazole and Benzimidazole Cationic Surface Active Ionic Liquids. In *23rd International Symposium and Summer School on Bioanalysis: Book of Abstracts*; Pocrnić, M., Ed.; University of Zagreb, Faculty of Science: Zagreb, Croatia, **2025**; p 72.

Sakač, N.; Glumac, N.; Drenovac, S.; Koščak, I.; Potočnik-Hunjadi, T.; Marković, D.; Madunić-Čačić, D.; Jozanović, M. New Surfactant Sensor Based on 1,3-Dioctadecyl-1H-1,2,3-Triazol-3-ium. In *1st European Green Conference: Book of Abstracts*; Habuda-Stanić, M., Ed.; International Association of Environmental Scientists and Professionals: Osijek, Croatia, **2023**; p 170.

Glumac, N.; Jozanović, M.; Madunić-Čačić, D.; Marković, D.; Koščak, T.; Sakač, N. Influence of Nonionic Surfactants on Response Properties of 2-Methyl-1,3-Dioctadecyl-1*H*-Benzo[d]imidazol-3-ium-Based Surfactant Sensor. In *19th Ružička Days – Today Science, Tomorrow Industry: Book of Abstracts*; Osijek, Croatia, **2022**; p 28.

Glumac, N.; Jozanović, M.; Madunić-Čačić, D.; Marković, D.; Tot, D.; Đurin, B.; Sakač, N. Development of a New Potentiometric Sensor for Surfactants. In *9th International Conference*

Water for All: Book of Abstracts; Faculty of Food Technology, Josip Juraj Strossmayer University of Osijek: Osijek, Croatia, **2022**; p 38.

Đambić, K.; Lubina, K.; Tot, D.; Sakač, N.; Madunić-Čačić, D.; Marković, D.; Šarkanj, B.; Pukleš, I.; Glumac, N.; Jozanović, M. Synthesis of New Cationic Amphiphiles with Antimicrobial Activities. In *Solutions in Chemistry 2022: Book of Abstracts*; Zagreb, Croatia, **2022**; p 122.

Tot, D.; Glumac, N.; Sakač, N.; Marković, D.; Jozanović, M. Synthesis and Application of New 2-Methyl-1,3-Dioctadecyl-1H-Benzo[d]imidazol-3-ium Cationic Surfactant. In *2nd International Student Green Conference: Book of Abstracts*; Osijek, Croatia, **2022**; p 14.

Glumac, N.; Kovač, I.; Rumenjak, D.; Sakač, N.; Novotni-Horčička, N. Nonlinear Time-Series Models of Annual Average Nitrate Concentrations in the Upper Aquifer Layer at the Prelog Well Field. In *Proceedings of the 2nd International Conference – The Holistic Approach to Environment*; Association for Promoting Holistic Approach to Environment: Sisak, Croatia, **2021**; pp 145–156.

Plantak, L.; Đurin, B.; Kodirov, S.; Glumac, N. Variability Analysis of the River Flow: Case Study River Gornja Dobra, Croatia. In *8th International Conference on Water and Flood Management: Book of Abstracts*; Idea Printers: Dhaka, Bangladesh, **2021**; p 70.

Dolar, D.; Ćurić, I.; Glumac, N. Direct Reuse of Municipal Wastewater for Irrigation by MBR-NF/RO. In *42nd International Conference Water Supply and Sewerage*; Association of Engineers and Technicians of Serbia: Belgrade, Serbia, **2021**; pp 342–348.

Đurin, B.; Glumac, N.; Sakač, N.; Pezeshki, A.; Dadar, S. New Assessment of the Analysis of Wastewater Quality from a Wastewater Treatment Plant Using the RAPS Method. In *Proceedings of the 5th European Conference on Water Sciences* **2020**, 1–7. https://doi.org/10.3390/ECWS-5-08019.

Dolar, D.; Racar, M.; Karadakić, K.; Čavarović, N.; Glumac, N.; Košutić, K. Reuse of Municipal Wastewater for Agricultural Irrigation by Membrane Processes. In *8th International Conference Water for All: Book of Abstracts*; Osijek, Croatia, **2019**; p 16.

Professional and Scientific-Professional Papers

Dolar, D.; Ćurić, I.; Glumac, N. Recovery of Municipal Wastewater for Irrigation of Agricultural Areas by Membrane Processes. *Hrvatske Vode* **2022**, *30*, 73–80.

Glumac, N.; Novotni-Horčička, N.; Sakač, N.; Kovač, I.; Dijanešić, Ž.; Golub, D. Application of "Green" Methods in Sludge Treatment at the Wastewater Treatment Plants of Čakovec and Varaždin. In *Proceedings of the Professional-Business Conference with International Participation "Current Issues in Water Supply and Sewerage"*; Croatian Water and Wastewater Utility Association: Vodice, Croatia, **2021**; pp 117–135.

Glumac, N.; Sakač, N.; Jozanović, M.; Novotni-Horčička, N. Surfactants: Methods of Determining and Removing Surfactants from the Environment. *Zb. Rad. Međimur. Veleuč. Čakovcu* **2022**, *13*, 14–21.

Glumac, N.; Sakač, N.; Remetović, M.; Jozanović, M.; Novotni-Horčička, N. Impact of Surfactants on the Environment. *Zb. Rad. Međimur. Veleuč. Čakovcu* **2020**, *11*, 7–14.

Sakač, N.; Glumac, N.; Kovač, I. Dynamics of Monitoring Nitrates, Phosphates and Detergents in Groundwater of the Međimurje County Water Supply System. *Rad. Zav. Znanst. Rad Varaždin* **2016**, *28*, 31–39. https://doi.org/10.21857/90836cd2qy.

7. APPENDICES

APPENDIX I: Supplementry Materials for the Paper I

Glumac, N.; Fizer, M.; Sakač, N.; Marković, D.; Vrban, L.; Vianello, R.; Šarkanj, B.; Kraševac Sakač, M.; Jozanović, M. Study of a 1,3-Dioctadecyl-1H-1,2,3-triazol-3-ium Cation for Potentiometric Surfactants Sensing Applications. *J. Mol. Liq.* 2025, *432*, 127831. https://doi.org/10.1016/j.molliq.2025.127831.

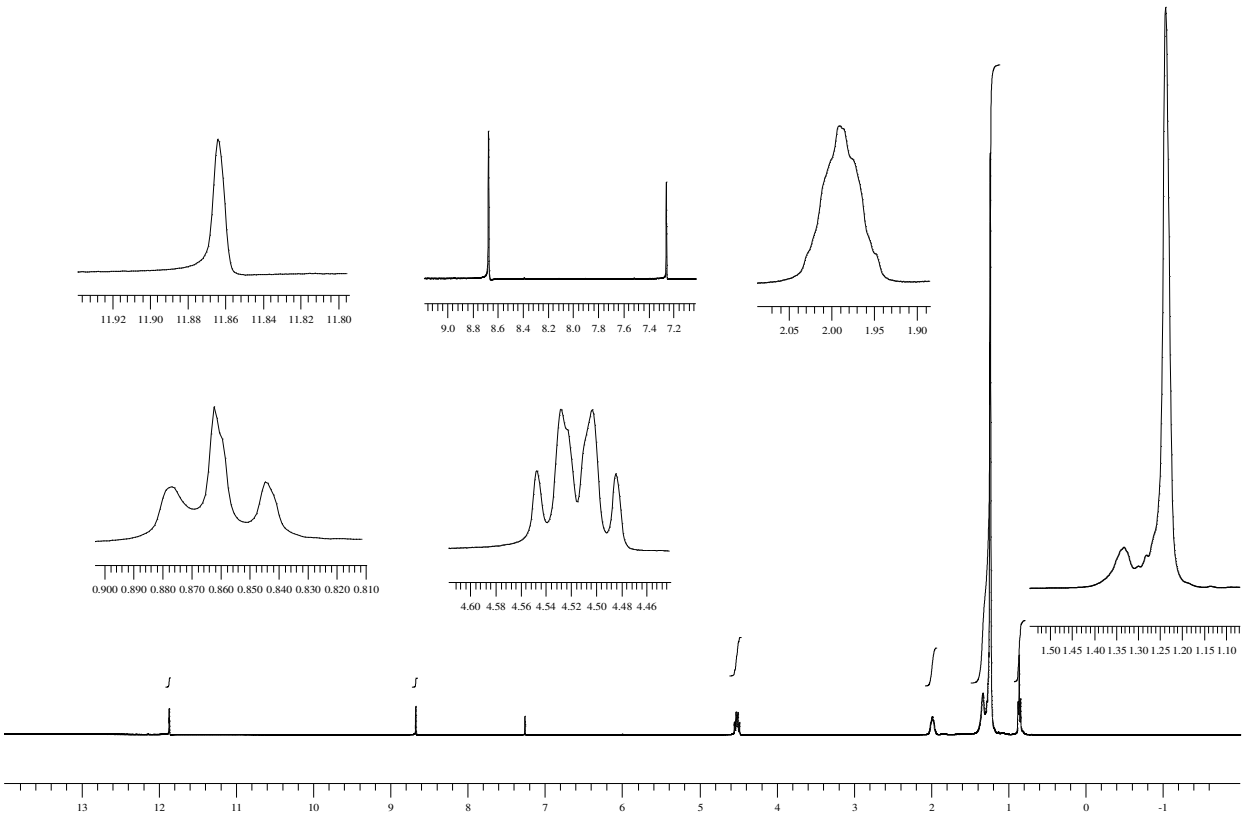

Figure S2. ^{1}H NMR (400 MHz; $CDCl_3$) of 1,3-dioctadecyl-1*H*-1,2,3-triazol-3-ium bromide (**1**).

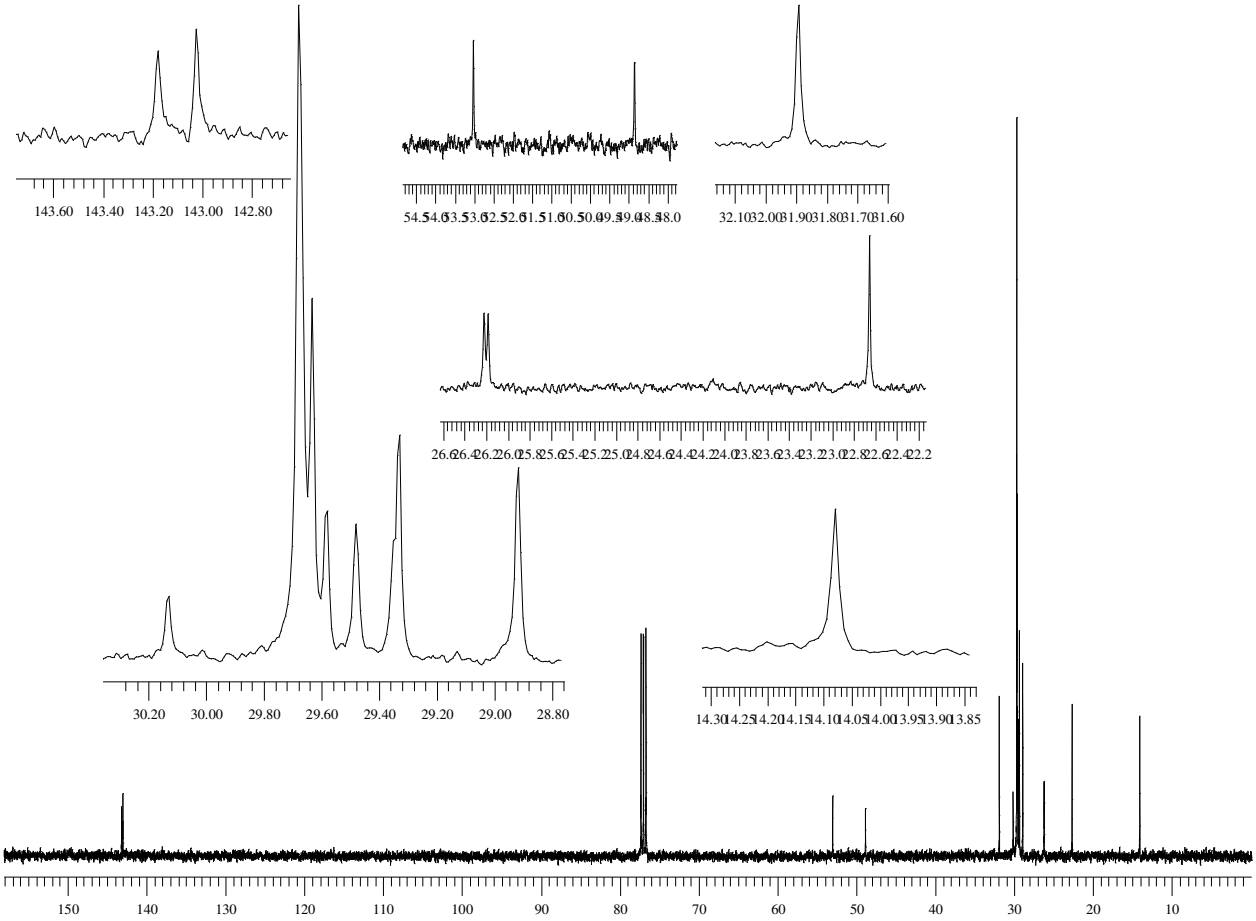

Figure S3. ^{13}C NMR (100.613 MHz; $CDCl_3$): of 1,3-dioctadecyl-1*H*-1,2,3-triazol-3-ium bromide (**1**).

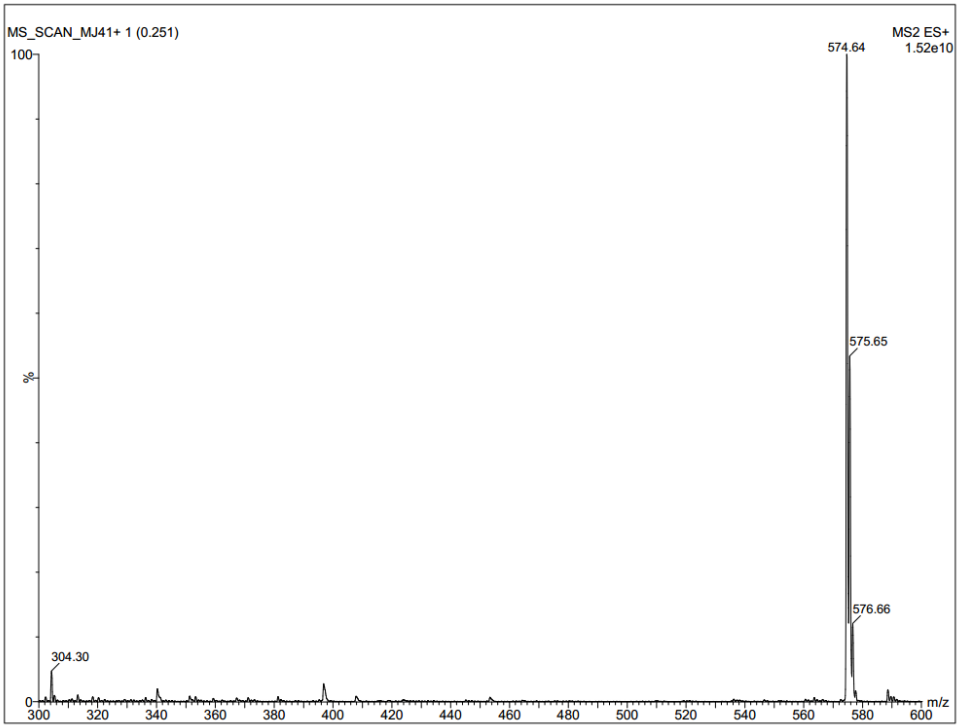

Figure S3. Positive ion mode ESI-MS/MS Q1 scan for 1,3-dioctadecyl-*1H*-1,2,3-triazol-3-ium bromide; infusion 10 µL min^{-1} at concentration 2.5 ng μL^{-1}.

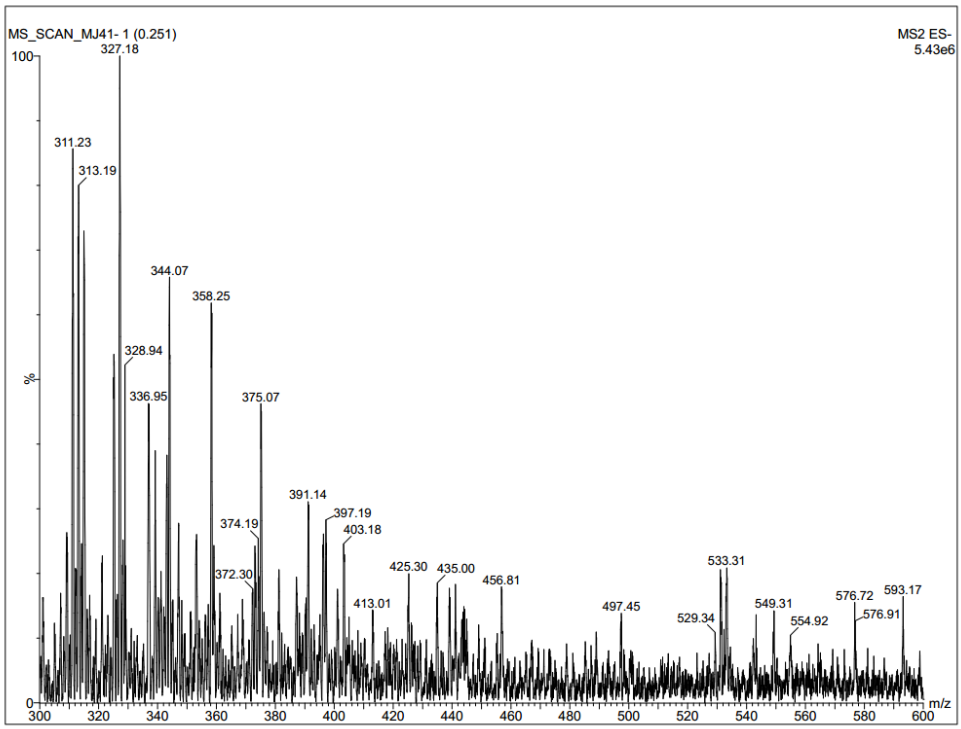

Figure S4. Negative ion mode ESI-MS/MS Q1 scan for 1,3-dioctadecyl-1*H*-1,2,3-triazol-3-ium bromide; infusion 10 µL min^{-1} at concentration 2.5 ng μL^{-1}.

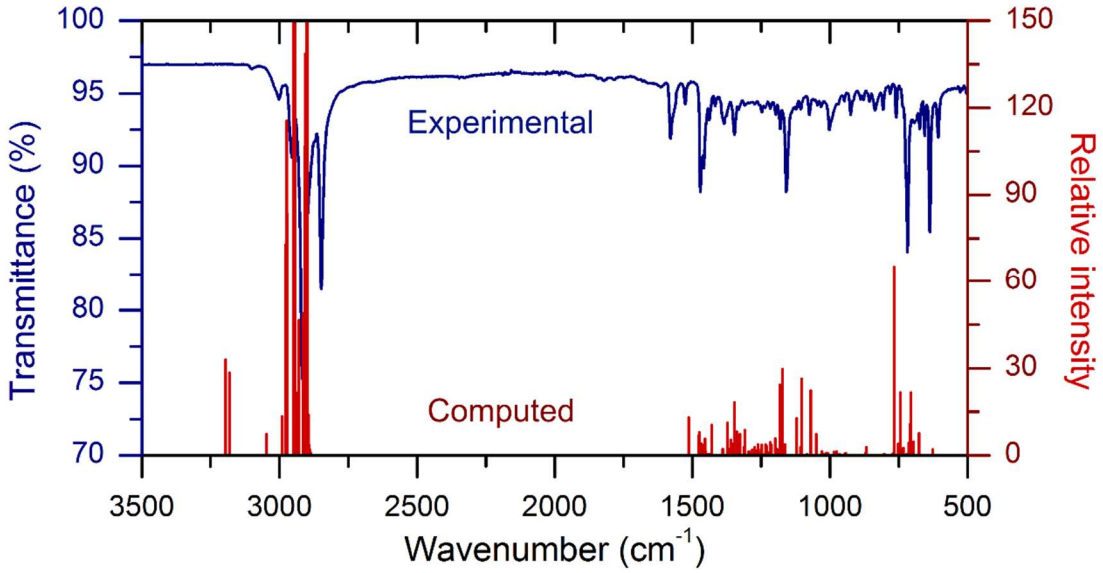

Figure S5. Experimental IR spectra of DODT bromide (blue), and computed with the CPCM-B3LYP-D3BJ/6-31G(d) theoretical method vibrational modes of DODT (red).

Peaks in the region of 2950–3000 cm^{-1} caused by C–H vibrations of the triazolium ring. The most intensive peaks at 2848 and 2916 cm^{-1} correspond to symmetric and asymmetric C–H stretching vibration of the CH_2 groups of alkyl chains. Medium intensity peak at 1579 cm^{-1} should be assigned to C=C vibration in the triazolium ring. Peaks in the region of 1160–1470 cm^{-1} related to stretching and bending vibrations in the triazolium ring. Intensive peaks in the region of 600–720 cm^{-1} can be assign to various torsion bending vibrations.

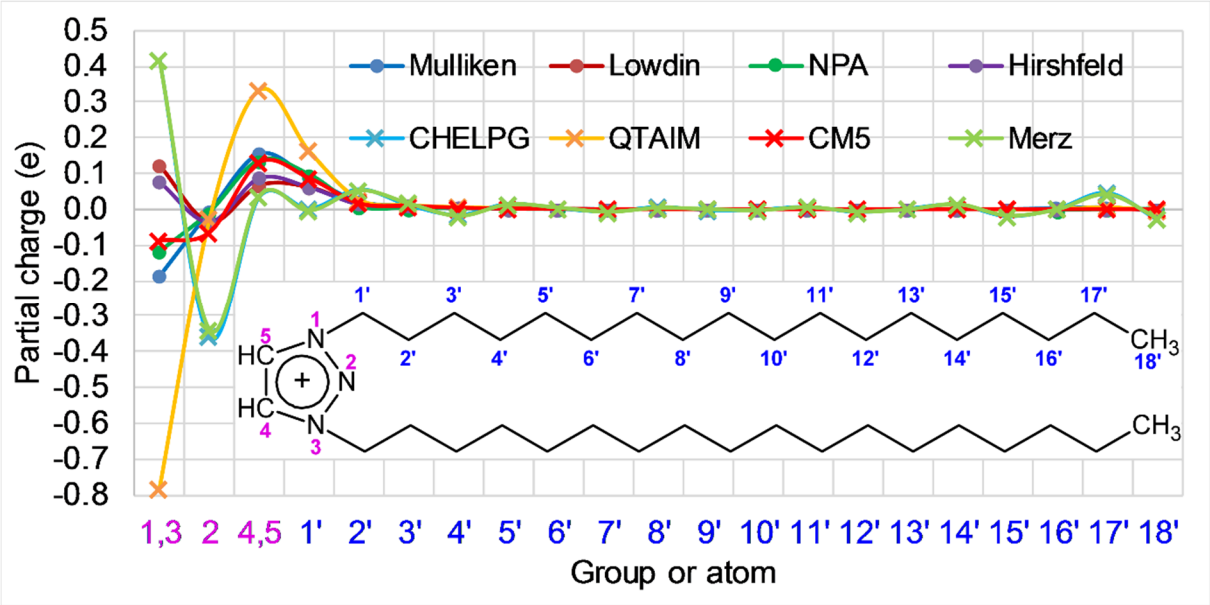

Figure S6. Delocalization of partial charges in DODT calculated via numerous partitioning schemes. Namely: Mulliken, Löwdin, natural population analysis (NPA), Hifshfeld and related charge model 5 (CM5), quantum theory of atoms in molecules (QTAIM), and charges from electrostatic potential calculations CHELPG and Merz-Kollman (Merz) charges.

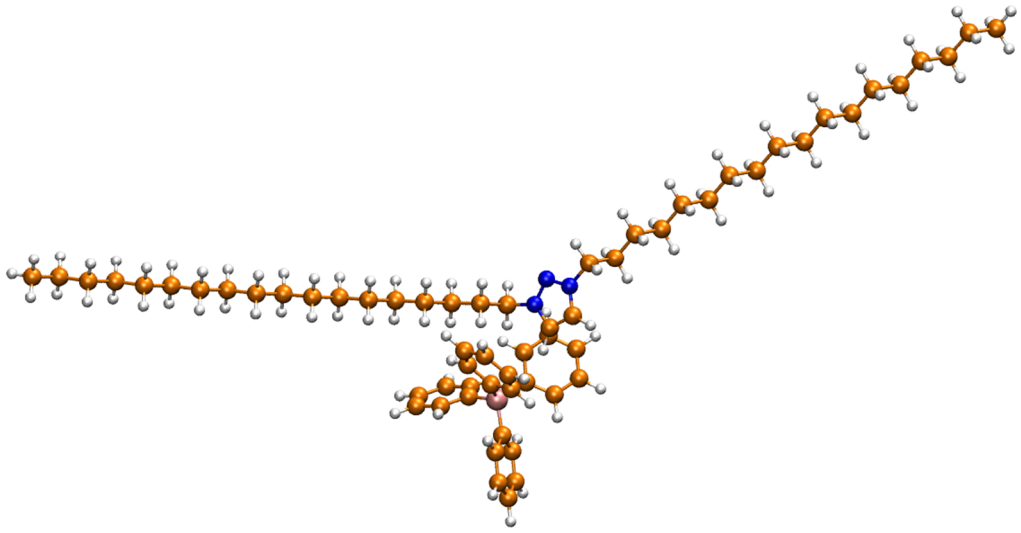

Figure S7. General CPK-type view of the DODT-TPhB associate optimized at the CPCM-B3LYP-D3BJ/6-31G(d) level of theory.

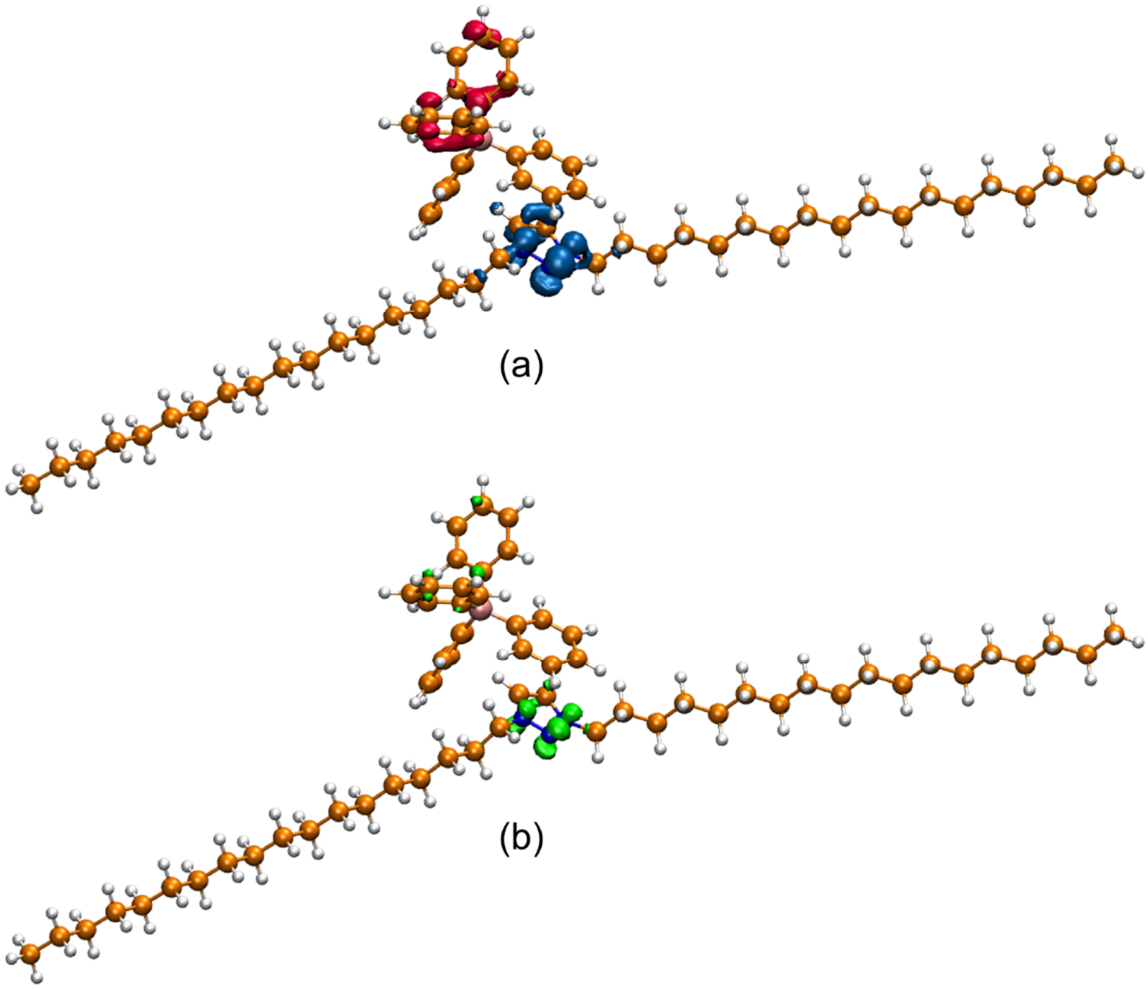

Figure S8. Electrophilic (red areas, a), nucleophilic (blue areas, a), and radical (green areas, b) Fukui function isosurfaces of the DODT-TPhB associate calculated at the CPCM-B3LYP-D3BJ/6-31G(d) level of theory.

APPENDIX II: Supplementry Materials for the Paper II

Glumac, N.; Vrban, L.; Vianello, R.; Jozanović, M.; Fizer, M.; Kraševac Sakač, M.; Velotta, R.; Iannotti, V.; Della Ventura, B.; Cvetnić, M. A DODTA–TPB-Based Potentiometric Sensor for Anionic Surfactants: A Computational Design and Environmental Application. *Chemosensors* **2025**, *13*, 321. https://doi.org/10.3390/chemosensors13090321

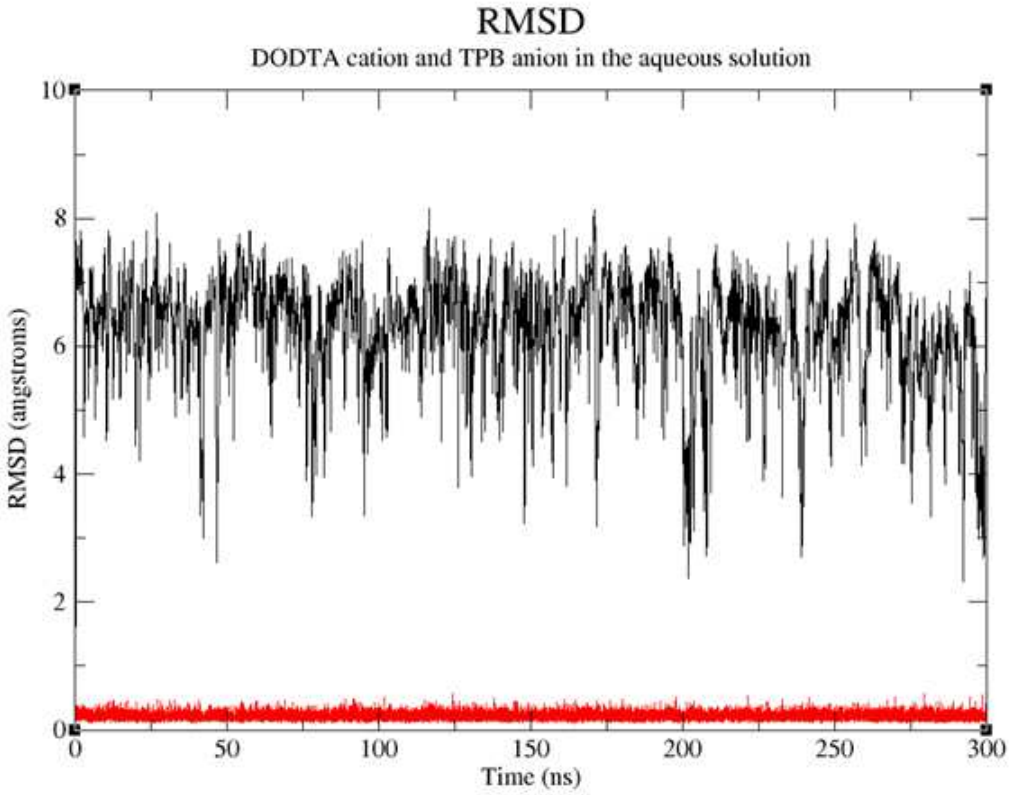

Figure S9. RMSD graphs from the molecular dynamics simulation of the $DODTA^+$ cation (in black) and the TPB^- anion (in red) in aqueous solution, showing significantly higher flexibility of the former.

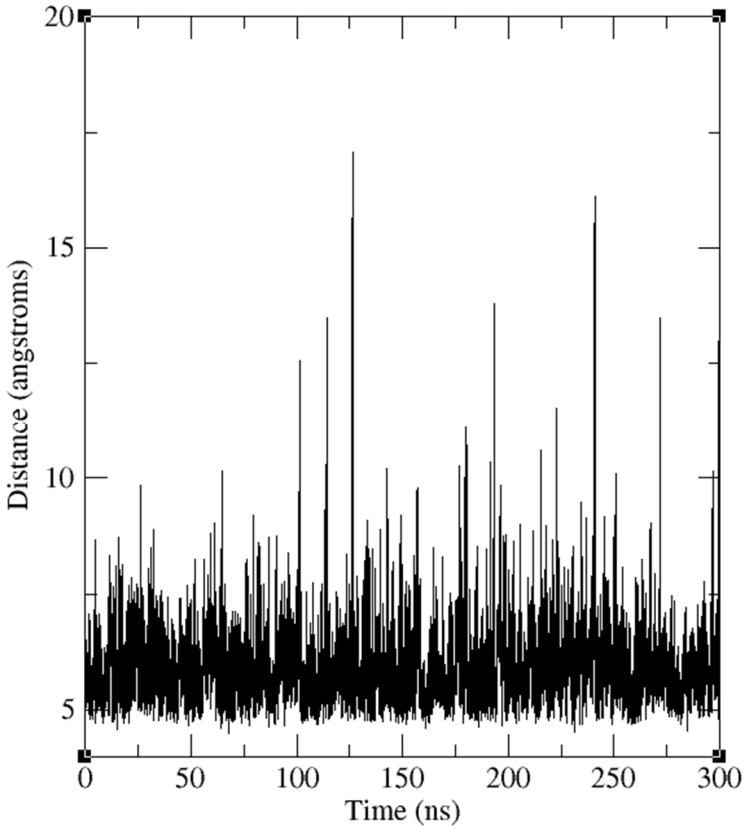

Figure S10. Evolution of the distance between the boron atom in TPB^- and the nitrogen atoms in $DODTA^+$ during the molecular dynamics simulation, indicating that the DODTA–TPB adduct formation is reversible and in equilibrium with the dissociated components.

ISOLATED COMPONENTS BEFORE THE ADDUCT FORMATION

DODTA⁺ cation		TPB⁻ anion		
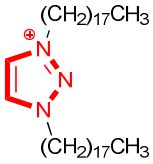	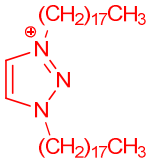	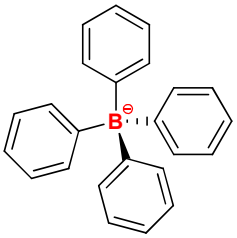	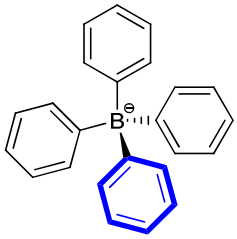	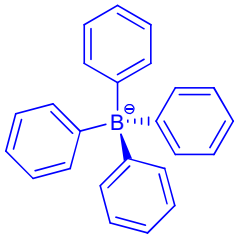
triazole ring	entire cation	boron atom	phenyl ring	entire anion
0.28 |e|	1.00 |e|	0.35 |e|	–0.34 |e|	–1.00 |e|

COMPONENTS WITHIN THE DODTA–TPB ADDUCT

DODTA⁺ cation		TPB⁻ anion		
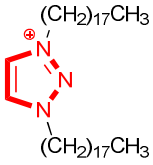		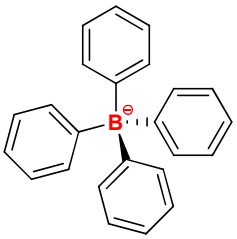	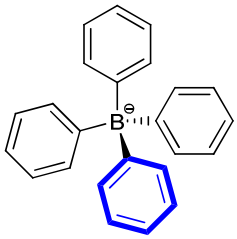	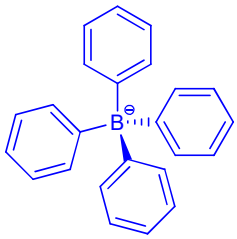
triazole ring	entire cation	boron atom	phenyl ring	entire anion
0.29 |e|	1.01 |e|	0.34 |e|	–0.33 |e|	–0.99 |e|

Figure S11. Charge distribution within the DODTA$^+$ cation and the TPB$^-$ anion, either isolated or within the elucidated representative structure of the DODTA–TPB adduct, as obtained from the NBO analysis at the (SMD)/M06–2X/6–31+G(d) level of theory in water. The specific set of atoms considered for the analysis is denoted by color (red for the cation, blue for the anion) and includes the attached hydrogen atoms. The results reveal that only 1% of the charge density is transferred between the overall components following DODTA–TPB adduct formation.